PALEOBIOLOGY OF A NEW “MACROBAENID” TURTLE (TESTUDINATA: PAN-CRYPTODIRA) FROM THE BLACKLEAF FORMATION, MONTANA

by

Brendan Aubrey Clark

A thesis submitted in partial fulfillment of the requirements for the

degree

of

Master of Science

in

Earth Sciences

MONTANA STATE UNIVERSITY
Bozeman, Montana

May 2026

ACKNOWLEDGEMENTS

I would like to thank my family: Lisa, Adam, and Gabe Clark, Taylor Manes, and more. The students, faculty, and alumni of the Earth Sciences Department at Montana State University are owed much thanks for the community they have welcomed me into. Next, my partner, Ryanne Stoddard, and our cats , (Blinky and Batman) have selflessly welcomed me (and my academic obligations) into their lives with unwavering support.

Dr. David Varricchio, along with Chris Organ and Tyler Lyson, have generously guided my development as a researcher and entrusted me with this amazing project. Walter Joyce, Giulio Panasci, Serjoscha Evers, Zakaria Hannebaum, and Haviv Avrahami have provided excellent guidance and advice on my research as well. I also thank the wonderful staff at the Idaho Museum of Natural History for inviting me to present this research at their Fall Fossil Fest in 2025. I thank Dr. Ladean McKittrick and the SubZero Research Laboratory on campus for their assistance acquiring scan data. Eric Metz, John Scanella, Lee Hall, Brian Helms, Laura Spicher, Ellen-Therese Lamm, and Dane Johnson at MOR have diligently provided collections access, correspondence, and histology training. I also thank the Dillon Ranger District of the United States Forest Service for land access where the specimen was retrieved.

This project was proudly supported by the Undergraduate Scholars program and Department of Earth Science funds. Both Montana State University and the Society of Vertebrate Paleontology have generously funded multiple travel opportunities to present my research via the Graduate Professional Development Grant, the CLS Dean’s Student Travel Award, and the SVP Jackson School of Geosciences Travel Award.

TABLE OF CONTENTS

TABLE OF CONTENTS CONTINUED

LIST OF FIGURES

Figure Page

LIST OF FIGURES CONTINUED

LIST OF FIGURES CONTINUED

LIST OF FIGURES CONTINUED

ABSTRACT

Across the Mesozoic fossil record, the stratigraphy between the Lower and Upper Cretaceous of North America has historically been understudied. Some fossils from this interval suggest diverse assemblages with both basal and derived turtles in many western North American formations. However, the fragmentary nature of these fossils has prevented more thorough reconstructions of their morphology, interrelationships, and ecology. A small fossil turtle, MOR 14891, was recently discovered in the Cenomanian-age Vaughn Member of the Blackleaf Formation in southwest Montana. This specimen includes a carapace and plastron surrounding other previously obscured elements, most of which are from the cranium and mandible. The specimen was micro-CT-scanned and digitally rendered using the software package 3DSlicer. Reconstructions of digital models were made using Blender. Additional synchrotron scans were acquired for the largest block. This permitted a subsequent description of the preserved elements. This specimen represents one of the most complete mid-Cretaceous North American turtle fossils found. Recent stratigraphic studies suggest the Blackleaf Formation dates to 100-101 Mya. As a result, MOR 14891 predates the oldest North American macrobaenid by about 8-9 myr.

Morphological features related to the internal carotid artery canals and parabasisphenoid suggest this specimen represents a new and oldest North American member of the problematic "Macrobaenidae." To test this identification, a global Bayesian phylogenetic analysis was conducted, placing MOR 14891 within a clade of "macrobaenids/sinemydids" branching just stemward of Testudines. MOR 14891 falls in a polytomy with other "macrobaenids"/ "sinemydids", with moderate node support. More specifically, MOR 14891 plots as a sister taxon to *Ordosemys* with similarly moderate node support. The presence of such an unusual, early

representative of the group provides valuable insight into the diversity of the Blackleaf Formation and the evolution of North American ecosystems through an underrepresented time range during the Cretaceous.

ICZN disclaimer: This thesis is not intended to meet the provisions of the ICZN (1999) regarding publication of new nomenclatural acts (Art 8.2). No name or nomenclatural act proposed herein should be considered available as defined by the ICZN.

CHAPTER ONE

INTRODUCTION

Despite turtles being united throughout time by their unique shell, the Mesozoic was a stage for large-scale evolutionary changes in turtles. From the earliest testudinates with a true turtle shell, trends in turtle evolution included the loss of teeth, cranial kinesis, and several additional shell bones (e.g., mesoplastra found in baenids and pleurodires (Joyce 2007)) by the end of the Jurassic.

Like the early Mesozoic, the middle Cretaceous featured transitions in turtle evolution of similar importance. Namely, Cretaceous ecosystems were transitioning from taxa (including turtles) typical of the early Mesozoic to taxa dominant in the ecosystems of the latest Cretaceous. For turtles, these latter assemblages would persist into the Paleogene. Prior to the middle Cretaceous of North America, turtles from extinct lineages, such as helochelydrids, pleurosternids (until the end of the Jurassic), and baenids dominated. The middle Cretaceous of North America specifically features basal turtles, such as helochelydrids and baenids, along with more derived turtles. Although the former are extinct, they are still closely related to lineages persisting to recent times, such as bothremydids (Pleurodira) and nanhsiungchelyids (Cryptodira, Trionychoidea) (Joyce et al., 2016; Clark et al., 2025).

Helochelydrids such as *Naomichelys* and the "Kate's Ridge Taxon" from the Mussentuchit Member of the Cedar Mountain Formation in Utah are non-testudine testudinates diagnosed by their "pustulose" sculpturing on both the carapace and plastron (Herzog, 2019; Joyce, 2017). These extinct turtles were restricted to the Cretaceous of Europe, with the exception of one described North American taxon, *Naomichelys* (Joyce, 2017). Pleurosternids and baenids are

basal Mesozoic testudinates within Paracryptodira, a clade uniting turtles that share similarities in their aberrant cranial vascularity, such as *Glyptops* and *Compsemys* (Joyce et al., 2021). Baenids occur in the Early Cretaceous to the Eocene of North America, while pleurosternids occur in the Late Jurassic to Early Cretaceous of North America and Europe (Joyce & Anquetín, 2019; Joyce & Lyson, 2015). Some authors argue that after the end of the Jurassic in North America, Cretaceous shell material referred to Pleurosternidae or *Glyptops* belongs to baenids. North American pleurosternid material from the Early Cretaceous consists of shell material with texture also found in baenids that occur in the same deposits or those that are stratigraphically equivalent (Joyce & Anquetín, 2019). Mentions of "*Glyptops*" in early Cretaceous faunal assemblages predate these authors' claims (Cifelli et al., 1999; Knell, 2012).

Yet another turtle group appearing in the Cretaceous of North America are the macrobaenids, likely close relatives of the Asian sinemydids. Macrobaenids are rare throughout the Cretaceous of North America but are first known from the Turonian of Arctic Canada (Vandermark et al., 2009). Later, they occur more frequently in the Campanian, Maastrichtian, and Paleogene, crossing the K-Pg boundary. Prior to the mid-Cretaceous, macrobaenids only occurred in Asia. The dispersal and evolution of North American macrobaenids from their Asian ancestors remains ambiguous due to the small sample size of North American macrobaenids from the mid-Cretaceous.

Various taxonomic issues currently prevent the phylogenetic distinction of "macrobaenids" from "sinemydids." As a result, these turtles will be collectively referred to as "macrobaenids/sinemydids" in quotations throughout this work, following the convention of Evers & Benson (2019). Unlike the other turtle families mentioned, "Macrobaenidae" (e.g.,

Macrobaena, *Judithemys*, *Hangaiemys*, *Kirgizemys*, and *Aurorachelys*), "Sinemydidae" (e.g., *Sinemys*, and *Manchurochelys*), and their constituents are not fully separable (Evers & Benson, 2019). In lieu of the phylogenetic resolution required to solve this problem, the terms "Macrobaenidae" and "Sinemydidae" (both isolated and together) and their informal counterparts (i.e., "macrobaenid" and "sinemydid") will refer to previously established, hypothesized representatives of each group (Evers & Benson, 2019).

"Macrobaenidae" is a proposed family of turtles representing anatomically plesiomorphic members of the total group of Testudines; namely, all taxa more closely related to the branch containing modern turtles than to any other branch. Macrobaenidae was erected by Sukhanov (1964) after the description of *Macrobaena mongolica* (PIN 333-4) (Tatarinov, 1959). Originally, Tatarinov (1959) first described this specimen as a baenid, but this family was established due to the aberrant morphology of *M. mongolica* warranting reidentification. Due to the specimen's inaccessibility and the lack of a sample size for the taxon, issues with resolving the phylogeny and even monophyly of "Macrobaenidae" ensued (Gentry et al., 2023). As more fossil turtles were assigned to Macrobaenidae, a general taxonomic pattern emerged where "macrobaenids" could be categorized into two groups: a small sized, Early Cretaceous grade with plesiomorphically rectangular neurals, and a predominantly Late Cretaceous to Paleogene grade of extremely large turtles with hexagonal neurals (Parham & Hutchison, 2003). The former type is exemplified by the morphology seen in "Sinemydidae," such as *Hangaiemys* and *Kirgizemys* (although other aspects of their shell anatomy are highly unusual, e.g., absence of a pygal bone, highly reduced epiplastra). The large-bodied turtle group is represented by *Aurorachelys, Appalachemys, Osteopygis, Judithemys, Gallica, Anatolemys, Macrobaena,* and the only Lower

Cretaceous large bodied taxon, *Yakemys* from Asia (Gentry et al., 2023; Parham & Hutchison, 2003). Tong et al., (2021) was the first to include *Macrobaena mongolica* in a phylogenetic analysis and this taxon will need to be included in future analyses to resolve the group's phylogeny. Despite its subsequent absence from most phylogenetic analyses of "macrobaenids", the role of *Macrobaena* in the establishment of the group has essentially rendered it the only internal specifier for the clade.

Regardless of the group's monophyletic status, Joyce et al. (2021) provides several characteristics in combination that have been used to distinguish these turtles from other anatomically plesiomorphic turtles: carotid fenestrae demarcating the ventrally open bifurcation of the internal carotid arteries, a lack of extragulars, a cruciform plastron, strap-like epiplastra, and a cervical vertebra formula of "1((2((3((4))5))6))7}}8" (where parentheses denote centrum shape (i.e., (2(is an opisthocoelous second cervical vertebra in macrobaenids and {} refer to ginglymoid/double articulations). Importantly, the latter two characters are homoplastic with Chelydroidea, which may parallel the frequent, independent evolution from a more plesiomorphic, or "mesochelydian" grade of morphology to that seen in some modern groups (esp. Trionychoidea (softshells), Kinosternoidea (mud turtles), Chelonoidea (sea turtles) (Miller et al., 2024)).

Evers and Benson (2019) also provided a set of characters used to distinguish "Macrobaenidae/Sinemydidae" from other turtles: a fossa on the lateral surfaces of the supraoccipital where it contacts the exoccipital and opisthotic, paired pits on the ventral surface of the parabasisphenoid, a long T-shaped entoplastron, and a lightly sutured to absent contact between the entoplastron and hyoplastron.

Turtle groups with similar anatomy and phylogenetic resolution include Xinjiangchelyidae and “Sinemydidae”. Xinjiangchelyidae occurs from the Middle Jurassic of Asia, to the end of the Early Cretaceous (Rabi, 2014), with “sinemydids” and “macrobaenids” occurring first in the Early Cretaceous of Spain and Asia (Pérez-García et al., 2012; Rabi, 2014). “Macrobaenids” were thought to have dispersed to North America from contemporaneous taxa in Asia during the early Late Cretaceous while “sinemydids” remained in Asia (Parham and Hutchison, 2003). Finally, Paleogene “macrobaenids” have been recovered from North America and Europe (Brinkman et al., 2010; Pérez-García, 2020). The oldest “macrobaenid” in North America is *Aurorachelys* from 92 Ma (Turonian) in Nunavut (Vandermark et al., 2009). Other North American forms include *Judithemys* from the Campanian to the Paleocene of Laramidia (see Brinkman et al. (2010)) for assignment of “*Clemmys” backmani* to *Judithemys)*, and *Osteopygis* from the Maastrichtian to Paleocene of New Jersey (Gentry et al., 2023).

Phylogenetic analyses of “Macrobaenidae” mostly place the group at an intermediate node between the divergence of Paracryptodira and Testudines, the modern turtles (Evers & Benson, 2019) (Figure 1D). However, some analyses place these turtles and their relatives in a grade within Cryptodira basal to Chelonioidea, making some “macrobaenids”/”sinemydids” stem sea turtles (Pérez-García et al., 2012; Pérez-García, 2012) (Figure 1C). Yet other analyses place sinemydids and xinjiangchelyids at the stem of Cryptodira with only macrobaenids nesting as sister taxa to chelonioids (Danilov & Parham, 2008; Menon & Joyce, 2025) (Figures 1B, 1E). This latter configuration may support the two aforementioned “macrobaenid” groups truly being separate. Regardless, the need for a redescription of *Macrobaena*, and inclusion of important taxonomic units such as *Macrobaena* in future phylogenetic analyses will hopefully yield well

resolved clades that can unite *Macrobaena* and other provisional “macrobaenids” separate from “sinemydids”. In turn, this would allow formal use of previously established phylogenetic definitions for these groups. Clearing this ambiguity could provide a more complete history of turtle biogeography and evolution in the Cretaceous (Rabi, 2014).

In 2021, an informative fossil turtle specimen referred to as MOR 14891 was discovered from the BL-1 locality of the Blackleaf Formation in southwest Montana. This specimen contributes an entire new family of turtles to the Blackleaf faunal assemblage and may represent the same taxon referred to Chelydridae by Ullmann et al. (2012). Both the BL-1 chelydrid material in Ullmann et al. (2012) and MOR 14891 share the same shell ornamentation. However, we describe and reconstruct the latter as distinct from Chelydridae. Reidentifying this chelydrid material may resolve the ghost lineage between it and the next oldest chelydrid fossils from the Santonian; on the other hand, both MOR 14891 and the Ullmann chelydrid material being identified as a “macrobaenid” means this taxon precedes earliest published dates for North American “macrobaenids” by 8-9 Ma (Gentry et al., 2023; Vandermark et al., 2009). Namely, recent stratigraphic work in progress suggests the Blackleaf Formation was deposited around 100-101 Mya (Varricchio pers. comm.). Here, we report and describe this new “macrobaenid” from the mid Cretaceous Blackleaf Formation of Montana. Its anatomy, especially the vascularity of the basicranial elements, warrants referral to this unusual family, making it the oldest “macrobaenid” found in North America. To extract as much data as possible from the many pieces of MOR 14891 obscured by matrix, the first goal of this work is to segment CT data for this specimen. Then, 3D models from the elements of MOR 14891 will contribute to a digital reconstruction of its skeletal anatomy.

This reconstruction will in turn contribute to a description of this taxon and a phylogenetic analysis to supplement its identification. Furthermore, the development of North American ecosystems during the Mesozoic will be better understood with the description of this new specimen. The completeness of the material available for MOR 14891 is atypical for the Blackleaf Formation, marking this new turtle as the third vertebrate taxon from the Blackleaf Formation identifiable from body fossils. The others include the small ornithischian dinosaur *Oryctodromeus cubicularis* (Varricchio et al., 2007) and the neosuchian *Thikarisuchus xenodentes* (Allen et al., 2025). In total, MOR 14891 provides significance beyond an addition to the faunal assemblage of the Blackleaf Formation. This specimen provides biogeographic and phylogenetic information for an enigmatic group in serious need of a larger sample size.

CHAPTER TWO

A NEW "MACROBAENID" TURTLE (TESTUDINATA: PAN-CRYPTODIRA) FROM THE ALBIAN-CENOMANIAN BLACKLEAF FORMATION, MONTANA

Contribution of Authors and Coauthors

Manuscript in Chapter Two

Author: Brendan Clark

Contributions: Conceived the study, segmented CT data, performed analyses, interpreted data and results, prepared figures, and authored the manuscript

Coauthor: David Varricchio

Contributions: Conceived the study, discussed data, results and interpretations, and edited manuscript drafts

Coauthor: Zakaria Hannebaum

Contributions: Prepared referred material, discussed analyses and results

Coauthor: Chris Organ

Contributions: Discussed analyses, data, results and interpretations, and edited manuscript drafts

Coauthor: Tyler Lyson

Contributions: Discussed results and interpretations, and edited manuscript drafts

Manuscript Information

Brendan Clark, David J. Varricchio, Zakaria Hannebaum, Tyler Lyson, Chris Organ

Status of Manuscript:

☒Prepared for submission to a peer-reviewed journal

☐Officially submitted to a peer-reviewed journal

☐Accepted by a peer-reviewed journal

☐Published in a peer-reviewed journal

Introduction

The Mesozoic witnessed some of the most significant changes in the evolution and ecology of turtles. For example, middle Cretaceous ecosystems transitioned from taxa (including turtles) typical of the early Mesozoic to taxa that would become dominant in the ecosystems of the latest Cretaceous. The middle Cretaceous of North America specifically features basal turtles, such as helochelydrids and baenids, along with more derived turtles. Although the former are mostly extinct, they are still closely related to lineages persisting to recent times, such as bothremydids (Pleurodira) and nanhsiungchelyids (Cryptodira, Trionychoidea) (Joyce et al., 2016; Clark et al., 2025).

Yet another turtle group appearing in the Cretaceous of North America are the macrobaenids, likely close relatives of the Asian sinemydids and xinjiangchelyids. "Macrobaenidae" is a proposed family of turtles representing anatomically plesiomorphic members of the total group of Testudines, namely, all taxa more closely related to the branch containing modern turtles than to any other branch. Macrobaenidae was erected by Sukhanov (1964) after the description of *Macrobaena mongolica* (PIN 333-4) (Tatarinov, 1959). Originally, Tatarinov (1959) first described this specimen as a baenid, but this family was established due to the aberrant morphology of *M. mongolica* warranting reidentification. Due to the specimen's inaccessibility and the lack of a sample size for the taxon, issues with resolving the phylogeny and even monophyly of "Macrobaenidae" ensued, preventing the phylogenetic distinction of "macrobaenids" from "sinemydids" (Gentry et al., 2023). As a result, these turtles will be collectively referred to as "macrobaenids"/"sinemydids" in quotations throughout this work, following the convention of Evers & Benson (2019).

Macrobaenids are rare throughout the Cretaceous of North America but are first known from the Turonian of the Canadian arctic (Vandermark et al., 2009). Later, they occur more frequently in the Campanian, Maastrichtian, and Paleogene, crossing the K-Pg boundary. Prior to the mid Cretaceous, “macrobaenids” only occurred in Asia. The dispersal and evolution of North American macrobaenids from their Asian ancestors remains ambiguous due to the small sample size of North American macrobaenids from the mid Cretaceous.

As more fossil turtles were assigned to Macrobaenidae, a general taxonomic pattern emerged where “macrobaenids” could be categorized into two groups: a small-sized, Early Cretaceous grade with plesiomorphically rectangular neurals, and a predominantly Late Cretaceous to Paleogene grade of extremely large turtles with hexagonal neurals (Parham & Hutchison, 2003). The former type is exemplified by the morphology seen in “Sinemydidae,” such as *Hangaiemys* and *Kirgizemys* (although other aspects of their shell anatomy are highly unusual, e.g., absence of a pygal bone, highly reduced epiplastra). The large-bodied turtle group is represented by *Aurorachelys, Appalachemys, Osteopygis, Judithemys, Gallica, Anatolemys, Macrobaena,* and the only Lower Cretaceous large-bodied taxon, *Yakemys* from Asia (Gentry et al., 2023; Parham & Hutchison, 2003).

Suites of characters have been identified that unite “Macrobaenidae” such as the following from Joyce et al. (2021): carotid fenestrae demarcating the ventrally open bifurcation of the internal carotid arteries, a lack of extragulars, a cruciform plastron, strap-like epiplastra, and a cervical vertebra formula of “1((2((3((4))5))6))7}}8” (where parentheses denote centrum shape (i.e., (2(is an opisthocoelous second cervical vertebra in macrobaenids and {} refer to ginglymoid/double articulations). While they could not separate “macrobaenids” from

"sinemydids," Evers and Benson (2019) provided the following characters uniting their group, "Macrobaenidae/Sinemydidae": a fossa on the lateral surfaces of the supraoccipital where it contacts the exoccipital and opisthotic, paired pits on the ventral surface of the parabasisphenoid, a long t-shaped entoplastron, and a lightly sutured to absent contact between the entoplastron and hyoplastron.

Phylogenetic analyses of "Macrobaenidae" mostly place the group at an intermediate node between the divergence of Paracryptodira and Testudines, the modern turtles (Evers & Benson, 2019) (Figure 1D). However, some analyses place these turtles and their relatives in a grade within Cryptodira basal to Chelonioidea, making some "macrobaenids"/"sinemydids" stem sea turtles (Pérez-García et al., 2012; Pérez-García, 2012) (Figure 1C). Yet other analyses place sinemydids and xinjianchelyids at the stem of Cryptodira with only macrobaenids nesting as sister taxa to chelonioids (Danilov & Parham, 2008; Menon & Joyce, 2025) (Figure 1B, 1E).

In 2021, an informative fossil turtle specimen Museum of the Rockies (MOR) 14891, was discovered from the BL-1 locality of the Blackleaf Formation in southwest Montana. Here, we report and describe a new "macrobaenid" from the mid Cretaceous Blackleaf Formation of Montana. Its anatomy, especially the vascularity of the basicranial elements, warrants referral to this unusual family, making it the oldest "macrobaenid" found in North America. To extract as much data as possible from the many pieces of MOR 14891 obscured by matrix, the first goal of this work wass to segment CT data for this specimen. Then, 3D models from the elements of MOR 14891 contributed to a digital reconstruction of its skeletal anatomy.

Methods

CT scanning of mid-Cretaceous fossil turtles has been limited. Normally, a specific project regarding a turtle specimen necessitated CT scanning, e.g., describing eggs from a gravid specimen or analyzing the braincase (Joyce et al., 2014; Lawver & Jackson, 2014; Paulina-Carabajal et al., 2019). While not the subject of CT scanning, more complete turtle fossils have been preserved with material retracted between the carapace and plastron (Meylan & Sterrer, 2000). Particularly in small fossils, these unusually preserved specimens are best treated with CT scanning to appropriately study their elements without incurring significant data loss that might aride using manual preparation methods.

Specimen MOR 14891 consists of numerous fragments with varying levels of exposure from their surrounding matrix. These mm to cm scale carapace, plastron, and other skeletal fragments range from completely free of matrix to mostly embedded in matrix, obscuring diagnostic material. This latter condition initially necessitated the use of a first round of micro-CT scanning for five of these pieces marked as high priority. The largest block is 6.5 cm by 3 cm by 1.25 cm containing the anteromedial portions of the carapace and plastron. Between the two, many elements are obscured. The remaining pieces are sub-cm to cm scale blocks of matrix surrounding fragmented and disarticulated elements. The scans were conducted using a Bruker Skyscan 1173 from the Subzero Research Lab at Montana State University, and completed using GPU-accelerated FDK reconstruction.

Scan data was segmented using 3DSlicer Version 5.6.2 (Fedorov et al., 2012) and Dragonfly Version 2024.1 (Object Research Systems, 2024). When using 3DSlicer, the segmentation method employed the “Fill between slices” tool for quickly segmenting isolated

elements. However, the “Grow from seeds” tool was primarily used for segmentation, where initial, incompletely painted areas of the scan data were propagated to the rest of a region of interest using an algorithm that considers these painted areas relative to others throughout the scan. Where nearby matrix could not be separated from the other elements using this tool, a smoothing tool was applied to the segment before exporting. Gaussian smoothing was used to keep contours smooth and remove extrusions without excessively removing data from openings as would occasionally happen using the “Opening” smoothing tool. The final segment files were reconfigured to pre-taphonomic conditions when possible, using Blender (4.2). These digital models are the subject of this description, and their anatomy will be compared to other turtles.

Due to scanning artefacts or software limitations in 3D Slicer, Dragonfly was used on more complicated blocks. In Dragonfly, all bone was separated from matrix first. This was performed by painting training areas and forming a machine learning model using the Adaboost algorithm, and the “Moments” and “Gabors_MF” feature presets. Once bone was separated from matrix, the individual pieces were segmented apart using iterations of a watershed transform based on manually painted regions and an inverse distance map of the background (non-bone material). The watershed transforms were masked by restricting their growth to a region of interest (ROI) of multiple elements that prevent the watershed from being applied across the entire scan. This ideally allows the painted regions to grow to the extent of each element in a semi-automated fashion.

To extract the maximal number of elements for a digital reconstruction of MOR 14891, the rest of the pieces recovered within the original jacket were scanned at the same Subzero Research Lab. This included about 500 pieces up to ~1cm^3 that were scanned en masse. To

facilitate this scanning, the workflow from Hipsley et al. (2020) was utilized with slight modifications. About 36 large pieces were wrapped in archival foam, arranged, and stabilized in a cup to allow multiple blocks of matrix to be scanned without risking excessive movement, or empty space reducing resolution. Smaller pieces were wrapped in archival tissue, placed in pill capsules and arranged in plastic straws inside pill bottles so dozens of pieces could be lined in a cylindrical pattern in a singular container with low risk of movement during scanning. The rest of the workflow described previously, including digital reconstruction in Blender, ensued.

The juxtaposition of ontogenetically plastic features in MOR 14981 (i.e., well-ossified carapace and plastron, lack of a central plastral fontanelle versus extremely small body size) complicates estimation of its age. Furthermore, the only limb bones free from matrix and other elements are not attributable to the same individual as MOR 14891. Cross sections of a femur and scapula were assessed in the scan data to compare compactness profiles with those recorded in extant turtles over ontogeny.

Turtles have historically been subject to histological studies including but not limited to age estimation (Scheyer & Cerda, 2021). Scute annuli count, carapace length, plastron length, and typical skeletochronology via limb thin sectioning have been used to age modern and fossil turtles (Ehret, 2007). However, a recent increase in research has demonstrated that turtle skeletal histology can provide insight into many diverse aspects of their biology, from the origin and development of the turtle shell to the intended focus in this study, skeletochronology (Scheyer & Cerda, 2021).

Growth curves and qualitative descriptions have been reported for many extant taxa across ontogeny, mainly focusing on the humerus or femur. This prevalence of sectioned limbs in the

literature is a useful reference for interpreting the skeletal maturity of MOR 14891. Since fiber arrangement and distribution, vascularization pattern, and the skeletochronology of extinct taxa remain understudied, the range of focus on turtle bone histology is limited, making further inferences about the histology of MOR 14891 largely outside the scope of this study (Scheyer & Cerda, 2021).

Importantly, histological observations can be problematic without considering the displaced ossification center of turtle limb elements, a unique developmental feature among amniotes (Scheyer & Cerda, 2021). Unlike the midshaft ossification center of other amniotes, this structure occurs slightly proximal in the limb diaphyses of turtles (Scheyer & Cerda, 2021).

Other caveats follow with this methodology. The lack of sampling both within and immediately related to the Blackleaf taxon may prevent optimally accurate estimations of ontogenetic age and growth ring counting. As shown by Scheyer and Cerda (2021), even in modern turtles of the same genus, the same element can exhibit significant variation in limb histology. It is important to note in their study that ontogenetic age is not listed for the sampled specimens. Both hatchlings and the oldest individuals can show little to no rings in thin section (Ehret, 2007). In older specimens, secondary remodeling in the form of secondary osteons and erosion cavities are present in thin sections (Scheyer & Cerda, 2021). In young specimens, embryonic bone and a significantly thicker ring, the hatch line, are visible (Bhat & Cullen, 2025).

MrBayes was used for phylogenetic analysis (Ronquist et al., 2012). The data consisted of a matrix modified from Menon and Joyce (2025), which in turn is a modification of Evers and Benson (2019). This was chosen due to the number of characters based on CT data. The authors

of these previous studies noted the prevalent homoplasy across turtles and remedied this using implied weighting. Since this Bayesian approach is prioritized in this study, and because implied weighting is dependent on parsimony, the matrix and subsequent commands were modified to allow for appropriate emphasis of more slowly evolving, less homoplastic characters. While not a direct analog of the implied weighting used in previous studies, these priors offer explicit probabilistic models of character evolution not performed by implied weighting in parsimony analysis. To remedy the prevalent missing data in this matrix while allowing for *Microbaena* to be included in the analysis (at ~ 63% missing data), this tree was trimmed in a subsequent analysis to remove taxa with over 75% missing data. Invariable characters from the original Menon & Joyce (2025) matrix were deleted, so the current matrix includes 95 taxa and 351 characters. For the rate variation, the "gamma" model was selected as a prior due to it being the simplest model that accounts for variability in substitution rates for each morphological character (Ronquist et al., 2019), and substitutions were given the same rate. Coding bias was set to variable to account for these deletions. The rate prior was set to variable to allow for different rates across partitions.

A relaxed clock model was used, allowing the variance of branch length to increase over time via an independent gamma rates (IGR) prior using an exponential distribution set to 1. A fossilized birth-death model (FBD) was paired with this relaxed clock model. For the FBD model, a speciation prior was set as a default exponential distribution (exp(10)). The extinction prior and fossilization prior were set as a beta distribution with default values (2,2). Sample probability was set to .085 to account for the number of sampled extant taxa out of total extant species (TTWG, 2021).

Because of the lack of agreement between morphological and molecular phylogenetic analyses for modern turtles, a backbone constraint was configured in the matrix using the topology recovered by Pereira et al., (2017) for modern turtles (Testudines, Pleurodires, Cryptodires, and all more inclusive clades). This style of constraint (partial) allows taxa to freely enter or leave a clade unless specified in the constraint. The following characters were ordered in this work's matrix as per Menon and Joyce (2025): 7 15 19 22 35 62 66 68 75 78 80 91 95 105 109 119 125 132 133 140 144 149 207 210 225 256 291 302 315 335 346 347.

A root prior was made, with the minimum age represented by an offset exponential distribution. The minimum was chosen using the earliest occurrence date for the earliest confirmed turtle, *Proganochelys quenstedti*, at 205.7 Ma. The rate parameter for this exponential distribution was set to .05 to account for the 20 million year range from the mean to earliest age (i.e., (.05, 205.7)). Calibrations included an ingroup containing all taxa except for *Proganochelys quenstedti*. Ingroup age was set as an offset exponential distribution. The minimum was set to the earliest verified turtle occurrence, *Proganochelys* at 205.7 Ma (PaleoBioDB), with earliest tentative turtle occurrence, *Chelonipus* at 249.9 Ma (PaleoBioDB) as the maximum. A mean of 227.8 was formed by averaging min and max ages.

Tip dates were retrieved and used for each extinct taxon to calibrate branch length, including *Microbaena*, which was set at 95 Ma. All other taxa were fixed according to their LAD recorded on the Paleobiology Database (https://paleobiodb.org (Peters & McClennen, 2016)). Calibrating the node date for Testudines using an offset exponential prior utilizing the MCMC mean divergence date from Joyce et al. (2013) was considered but not chosen due to the inability of MrBayes to constrain node dates from a partially constrained Testudinata, which itself cannot

be expended due to the ambiguity surrounding the phylogenetic placement of many fossil taxa in the matrix (i.e. it would be inappropriate to remove them from crown Testudines). Chains were set to 5 and runs were set to three to allow for adequate sampling of trees. The burn-in was set to 50% on our analysis consisting of 75 million generations.

The phylogeography was interpreted from a consensus tree derived from the phylogenetic analysis performed above and was mapped using parsimony ancestral state reconstruction using Mesquite. Taxa were categorized by their continent of origin (North American, South America, Africa Europe, Asia, Australia), and were listed as "polymorphic" (e.g., 0/1) if found on multiple continents.

Geological Occurrence

The middle Cretaceous Blackleaf Formation has only recently been explored in terms of its vertebrate faunal assemblage. The numerous formations representing middle Cretaceous Laramidia (e.g. Blackleaf, Frontier, Wayan, and Cedar Mountain) have begun to reveal the evolution of western North American ecosystems during a relatively undersampled portion of deep time.

The Albian to Cenomanian Blackleaf Formation in southwestern Montana is demarcated by the following four lithofacies in ascending order: a lower coarser grain lithofacies, a lower mudstone shale facies, an upper clastic lithofacies, and a much thicker volcaniclastic lithofacies (Dyman & Nichols, 1988). Specifically in the Lima Peaks area, the lowest in the Blackleaf Formation is the Flood Member. This unit contains marine shales between fluvial sandstones which correlates with Idaho's Smiths Formation (Dyman & Nichols, 1988; Krumenacker, 2020;

Ullmann et al., 2012). The Vaughn Member lies above the Flood Member in this region, consisting of a volcaniclastic lithofacies (Dyman and Nichols, 1988). Bone fragments and fish scales constituted the only known vertebrate material from the Blackleaf Formation prior to more recent discoveries such as those described in Varricchio et al. (2007) and Ullmann et al. (2012) (Dyman & Nichols, 1988).

The specimen MOR 14891 was discovered in BL-1, the microvertebrate site described in Ullmann et al. (2012), which is located within the Vaughn Member of the Blackleaf Formation in the Lima Peaks region of southwestern Montana. BL-1 appears to occur in this member instead of the Flood Member as mentioned in Ullmann et al. (2012), lying about 80 meters below the lower boundary of the Frontier Formation (Varricchio pers. comm.).

The fossiliferous unit in BL-1 is a green sandy siltstone with (~80% silt) (Ullmann et al., 2012). According to Ullmann et al.'s study, the sand clasts are subangular or subrounded, fine to very fine sized quartz grains, along with well rounded, fine sized chert grains and some very fine sized biotite flakes. The geometry of the bed containing BL-1 is somewhat lenticular and discontinuous. This unit fines upward with a decrease in the number of fossils. BL-1 has produced fossil material from neopterygians, crocodilians, and other turtles, indicating a less terrestrial environment than BL-4, a locality from the same Lima Peaks region known for producing fossils of a more terrestrial signature, such as dinosaur eggshell and *Oryctodromeus* (Ullmann et al., 2012). Prior to the discovery of MOR 14891, turtles recovered from BL-1 included only fragments of "*Glyptops*", another taxon similar to *Adocus* in shell texture, a chelydrid which we reidentify here as a macrobaenid, and a small humerus from a pond turtle-like animal found outside of BL-1 (Ullmann et al., 2012). The work of Ullmann et al. therefore

provides a rich faunal assemblage of turtles including taxa both basal and derived relative to crown Testudines.

While the Blackleaf Formation has produced a noteworthy assemblage of fossil turtles, equivalent layers across western North America are also reported to contain similar taxa. Strata equivalent to the Vaughn Member include the Wayan Formation of Idaho, the Willow Tank Formation of Nevada, and the Mussentuchit Member of the Cedar Mountain Formation in Utah (Bonde, 2008; Krumenacker, 2020; Suarez et al., 2012). The Wayan Formation has produced indeterminate turtle fossils. On the other hand, the Willow Tank Formation contains *Naomichelys*, a baenid, and trionychid-like and *Adocus*-like testudines (Bonde, 2008; Krumenacker, 2020; Ullmann et al., 2012). Finally, the Mussentuchit Member has produced baenid, adocid, trionychid-like, helochelydrid, and possibly pleurosternid ("*Glyptops*") specimens (Avrahami, 2018; Cifelli et al., 1999; Goldberg, 2000; Herzog, 2019; Ullmann et al., 2012).

Systematic Paleontology

Class REPTILIA (Laurenti, 1768)

TESTUDINATA (Klein, 1760)

PAN-CRYPTODIRA (Joyce et al., 2004)

Family "MACROBAENIDAE" (Sukhanov, 1964)

MICROBAENA gen. nov.

Type species: *Microbaena quadratosternon* sp. nov.

Generic Etymology and Gender: *Microbaena*: In reference to the internal specifier for "Macrobaenidae" (Sukhanov, 1964), *Macrobaena mongolica* (Tatarinov, 1959), with Macro-

replaced with Micro-, to denote the small size of this taxon relative to other North American members of the group.

Diagnosis: See diagnosis for species (genus is monotypic)

Specific Etymology and Gender: quadratosternon: quadrato- square, sternon- chest/breastbone, name refers to the squared anterior edge of the plastron, a shape not seen in the anterior plastra of other “macrobaenids”/”sinemydids.”

Diagnosis: A turtle with carotid fenestrae sensu Rabi (2014), paired pits on the ventral surface of the parabasisphenoid, weak contact between the entoplastron and hyoplastron as in other members of “Macrobaenidae/Sinemydidae”, circular (not elongate) fenestra caroticus as in *Judithemys sukhanovi* and *Sinemys* but not *Ordosemys sp.* (IVPP 12092) or *Dracochelys bicuspis*, anterior central plastral fontanelle absent as in *Judithemys sukhanovi*, *Changmachelys*, and *Kirgizemys*, pterygoid contacts the basioccipital as in other members of “Macrobaenidae/Sinemydidae” at the exclusion of *Sinemys*. Apomorphies include the following: paired pits on parabasisphenoid highly reduced , large, strap-like epiplastra with squared anterior edges.

Description

Morphological nomenclature primarily follows that of Evers and Benson (2019). The purpose of this is to maintain consistency between this description and its phylogenetic analysis (made from an iteration of the Evers & Benson (2019) matrix, and the character definitions provided by Evers and Benson’s original study).

Skull

The skull of *Microbaena* is dorsoventrally flattened (Figures 2E, 3E, 10). Anteriorly, the geometry of the maxilla suggests a shortened antorbital region in lateral view. What is reconstructed of the skull roof and facial skeleton suggests the orbits were large, likely comprising over half the height of the cranium. Posteriorly, the elements are more fragmentary, but suggest the cavum tympanum, the concavity covered by the eardrum in life, was similarly shallow (Figures 2E, 3E, 4A). The skull of MOR 14891 is highly disarticulated, but preserves incomplete elements from the posterior facial skeleton, skull roof, basicranium, and portions of the braincase. Most of the cranial elements are preserved between the carapace and plastron, but some of the facial skeleton (i.e. a fragmentary maxilla, postorbital) is preserved elsewhere.

Maxilla: Only the anterior region of the left maxilla is preserved. It has an angled lateral surface in anterior or posterior view, forming an oblique shelf dorsally. In ventral view, the maxilla is flat, except for the margin, which extends ventrally forming the labial ridge at the edge of the mouth (Figures 2B, 3B). Fragments of the maxillae are present throughout the various blocks constituting MOR 14891. The anteromedial (palatal) portions of the maxillae are missing, and their medial contact with other elements or each other is therefore unknown. The triturating surface of the maxilla is simple, only bearing a labial ridge (Figure 2B). As a result, no lingual or accessory ridges were present in life.

Jugal: The well-preserved left jugal is mediolaterally narrow, forming a crescent shape in lateral view, with the concave dorsal margin forming the contribution of the element to the orbit. The small medial process of the jugal is present extending medially from the posteromedial region of the element, where it would contact the anterolateral edge of the pterygoid just medial

to the processus pterygoideus externis (Figures 2B, 3B, 7). The jugal contacts the postorbital dorsally with a thin, posterodorsal process that is rounded in lateral view (Figures 3C). The jugal provides no contribution to the temporal emargination of MOR 14891. How the jugal may contact the maxilla or palatines is unknown due to their incomplete preservation in MOR 14891.

Quadrate: The quadrates are complex in their form, though each is incompletely preserved. The left quadrate preserves only the dorsomedial region of the cavum tympanum, and the right preserves the descending process that leads to the mandibular condyle (Figure 2A). In lateral view, mirrored pieces of these elements suggest a large, laterally embayed shape to the quadrates, with two lobes (Figure 4A). The larger ventral lobe contains the cavum tympanum, where the eardrum was housed in life. The smaller, flatter, posterior lobe contains the antrum postoticum, which is open dorsally due to incomplete preservation of the squamosal. These two, embayed lobes of the quadrate form the kidney-shaped opening seen in lateral view of the quadrates. In ventral view, a medial lip is formed where the mandibular ramus of the quadrate contacts the pterygoid. The mandibular condyle is visible in this view, extending posterolaterally. The left and right quadrates are preserved, but some detail is lost from a significant break through the right element, and loss of the ventral half of the left (Figure 2, Figure 4). The region of the quadrate containing the incisura columella auris is broken but visible, revealing a posteriorly opened incisura columella auris as is seen in other “macrobaenids”/”sinemydids” (Figure 4C). This region has small, blocky processes on the dorsal and ventral edge of the incisura. The cavum tympani deeply extend medially and posteriorly. The quadrate has a flat, broad process that floors the contribution of the quadrate to the antrum postoticum. The antrum postoticum is partially formed by the quadrate, which itself is fenestrated posterodorsally. This

fenestra leads into the rest of the antrum postoticum, which is completed by the squamosal when articulated. A mandibular condyle is preserved, extending ventrolaterally from the quadrate's medial contact with the pterygoid, where a lip is formed between the two elements (Figures 2B, 3B).

Skull Roof

In dorsal view, the skull roof is rectangular, widening around the posterodorsal margins of the orbits, then narrowing posteriorly with the tapering posterior extent of the parietal (Figures 2A, 3A). The skull roof consists of paired frontals anteriorly and is dominated by the parietals immediately posterior, along with the postorbitals lateral to the frontals and parietals, and the squamosal posterior to the postorbitals. Although breaks throughout the skull roof preclude determining the full extent of this temporal emargination, the elements of the braincase and basicranium are exposed in dorsal view via the temporal fossa.

Parietal: The skull roof of *Microbaena* appears to largely consist of the kite-shaped, dorsalmost parietal (Figures 2A, 3A), indicative of a moderate to high degree of temporal emargination. The parietal appears broken at the anterolateral edges, but preserves a wide, somewhat rounded anterior extent in dorsal view, tapering posteriorly to a point where the supraoccipital would be located when articulated. This element appears to lack crenulations or sculpturing (Figures 2A, 3A). Anteriorly, the skull roof is shaped to allow for the jugal and maxilla to be visible in dorsal view, causing the orbits to face dorsolaterally. The anterior margins of the parietals have a stepped articular facet for contacting the frontals (Figures 2A, 3A). The short, paired, descending processes of the parietal in *Microbaena* articulate with the left and right pterygoids (Figures 2B, 2C). As they descend from the parietal, these processes

bifurcate then bifurcate again closer to the wider anterior margins in ventral view. This matches some baenids, where these descending processes are illustrated to bifurcate in the same pattern on the ventral side of the parietal (Gaffney, 1979). Contact with the epipterygoids is unknown since neither epipterygoid was recovered. However, it is important to note that few reported observations of the parietals of turtles in ventral view have been made, so the currently published extent of this characteristic among turtles is not representative of the expression of this character across the clade. A small, anterolaterally directed ridge is present on the anteroventral surface of the parietal (Figure 3E). Here, the temporal and orbital fossae are separated by this ridge. This structure is equivalent to that first described by Evers and Benson (2019).

Frontal: In *Microbaena*, the frontal is a rectangular element in dorsal view, with a distinct ventromedially directed process in anterior view (Figures 2A, 2C, 3A, 3C). The element is broken transversely in the middle and is missing the anteriormost material at another transverse break. The frontal forms the margin of the orbit along with the postorbital. While a singular element is preserved, its isolation suggests an absence of medial fusion between the paired frontals. Ventrally, the single preserved right frontal is embayed by the sulcus olfactorius, forming a trough bordered laterally by a shelf-like ridge continuing parasagittally along the medial edge of each frontal.

Postorbital: A disarticulated left postorbital is preserved and fits with the cranial material from the largest block containing the flattened, partial carapace and plastron. It contacts the parietal dorsomedially, and the jugal ventrally. In lateral view, the postorbital is a shallow, sinusoidal element, which extending posteriorly, then bends ventrally upon reaching its contact with the jugal (Figure 3E). At this bend, the postorbital contacts the parietal in dorsal view

(Figures 2A, 3A). The complex shape of the anterior edge of the postorbital is obscured by a break at the contribution of the element to the orbit

Squamosal: The squamosal is present as a flat fragment in the cavum tympanum of the quadrate. In dorsal view, this region of the squamosal is paddle shaped, and expands posteriorly. This region of the element marks the boundary between the cavum tympanum and the antrum postoticum (Figures 2A, 3A).

Basicranium and Braincase

Pterygoids: The pterygoids of *Microbaena* are complex in their shape. In ventral view, they are wide anteriorly, with clear suturing on the anterior edge of the element; they extend laterally in this region with a somewhat stout process (processus pterygoideus externis) (Figures 2B, 3B, 5). This process bears a second process that projects posteriorly into a large fenestra bound by the lateral concavities formed by the basicranium. Continuing posteriorly in ventral view, the pterygoids narrow. This narrowing is abrupt where the pterygoids bear a medial process that contacts the ventral surface of the parabasisphenoid. The shape of this process forms a "hook" projecting from the medial pterygoid at the level of the extreme narrowing ("waist") of the element. Further posteriorly, the elements widen with two lobes forming the posteromedial and posterolateral edges of the element in ventral view. In lateral view, the pterygoids are dorsoventrally flattened except for near the midline where dorsal projections (such as the "cryptodire flange" sensu Gaffney (1979)) contact the descending processes of the parietal.

Both pterygoids represent some of the best-preserved cranial elements in the entire specimen and facilitates comparison with other turtles (Figures 2B, 3B, 5, 6). However, the right pterygoid appears to be missing the medial portion that would suture with the right lateral margin

of the basisphenoid (Figures 2B, 3B, 5). The processus pterygoideus externis extends laterally and hooks posteriorly into the opening of the subtemporal fenestra as in *Chelydra*, baenids, and macrobaenids/sinemydids (Figures 2B, 3B, 5) (Gaffney, 1979; Evers & Benson, 2019). This condition is reported by Evers & Benson (2019) to be very similar to but separate from another condition seen in testudinoids, and most kinosternids and cheloniids. In this separate condition, the anterolateral margin of the pterygoid has a hookless, triangular process that is dorsoventrally thinner but anteroposteriorly wider than that seen in *Microbaena* and other "macrobaenids"/"sinemydids". *Microbaena* instead has a hooked, posterior extension from the transversely oriented processus pterygoideus externis posterior to the element's contact with the maxilla. A digital model of *Ordosemys sp.* (IVPP V12092) (Miller et al., 2024, supp. mat.), exhibits the same morphology of the pterygoideus processus externis matching that of *Microbaena*. Because *Ordosemys* was initially reported to have the hookless, triangular process not seen in other macrobaenids/sinemydids, this character was recoded in the matrix used in this study. Another shared character between *Ordosemys* and *Microbaena* in agreement with this recoding is the dorsoventral, laterally flattened expansion or "vertical flange" sensu Evers & Benson (2019) of the processus pterygoideus externis.

The pterygoids contact the parabasisphenoid posteromedially, forming a single, continuous surface ventrally except for the fenestrae carotici (Figures 2B, 3B, 5). Posteriorly, the medial edge of the pterygoids contact the basioccipital as in other "macrobaenids"/"sinemydids", and posterolaterally, they contact the quadrate. At the sutured contact between the pterygoids and parabasisphenoid, basipterygoid processes are absent. The limited medial extent of the

posteromedial wings of the pterygoids renders the parabasisphenoid and basioccipital fully exposed in ventral view.

Anteromedially, the pterygoids contact each other along the midline of the skull for a length subequal to the rest of the pterygoids. In this region, each pterygoid contacts the anteroventral region of the parabasisphenoid along a W-shaped articular facet. These facets receive the aforementioned medial "hook" of the pterygoid that contribute to the strong pinching or "waist" at the middle of the pterygoid. A paired opening is formed by the posterior concavities of the medial pterygoid "hooks" combined with paired fossae formed by the lateral edges of the parabasisphenoid. This is the fenestra caroticus, seen in almost all "macrobaenid" taxa such as *Judithemys* and *Sinemys gamera* (Rabi, 2014; Tong & Brinkman, 2013). It accommodates the ventrally exposed split between the cerebral and palatine branches of the internal carotid artery. On the ventral surface of the pterygoids, there are a pair of ridges positioned along the level of the parabasisphenoid. They start posteriorly, continue obliquely, then parasagittally, and end about halfway along the anteroposterior length of the pterygoids. These truncated pterygoid ridges are seen in representatives of crown group Chelonioidea. Unlike the deep fossae in Chelonioidea, shallow pterygoid fossae are formed by these ridges as a result.

In dorsal view (Figure 7), the pterygoids are devoid of the paired, pulley-like processes which impart mechanical advantage to the jaw adductor muscles found in Pleurodira (i.e. the processus trochlearis pterygoidei). The pterygoids also lack the foramen palatinum posterius. Due to the palatines not being recovered, the presence of the foramen palatinum posterius itself remains ambiguous. The position of these foramina varies among turtles, perforating the palatine (e.g., trionychids, baenids), the contact between the palatine and maxilla (e.g., most other

cryptodires), or the contact between the pterygoid and palatine (and possibly other elements) (e.g., pleurodires) (Gaffney, 1979). Finally, the lateral margin of the posterior left pterygoid of this specimen preserves a dorsally oriented flange, which is referred to as the "cryptodire flange" in Gaffney (1979) (Figure 7). This flange contacts the prootic, rendering it unexposed in ventral view as is the case for cryptodires (Gaffney, 1979).

Prootic: The left prootic appears completely preserved but fragmented with the rest of the left braincase (Figures 6, 7). What is visible of the prootic is reduced, dominated by a dorsal, saddle-shaped process. The complex canals and foramina often found in the prootic are not clearly visible in MOR 14891. The fragmentary nature of the prootic renders contacts difficult to reconstruct, though the prootic contacts the opisthotic posteriorly, and likely contacts the parietals medially, the quadrates laterally, and the pterygoids anteriorly and ventrally.

Opisthotic: Only an incomplete left opisthotic is preserved in MOR 14891, with breaks causing the dorsal half to be missing (Figures 6, 7). Its shape is complex, contacting the prootic anteriorly, extending posteriorly and curving laterally around the cavum tympanum. Posteroventrally, a pronounced ridge on this curved region forms the border of a saddle-shaped convexity on the ventral surface of the opisthotic near its contact with the quadrate (Figure 4). In between the anterior cavum acoustic-jugulare and the posterior recessus scalae tympani, the processus interfenestralis is expressed as a component of the basicranium and the floor of the inner ear as a small footplate contacting the pterygoid dorsally (Figures 2B, 3B, 5, 6). Importantly, the footplate of this process remains on the dorsal surface of the basicranium in *Microbaena* without its ventral margins contacting other basicranial elements, as in *Sinemys* and testudinids such as *Gopherus polyphemus* (Evers and Benson, 2019). Rather, reconstructions of

the skull of *Microbaena* with mirrored elements suggest this footplate is excluded from the space occupied by the contact between the pterygoid and basioccipital (Figures 2B, 3B). Rabi (2014) noted that the genus *Sinemys* could be excluded from other "macrobaenids"/ "sinemydids" due to the lack of contact between the pterygoids and basioccipitals, a trait shared by the rest of the group. The expansion of this footplate in *Sinemys* may permit the separation of these elements in this genus, in turn explaining the dichotomous character expression seen between *Sinemys* and other "macrobaenids"/ "sinemydids" such as *Microbaena*.

(Para)basisphenoid: Given that almost all turtles are likely to have a parasphenoid contribution to their basisphenoid in development or ontogeny, the element here referred to as the parabasisphenoid assumes these two elements are united (Gaffney, 1979; Raselli, 2018). The parabasisphenoid is largely complete except for some small breaks in the anterior region of the element, where a complete rostrum basisphenoidale and processus clinoidei would occur (Figures 2B, 2C, 3B, 3C, 5). The base of the rostrum basisphenoidale, in cross section suggests the region had a flat shape when complete. In anterior view, three pits are present, separated by vertical ridges. The middle pit bears two large, paired foramina revealing the exit of the cerebral branch of the internal carotid artery. A foramen can be found on each side of the lateral pair of pits (the retractor bulbi pits). In dorsal view, the rectangular form of the element can be appreciated along with raised lateral walls surrounding a large, shallow fossa, which both sit on a raised platform comprising the majority of the parabasisphenoid in dorsal view (i.e., dorsum sellae) (Figure 7). Anteriorly, there is a step from this fossa to a ventral, flat anterior edge of the parabasisphenoid (i.e., the rostrum basisphenoidale). The dorsum sellae bears very weakly

developed processus clinoidei. This dorsum sellae is low and extends anteriorly at an extremely low angle with the posterodorsal surface of the element.

The parabasisphenoid is a rectangular element in ventral view, with a W-shaped articular facet near its anterior margin. This facet receives the pterygoids ventrally where it contacts the parabasisphenoid laterally and anteriorly. The ventral floor of the parabasisphenoid slopes posterodorsally near its contact with the basioccipital posteriorly (Figures 2B, 3B). In *Microbaena*, the parabasisphenoid bears highly reduced, paired pits. The presence of paired pits is an unambiguous synapomorphy for "macrobaenids/sinemydids," and are almost always associated with a short, rounded fenestra caroticus. *Ordosemys* is an exception to this with an elongate fenestra and distinct pits. Xinjiangchelyids and *Dracochelys* always have an elongate fenestra caroticus but lack these pits. The reduced size of these pits in *Microbaena* is therefore highly unusual for "macrobaenids"/"sinemydids" with anteroposteriorly shortened, round fenestrae carotici. The reduction of these pits in *Microbaena* is naturally accompanied by a flat palatal surface of the parabasisphenoid. The only exceptions to this are a pair of ventrolateral embayments. These receive canals for the paired cerebral branches of the internal carotid arteries (Figures 2B, 3B, 5). With the carotid fenestrae and parabasisphenoid pits of MOR 14891, an expanded suite of expressed character states can be appreciated for this group of turtles. However, this increasing complexity suggests a reevaluation of expressed characters in macrobaenids is needed.

Basioccipital: In ventral view, the basioccipital is mostly flat, squared anteriorly, and roughly hexagonal posteriorly, with two short, wing-like processes projecting posterolaterally, referred to as the basal tubera (Figures 2B, 3B). The basioccipital region of the occipital condyle

and the left ventral region are not well preserved. These basal tubera are broken, leaving only the basioccipital with remnants of this structure. Therefore, the contributions of other braincase elements to the basal tubera remain unknown. This unknown anatomy is exacerbated by the missing exoccipitals, which would likely contact the basioccipital dorsolaterally. The basioccipital contacts the basisphenoid anteriorly. The basioccipital of MOR 14891 can be seen contacting the pterygoids along its lateral margins (Figures 2B, 3B). In dorsal view, the crista dorsalis basioccipitalis is about half as high as the lateral walls of the element (Figure 7). The basal tubera differ from the much larger ventral tubercles seen on the anterior basioccipital in the earliest turtles (Evers and Benson, 2019). In *Microbaena*, the contribution of the basioccipital to the basal tubera indicates a reduced structure. On the other hand, the ventral tubercles of earlier turtles are large, bulbous structures positioned ventrally and importantly, sagitally on the basioccipital.

Processus Trochlearis Oticum

The processus trochlearis oticum is a laterally oriented, saddle-shaped region of the skull, known to span the prootic and quadrate in *Microbaena* (Figures 2A, 3A, 7). In cryptodires and some earlier turtles such as *Microbaena,* the processus trochlearis oticum is present. This structure is an area on the anterodorsal surface of the otic region modified into a pulley (the musculatory facet), that provides jaw musculature with mechanical advantage (Gaffney, 1979). The processus trochlearis oticum is recovered only on the quadrate and prootic and is itself, reduced so that the musculatory facet is only found on the prootic. However, since the ventral processes of the parietal have not been fully recovered, we cannot preclude the parietal as one of the contributors to the musculatory facet of the processus trochlearis oticum.

The contribution of the quadrate to the processus trochlearis oticum is reduced and the structure is mostly formed by the prootic. This configuration of the processus trochlearis oticum is seen sporadically in kinosternoids, chelonioids, plesiochelyids, and “macrobaenids”/ “sinemydids” (Evers and Benson, 2019).

Cranial Vascularity

The pattern of arterial canals through the cranium is highly valuable in identifying and classifying turtles (Gaffney, 1979; Rabi, 2014). *Microbaena* has a traceable pattern of vascularity across multiple elements. In ventral view, the paired canals corresponding to the internal carotid arteries begin with the foramen posterius canalis caroticus interni (Figure 6). These are located on the posteromedial edge of the pterygoid ventral to the laterally offset fenestra postotica, a larger opening between the pterygoid and opisthotic. Continuing anteriorly on each pterygoid, four canals (two pairs) for the cranial vasculature are distinguishable in dorsal view (Figure 7). Laterally, the canal for the lateral head artery runs anteromedially along the length of the pterygoid (Figure 7). This canal, the sulcus cavernosus, seems to end at the medial edge of the thin central region (“waist”) of the pterygoid between the pterygoid and parabasisphenoid. Medial to the sulcus cavernosus is the canalis caroticus internus, where the pterygoid contained the internal carotid artery in life (Gaffney 1979). The canalis caroticus internus connects to paired foramina in the lateral margins of the parabasisphenoid, where the canals continue.

In ventral view, the canals for the internal carotid artery continue past the “waist” of the pterygoid. In this region, the canal is visible in ventral view through the paired fenestrae caroticus. Here, the canal for the internal carotid artery branches into the more medial cerebral branch and the lateral palatine branch. The cerebral branches obliquely enter the ventrolateral

margin of the basisphenoid through the foramen posterius canalis carotici cerebralis (Figures 2B, 3B, 5). These canals straighten into a parasagittal orientation, exiting the anterior margin of the basisphenoid as the foramina anterius canalis carotici internus. Due to the thinness of the latter canal, we tentatively interpret the palatine artery to travel anteriorly and lateral to the W-shaped articular facet on the parabasisphenoid, between the pterygoid ventrally and the parabasisphenoid dorsally.

Mandible

Dentary: The left dentary is complete but broken in several areas throughout its length. The right hemimandible is missing except for a single tentative element (a possible prearticular). In lateral view, the dentary is a dorsoventrally low, curved element. The anterior end of the dentary curves dorsally, revealing a modest hook. The dentary broadens posteriorly with the posterodorsally expanded coronoid process. The triturating surface of the dentary is simple and narrow, being flat to slightly concave. Some larger neurovascular foramina appear visible at the labial edge of the dentary (Figure 8A). In posterolateral view, a pair of small foramina are present at the base of the coronoid process (Figure 9A). A corresponding, similarly sized foramen at a similar position is present in medial view within the Meckelian fossa (Figure 9C). The lateral pair corresponds to the foramina dentofaciale majus, and the latter may be the foramen alveolare inferius (Evers et al., 2023). A paired foramina dentofacial majus is not seen in *Chelydra*, though two or three foramina corresponding to the foramina dentofacial majus are common in kinosternids (e.g. *Sternotherus*) (Evers et al., 2023). The presence of this in extinct taxa remains ambiguous.

Coronoid: The coronoid is a complex triangular shape, with a dorsally oriented apex. The element is kidney-shaped in cross section. Only a left fragmentary coronoid is preserved, with breaks at the ventral processes of the element. The coronoid forms rounded contacts with the dentary anteromedially and posteromedially. Nevertheless, it preserves the coronoid process, which the coronoid predominantly forms. This process is high and points posterodorsally (Fig 8B).

Splenial: The left splenial is complete, while the right is missing. The splenial is a large, flat element in medial view. It has a squared medial aspect, and laterally contacts a short length of the posteromedial region of the dentary. The Meckelian groove traverses through the element forming the lateral wall of this structure at the middle of the dentary (Fig 8B).

Surangular: The surangular is a smaller, lateral mandibular element contributing to the lateral margin of the mandibular fossa where it contacts the articular medially (Figure 8A).The surangular has a flat lateral aspect, forming the posterodorsal region of the mandible, contacting the dentary anteriorly and the angular ventrally. The surangular is complete on the left side along with the rest of the left hemimandible. In anterior view, a pair of foramina in a larger fossa are present, what this corresponds to is currently unknown (Figure 9B).

Angular: The left angular is complete. It is thin, strap-like and dorsally concave. The angular is preserved following the ventromedial margin of the dentary (Figure 8). It contacts the surangular and articular dorsally and shares medial contact with the prearticular and articular with the surangular (Figures 8D, 9B).

Prearticular: The prearticular is thin, with curved medioventral regions preserved within the opening formed by the Meckelian groove. The complete, left prearticular medially contacts the articular with a lip on the ventral edge of the lateralmost surface. This was used to tentatively identify another disarticulated prearticular found in another block from the specimen. Artifacts in the scan containing the complete left hemimandible, which also contains the articulated prearticular, prevent a more confident identification of the isolated prearticular (Figure 8).

Articular: The articular is complete, forming a blocky element in the posterodorsal region of the dentary. It tapers anteriorly, and expands posteriorly, accommodating the mandibular fossa. It is the primary contributor to the mandibular fossa along with the surangular. The articular contacts the surangular laterally along with the prearticular, which is preserved anterolateral to the articular. The articular sits in a recess formed by the concave dorsal margin of the angular. The retroarticular process is reduced (Figure 9A). The entire dorsal surface of the articular acts as an articular facet for the quadrate, and the articular makes up most of this surface. The anteroposterior ridge subdividing the mandibular fossa is extremely faint (Figure 9A).

Carapace

Carapace Shape: The carapace is highly fragmented, allowing only a partial, reconstruction limited to the anteromedial portion, and some peripherals forming the edge of the shell. Other fragments exist but cannot be fitted to the reconstructed portion (Figures 11, 12). The carapace material preserved in the largest block (nuchal and first four neurals) is about 6.5 cm in length, suggesting a total carapace midline length of only 15 cm (Figure 11). The midline

carapace length is highly varied in Macrobaenidae/Sinemydidae, with some taxa measuring below 30 cm, and others, such as *Anatolemys*, *Macrobaena*, and *Judithemys* reaching over 40 cm, and sometimes exceeding 50 cm (i.e. *Appalachemys* at 80 cm) (Gentry et al., 2023). As a result, the estimated carapace length of MOR 14891 raises questions about its ontogenetic age, which could explain why this specimen deviates so greatly from the body size seen in the large bodied "grade" of macrobaenids as defined by Parham and Hutchison (2003). Although crushing was evident in MOR 14891, the carapace was likely very flat in life. Sculpturing is present on the medial portions of the carapace. These plications run parasagittally on the neurals and shift their trajectory obliquely, causing a radial pattern of plications more laterally on the proximal costals.

Nuchal: The nuchal is preserved, but fragmentary. The right first costal is preserved, delineating the lateral extent of the nuchal. The nuchal is wider than long as a result.

Neurals: Only the four anteriormost neurals are articulated. Three other neurals are preserved, allowing for a more complete reconstruction. The edges of the neurals are smooth, lacking jagged sutures. The neurals are slightly longer than wide and are hexagonal, forming a coffin shape. Namely, the anterior margin of the neural is often wider than the posterior margin. Within the confines of an individual neural, plications are truncated anteriorly by a transverse, sinusoidal scute sulcus, where a smooth texture follows (Figure 11, 13).

With other neurals, they articulate anteriorly with a concave margin and with a convex margin posteriorly. The neural formula cannot be calculated, but the second neural remains hexagonal instead of quadrate.

The reconstructed carapace reveals that the sixth neural bears the sulcus separating vertebral scutes 3 and 4. This sulcus is W-shaped, matching the pattern seen in xinjiangchelyids and macrobaenids (Figures 11, 13A). Interestingly, this sulcus separating vertebrals 3 and 4 is instead on the fifth neural in macrobaenids and sinemydids, with only some xinjiangchelyids such as *Annemys levensis* having this sulcus on the 6th neural as in *Microbaena*.

Costals: Only the second left costal of the reconstructed specimen is well preserved, though fragments of the first and third pair are also articulated. Numerous small fragments were also recovered and identified based on their texture and asymmetry (the latter of which is not found in the similarly textured neurals). This anterior costal is elongate and T-shaped in lateral view, with an elongate, thickened process corresponding to the rib. This rib fits into the medial edge of the peripherals leaving no space for fontanelles (Figure 11). The medial region of the costals also bear craniocaudally oriented plications, which become more radially oriented, then less conspicuous or absent laterally (Figure 11, 12). The costal's texture is interrupted at the scute sulci in a manner similar to the posterior neurals. The rest of the costals lack texture other than the scute sulci (Figure 11, 12, 13). The costals are dorsoventrally thin compared to the plastron. Their lateral extent and contacts with the marginals, inguinal, or axillary buttresses cannot be assessed currently due to the preservational condition of these areas. The first costals are medially separated in dorsal view by the first neural and the nuchal anteromedially.

Suprapygal: At least a single, complete suprapygal is preserved but disarticulated from the specimen, it is hexagonal in shape. A second suprapygal is often found in "macrobaenids"/"sinemydids," suggesting the second was not preserved.

Pygal: The singular pygal was preserved but disarticulated. It is a symmetrical, squared element in dorsal view, and has a tapered posterior (Figure 11) The pygal bears a transverse scute margin near its anterior margin, and another oriented sagittally. The pygal is positioned in the posteriormost region of the edge of the carapace in between the final pair of peripherals. It resembles a peripheral but differs in its bilateral symmetry, which is not found in peripherals. Due to its fit with an articulated series of peripherals, the pygal has been reconstructed at the posteriormost, median edge of the carapace alongside these posterior peripherals (Figure 11).

Peripherals: Despite being frequently disarticulated, the peripherals range from fragmentary to complete, and are the best represented out of all of the bones of the carapace in MOR 14891. Specimen MOR 14891 preserves 20 complete to near complete peripherals. Anteriorly, the peripherals are flat but thick (Figure 11). Posterior to these anteriormost peripherals, the peripherals meeting the bridge of the shell are thinner, but angled so that they are dorsoventrally deep. A strong peripheral gutter forms at the peripherals ranging from immediately anterior to posterior to the bridge. This gutter is absent on the anteriormost and posteriormost peripherals. The peripherals strongly flatten and broaden posteriorly.

Scute Pattern: On the dorsal surface of the anteromedial region of the carapace, grooves corresponding to the boundaries between the vertebral and pleural scutes appear to extend from the midline laterally to the medial portions of the costals, where they form a deep channel running anteriorly to posteriorly or posteromedially on the element (Figure 11). This is best seen in the posterior region of the main carapace block of the specimen, where the costals lateral to the third neural appear to have scute grooves for two abutting vertebral scutes on one element (Figure 11). The preserved vertebral grooves form a rectangular outline, with roughly parallel

sides running parasagittally along the proximal costals. Several marginals are preserved, being restricted to their corresponding peripherals. The neurals and medial regions of the costals bear parallel, parasagittally oriented plications. These do not pass anterior to the anteriormost vertebral scute in this specimen. Traditionally, the parallel to radial plications found on the medial regions of the costals and vertebrals have been used as a diagnostic trait for Chelydroidea. However, this texture appears to be ubiquitous across anatomically plesiomorphic turtle taxa, and is especially pronounced in juveniles or subadults (Danilov & Parham, 2008). These plications are reported in thalassochelydians (Mlynarski, 1976), chelydroids (Joyce et al., 2023), xinjiangchelyids (Rabi et al., 2014), and sinemydids/macrobaenids (Zhou & Rabi, 2015).

Plastron

Plastron Shape: The cruciform shape of the plastron can be inferred from the preserved fragments in MOR 14891. Nevertheless, its overall shape is highly unusual, being squared anteriorly as opposed to the triangular to ovoid condition found in other "macrobaenids/sinemydids". Interestingly, some of the posterolateral margins of the plastron preserve the full extent of the element in that area, which curves anterolaterally and could have followed the margins of the missing lateral processes of the hyoplastra and hypoplastra. Fragments of the lateral edges of the plastron suggest serrated margins of the hyo/hypoplastra and a ligamentous connection to the carapace. The posterior plastral lobe shape cannot be readily determined. The main plastron fragment consists of the medial portion of all plastral elements except for the xiphiplastra, and measures only 4.5 cm long. Despite this size, plastral fontanelles are absent, as in *Judithemys sukhanovi* and *Krigizemys hoburensis* (Rabi et al. 2014). This further

suggests close affinities to *Judithemys* and may indicate a lack of these fontanelles through ontogeny in these taxa.

Epiplastra: The epiplastra are the best preserved elements in the plastron being complete, with only one epiplastron being disarticulated and unnaturally displaced into the internal cavity formed by the shell. The epiplastra are strap-like, covering about a third of the lateral margin of the hyoplastra (Figure 15). The epiplastra are shaped in a way that is difficult to characterize among other similar turtles. While this region is missing material, the fitted pieces of the anterior epiplastra indicate a small, midline, triangular projection is present anteriorly. This is like other macrobaenids, although *Microbaena* lacks the narrow, uniformly tapering anterior plastral lobe seen in these other taxa. Instead, the epiplastra form a squared anterior margin in *Microbaena*, yet the elements are still elongate unlike the nearly square epiplastra in xinjiangchelyids. They narrow as they extend along the anterolateral margin of the hyoplastra.

Entoplastron: The entoplastron is complete and articulated with the hyoplastra. The entoplastron is noticeably thicker than the surrounding plastral elements. The element is roughly diamond-shaped and has a sagittal scute canal on the ventral surface. The entoplastron is truncated anteriorly, allowing the epiplastra to contact each other. Although the entoplastron contacts the hyoplastra, the suturing between them is minimal.

Hyoplastra: A few fragments of the lateral processes of the hyoplastra have been found. The suture in between each hyoplastron is open and interdigitating, but straight overall, lacking sinuosity (Figure 15). The hyo/hypoplastral suture is transverse but its texture cannot be

considered further due to breakage. Similarly, the ento/hyoplastral suture is smooth and progresses anterolaterally to accommodate the shape of the entoplastron. The anterolateral margins of the hyoplastra bear a groove for articulation with the epiplastra.

Hypoplastra: The lateral processes and the posterior regions of the hypoplastra have not been found. The right posterolateral margin of the hypoplastra appears to preserve the articular facet for the xiphiplastron that contains morphology atypical of the breaks surrounding the remaining margins of the element (Figure 15). This indicates a hypo/xiphiplastral suture oriented in the opposite direction of the epi/hyoplastral suture, namely, a suture propagating anteriorly when followed from its medial to lateralmost extent. The suture in between each hypoplastron is open and interdigitating, but straight, lacking sinuosity.

Xiphiplastron: Some fragments of the xiphiplastron are preserved. Some of these fragments are very thin relative to the other plastral elements and lack texture. One fragment was fitted with the posterior margin of the right hypoplastron, and preserves the femoral/anal scute sulcus on its posteromedial corner.

Scute Pattern: Reconstruction of the plastron has revealed an interesting scute pattern that provides insights into this specimen's taxonomic identity (Figure 15). There is a sinuous midline scute margin. Intergulars are absent. The pectorals are present and extensive but are restricted to the hyoplastra and hypoplastra (not reaching the posterior entoplastron) An anal scute sulcus is not seen given the corresponding region of the xiphiplastral being missing. However, the anal scute sulcus is not found crossing from the xiphiplastra to the posteromedial region of the

hypoplastra as in Xinjiangchelyidae. The gulars may be present as faint, transverse sulci on the anteriormost epiplastra, and are most distinguishable on the anteroventral left epiplastron. The entoplastron only bears a sagittal scute sulcus separating the left and right humeral. The hyoplastra bear the humeral/pectoral and pectoral/abdominal scute sulci. On the hypoplastra, the abdominal/femoral scute boundary is present, with the abdominals partially contacting each other on the hypoplastra.

Cervical Vertebrae

Two cervical vertebra have been recovered. One of these is an indeterminate cervical vertebra, preserving a fragmented neural arch and a small fragment of the centrum (Figure 16 G-L). The neural arch is long and dorsoventrally low, and the zygapophyses are elongate. The best preserved is cervical vertebra VIII, with a weak ventral keel, anteriorly placed transverse processes, and a procoelous, ginglymoid/double articulation between CV VII and VIII. This vertebra was identified by the postzygapophyses drastically hooking downward to the level of the centrum (Figure 16 A-F). In life this would facilitate the method of shell retraction typical of cryptodires, where the eighth and last cervical must remain articulated with the first dorsal vertebra when rotating ventrally to retract the neck in the sagittal plane (Evers & Benson, 2019; Hoffstetter & Gasc, 1969). The articulation between VII and VIII is much wider than high, as in cheloniioids. The height of CV III is subequal to the length. The neurocentral sutures are unfused. These sutures allow for complete separation of the centrum and neural arch of CV VIII, and their surfaces are flat, with no interdigitation at the sutural surfaces.

Caudal Vertebrae

A single, disarticulated caudal vertebra was recovered (Figure 18). The vertebra is complete and opisthocoelous. The size of this element (only about 2mm) and the resolution of the scan obscures some detail, but the right prezygapophysis is the only missing section. Detail is lacking at the neurocentral suture, but the vertebra is complete suggesting a connected, if not, closed neurocentral suture.

Appendicular Skeleton

Scapula: The scapula is a large element, with an elongated, narrow blade (Figure 19). The distal end of the scapula and the acromion process are not preserved (Figure 19). The glenoid is shallow, meeting the articular facet for the coracoid at an obtuse angle. The scapula lacks a lamina between the scapula's dorsal process and the acromion. Unlike in Cheloniioidea, the internal angle between the acromion and scapular processes is less than 110° (Evers & Benson, 2019).

Coracoid: A single disarticulated coracoid is preserved with only the proximal and distalmost edges missing (Figure 19). The element is proximally cylindrical to ovoid in cross section, flattening into a paddle shape distally. The area preserving the contribution of the coracoid to the glenoid is missing. The length of the humerus exceeds that of the coracoid, unlike in Chenonioidea, where the opposite relationship occurs (Evers & Benson, 2019).

Humerus: One distal and two proximal humeral diaphyses are preserved. The distal epiphysis bears an elongate entepicondylar foramen, and a small capitulum, although some may be missing due to breaks (Figure 20). Of the proximal epiphyses, one is missing the humeral head and lateral process, and the other is missing both processes (Figure 20). The head is

displaced from the processes and shaft by a short neck. The preserved medial process is short and in line with the shaft.

Radius: A distal epiphysis from the radius is preserved for MOR 14891 (Figure 22 Q-T). This piece is largely uninformative but was still identifiable due to the agreement between its morphology and that of other compared turtle osteological specimens.

Ulna: Two proximal ulnae are preserved, identified by the step-like, concave articular facet seen in other turtle ulnae (Figure 22 I-L).

Ilium: In the same block as the other pelvic elements, an ilium is preserved. The ilium lacks a sutural connection to the carapace, unlike the condition seen in pleurodires (Figure 21A, 20B).

Pubis: A single, disarticulated pubis is preserved with a small, columnar lateral process seen in most turtles (excluding Cheloniioidea (Evers & Benson, 2019)) (Figure 21C, 20D). An epipubic process is not preserved and is therefore likely unossified .

Femur: The femur of MOR 14891 is known from the proximal epiphysis to the midshaft (Figure 21E-H). The femur is a very narrow element with a midshaft diameter of about 2 mm. The femoral head is large and expansive proximodistally. The femoral head is deflected laterally. The medial process is distinct, as is the lateral process but the latter is confluent with the femoral head remaining even with the proximal extent of the head. The head is distally continuous with the shaft via a ridge in capitular view, though the head meets this ridge at a constriction so a small neck is present.

Fibula: A distal epiphysis from the fibula was preserved in MOR 14891. This identification agrees with fibula morphology seen in other turtle specimens (Figure 22 A-D).

Carpals/Tarsals: Given the preservational condition of MOR 14891, the scattered limb elements are subsequently challenging to identify. This and the following paragraphs describe more distal components of the limb in MOR 14891, all of which cannot be confidently identified as forelimb or hindlimb elements. In MOR 14891, a few tentative carpals/tarsals were recovered (Figure 23).

Metapodials: Several elongate metapodials were recovered, suggesting a lengthened manus or pes perhaps typical of more aquatic taxa (Figure 23) (Zhou & Rabi, 2015).

Phalanges: A few, shorter phalanges were recovered as well, this likely indicates more distal phalanges, rather than the combination of elongate metapodial elements and shortened phalanges (Figure 23).

Unguals: The five preserved unguals are narrow and somewhat straight, extending to 3-4mm in length (Figure 23). The neurovascular grooves on either side are prominent but cannot be traced past the proximal half of the elements (Figure 23). They are somewhat triangular in cross-section with a faintly biconcave condyle for articulating with a phalanx (Figure 23).

Results

Ontogenetic Age

The unusually small body size of MOR 14891 warrants a more comprehensive evaluation of its ontogenetic age. While the preserved material for MOR 14891 is evidently diminutive,

digital reconstructions of MOR 14891 reveal an individual with a carapace length of about 15 cm, which falls within the size range for smaller “sinemydid” individuals, namely the Early Cretaceous “macrobaenid/sinemydid” taxa from Asia sensu Parham and Hutchison (2003).

In hatchling turtles, the costals appear very similar to ribs, retaining a more ovoid cross section as opposed to the broadly expanded T-shaped cross section seen in more skeletally mature turtles. In mature turtles, the costals contact each other anteroposteriorly in sequence instead of being separated by large fontanelles as in hatchlings. At least in what is preserved for MOR 14891, the anterior and posterior costals not only retain this broad T-shaped cross section but also embed in the peripherals so that costoperipheral fontanelles are absent (Figure 10). The former indicates the dermal components of the carapace have ossified unlike what is seen in the least skeletally mature turtles. An important caveat to this is the extreme levels of plasticity seen across Testudines. Not only are fontanelles throughout the shell variable in size and presence within species (from sexual dimorphism or ontogenetic variability), but their sequence of development and closure often vary at the species level, with minimal phylogenetic signal (Wyneken et al., 2008). This is especially important with the lack of a central plastral fontanelle in MOR 14891. Given the possible ontogenetic age of this specimen, this trait may offer an example of this structure being absent either very early in ontogeny or absent altogether. Few other macrobaenids are known to have this condition, regardless of size or age (e.g., *Judithemys sukhanovi*).

In modern turtles, the cross sections of the limb diaphysis undergo a general transition. The youngest juveniles have thin outer rings of cortical bone surrounding an open medullary cavity. In some cases, this medullary cavity contains trabeculae that are proportionately extremely large. Young subadults undergo a reduction in the size of their medullary cavities in exchange for

thick cortical bone, which is often penetrated by canals. Finally, the medullary cavity reopens to a larger size in old subadults and adults, filling with small trabeculae from secondary remodeling. CT scans of limb cross sections reveal an organization of the skeletal tissue where the compactness of the bone is high, but there is a lack of texture indicating arrested growth at the superficial edges of the femur. The compactness appears transitional between that of the young and old subadults, with a larger, but filled medullary cavity containing proportionately thin trabeculae and possibly some canals (Figure 26). Furthermore, the preserved epiphyses bear texture indicative of an older individual. These together suggest MOR 14891 is a relatively skeletally mature individual, perhaps a subadult, that may not have experienced a cessation in growth before death.

The specimen MOR 14891 can be more confidently included in phylogenetic analyses without confounding risked by including specimens of an early ontogenetic age, and its diagnostic characters can be applicable to other mature individuals found in the future. The suite of taxonomic characters present in this specimen, including those which defensibly would persist across ontogeny, correspond well with the macrobaenid/sinemydid grades of earlier turtles. However, characters remain that conflict with identification of MOR 14891 as a preexisting taxon from this group, warranting a new genus and species.

Phylogenetic Analysis

Bayesian methods were chosen for a modular approach to applying a substitution model for characters, and to allow for a clearer way to depict branch support without using bootstrapping, which can become artificially lower when more taxa are added (Soltis & Soltis, 2003). Furthermore, the complexity of this analysis requires calibration via tip dating and

molecular backbone, which act as priors that can inform this analysis. Finally, a new approach to the model used for this analysis may provide new insights on the phylogeny of "macrobaenids"/"sinemydids." After all, an extensive set of phylogenetic analyses using parsimony have already been done using this matrix or an older iteration of it (Evers & Benson, 2019; Menon et al., 2024; Menon & Joyce, 2025).

Previous phylogenetic analyses of turtles mentioned below have gathered many significant findings about the evolutionary history of fossil and modern turtles. Testudinata includes all tetrapods with a complete turtle shell. An exemplary immediate outgroup is the plastron-bearing but carapace-lacking *Odontochelys semitestacea*. The first branches of Testudinata include very early, but fully shelled turtles such as *Proganochelys*, *Proterochersis*, and the more transitional "mesochelydian" taxon *Kayentachelys* (Joyce 2007; Danilov and Parham, 2008; Evers and Benson 2019). Then, more crownward clades include Meiolaniiformes, exemplified by the giant insular "tortoises" bearing tailclubs and horns from as recent as historic times in Oceania (Sterli 2015). Helochelydridae, including *Naomichelys*, a contemporaneous taxon with *Microbaena*, is more crownward yet (Evers and Benson 2019). The next prominent clade is Paracryptodira, including *Compsemys*, and a lineage including Pleurosternidae (*Glyptops*) and Baenidae (Joyce et al. 2016; Evers and Benson 2019). Occasionally, analyses recover Helochelyridae in Paracryptodira (Rollot et al., 2022). Furthermore, the likely grades including Xinjiangchelyidae, Macrobaenidae, and Sinemydidae branch more crownward of Paracryptodira in most analyses (Evers & Benson 2019). Paracryptodira and these grades are contentious in their placement, with analyses nesting either or both groups outside of the crown turtle clade

Testudines, or more crownward than Pleurodires, basal to most or all of Cryptodira (Figure 1C) (Pérez-García et al., 2012; Pérez-García, 2012).

In particular, the pan-Cryptodire grades (including "Macrobaenidae/Sinemydidae") are particularly poorly resolved, despite their high sample of taxa. They likely represent a grade of evolutionary development close to that expressed by crown, modern turtle groups, which emphasizes the importance of their resolution as a clade. Namely, modern turtle lineages often include stemward representatives that ancestrally retain more plesiomorphic anatomy (such as Kinosternoidea, Trionychoidea, and Cheloniioidea) requiring independent evolution of "neochelydian" anatomical features across modern turtle taxa (Miller et al., 2024). These pan-Cryptodire grades normally fall in the following locations: immediately stemward of Testudines, the crown turtle clade consisting of Pleurodira and Cryptodira (Evers & Benson 2019); within Testudines, but only stemward of crown Cryptodira (between Cryptodira and Pleurodira (Joyce, 2007); or as a polyphyletic group with taxa both outside Cryptodira and in stem-Chelonoidea, the cryptodire sea turtle lineage (Menon et al. 2024; Menon and Joyce 2025).

For "macrobaenids/sinemydids" specifically, there is a dichotomous outcome to their phylogenetic placement in recent work. Evers and Benson (2019) typify the consensus phylogenetic placement where "Macrobaenidae/Sinemydidae" is placed immediately stemward to Testudines. A series of other works focusing on similar turtles from the Early Cretaceous of Europe highlight a second hypothesis placing at least some "macrobaenids/sinemydids" as stem-chelonioids. This is supported by more recent phylogenetic analyses from Menon et al. (2024) and Menon and Joyce (2025). These latter two utilized a modified matrix from Evers and Benson (2019) and utilize implied weighting at the same time

The presented tree reveals a grade of the earliest turtles (e.g., *Proganochelys*, *Eileanchelys*) stemward of a polytomy formed by Meiolaniiformes (*Meiolania*, *Kallokibotion*, and *Chubutemys*), Paracryptodira (pleurosternids and baenids), and a large clade containing all other turtles (Figures 24, 25). Angolachelonia (sandownids, thalassochelyids, and plesiochelyids) forms the basalmost branch of this large clade with moderate node support. Xinjiangchelyidae forms the next most basal group with strong node support, followed by a large polytomy representing "Macrobaenidae/Sinemydidae," acting as the outgroup to all modern turtes (Testudines). This polytomy is united with moderately weak node support, with four branches consisting of *Dracochelys*, a strongly supported polytomy containing the two sampled species of *Kirgizemys* and *Judithemys*, and two clades with nearly equal, moderate node support. One contains the two sampled species of *Sinemys*, and the other containing *Ordosemys* and *Microbaena*. The "macrobaenids/sinemydids" are united by the following unambiguous synapomorphies: fossa formed on the lateral surface of the supraoccipital, paired pits on the ventral surface of the parabasisphenoid, absent anteromedial process of the coronoid, vertebral scute I enters the anterior margin of the carapace, and reduced suturing between entoplastron and hyoplastra. *Microbaena* nests with *Ordosemys* due to sharing the following synapomorphies: processus trochlearis oticum primarily formed by prootic, limited to the medial portion of the skull, and an oblique, posteromedially oriented suture between the xiphiplastron and hypoplastron.

The resulting phylogeographic reconstructions suggest an Asian origin for "Macrobaenidae/Sinemydidae" (Figures 24, 25). However, the topology of the tree provides weak support for the independent incursion into North America by *Microbaena quadratosternon*

and *Judithemys sukhanovi*. Increased resolution of this region of the tree could further support a more detailed phylogeographic history of these turtles.

Discussion

Microbaena seems to fit in a unique position among these turtles when considering the two grades of "macrobaenids/sinemydids" delineated by Parham and Hutchison (2003). All other North American macrobaenids have been recovered after the Cenomanian, exemplified by the next oldest, *Aurorachelys*, from the high Arctic of Canada (Vandermark et al., 2009). All "macrobaenids/sinemydids" older than *Microbaena* are from Asia. The older, Asian taxa typify the Early Cretaceous, small bodied, sinemydid-like group while the younger, larger, North American and Asian taxa typify the other, macrobaenid-like group. *Microbaena* is a much smaller bodied, Early Cretaceous taxon occurring in North America, and may bridge the gap between these similar, but nevertheless distinct groups of turtles recognized by earlier researchers. The initial description of the faunal assemblage at BL-1 listed the tentative earliest occurrence of Chelydridae based on shell fragments. These included peripherals with pronounced upturned lips and shingling texture, where the scute margins are offset, creating a step between the regions of bone that correspond to neighboring scutes. Additionally, these shell fragments exhibited plications, fine parallel ridges running sagittally or parasagittally along the carapace. All these traits are found in the carapace of MOR 14891. Furthermore, inspection of the referred chelydrid material from this site revealed that these shell fragments were the same size as those found in MOR 14891. Given the comprehensive agreement of the diagnostic features between these specimens, the previously described fragments are hypothesized to represent a second individual of this taxon, therefore representing "macrobaenid" shell material instead of chelydrid.

While macrobaenids and chelydroids share many convergent traits, some notable characteristics distinguish the two groups. Unlike macrobaenids, chelydroids ubiquitously lack carotid fenestrae, lack pectoral scutes (some fossil taxa may be an exception), and bear costiform processes on the nuchal that form articulations with the first peripherals (Joyce et al. 2021). Larger elements matching MOR 14891 in appearance have not been recovered from BL-1, supporting the notion that MOR 14891 is a more skeletally mature individual. The assignment of these first shell fragments to "Macrobaenidae/Sinemydidae" allow for a more parsimonious divergence time for Pan-Chelydridae and Chelydroidea. With the exception of fragmentary Santonian material referred to Pan-Chelydridae, no taxa from these latter two groups have been demonstrated to occur before the Campanian (Joyce, 2016; Joyce & Bourque, 2016).

The stark contrast between the completeness of MOR 14891 and other BL-1 fossils still raises questions regarding its taphonomy. One possible hypothesis accounting for this difference in preservation is that MOR 14891 is a coprolite containing turtle material. The resolution of current CT data complicates the detection of gastric etching or other features associated with ingestion.

Conclusion

The discovery of *Microbaena* from the Ullmann microsite (BL-1) of the Cenomanian Albian Blackleaf Formation in Montana has provided a more thorough reconstruction of the morphology, interrelationships, and ecology of Mesozoic turtles. Morphological features related to the internal carotid artery canals and parabasisphenoid suggest this specimen represents a new member of "Macrobaenidae." The skull shares carotid fenestrae and paired pits on the

parabasisphenoid with “Macrobaenidae/Sinemydidae,” and uniquely these paired pits are highly reduced. Additionally, this turtle has an apomorphic, squared anterior plastron, formed by large, elongate epiplastra.

This specimen likely represents one of the smallest and most complete mid-Cretaceous North American turtle fossils found, representing an individual with a carapace length of about 15 cm. *Microbaena* has a flat cranium and shell, long metapodials, and dentary morphology suggestive of a more aquatic taxon. Namely, the shape of the triturating surface of the dentary suggests a molluscivorous diet (Joyce 2016). Overall, these traits fit well with the aquatic depositional environment this specimen was discovered in. Matching texture on the carapace of *Microbaena* indicates that this taxon is likely the same as the producer of the shell material referred to Chelydridae by Ullmann et al. (2012). The discovery of MOR 14891 is important in that it is the only substantially complete body fossil from BL-1, and is one of three named taxa from the Blackleaf Formation. North American “macrobaenids” are otherwise only known from after the Cenomanian, making *Microbaena* the oldest of these currently known by about 8-9 myr. *Microbaena* not only supplements the known faunal assemblage of the Blackleaf Formation but also has unique phylogenetic and biogeographic significance. This study’s Bayesian phylogenetic analysis places MOR 14891 within a clade of “macrobaenids/sinemydids” branching just stemward of Testudines. MOR 14891 falls in a polytomy with other “macrobaenids”/ “sinemydids”, with moderate node support. More specifically, MOR 14891 plots as a sister taxon to *Ordosemys* with similarly moderate node support. Given this similarity to *Ordosemys* relative to *Judithemys*, phylogeographic reconstructions suggest independent migrations from Asia to North America for *Microbaena* and *Judithemys*.

Hopefully, a large sample size of more complete and articulated specimens can provide more refined insight into the anatomy and biology of this taxon and in turn, the mysterious "macrobaenids"/"sinemydids." Combining these conclusions with a more comprehensive approach and sample size in future studies can yield further invaluable data on the development of middle Cretaceous vertebrate clades and ecosystems. Despite its size, this specimen is one of the most complete North American turtle fossils of its time, which suggests a greater possibility of discovering similar specimens than previously thought. In turn, the nature of middle Cretaceous formations of North America can further uncover the evolution of life in this pivotal time and region than previously thought.

Unlike many common Mesozoic turtle fossils, *Microbaena* offers insight into the evolution of turtles in North America in a manner far more expansive than initially expected. "Macrobaenids"/ "sinemydids" have escaped phylogenetic resolution for six decades, with taxa spanning across an entire hemisphere for most of the Mesozoic and part of the Cenozoic for "macrobaenids." A phylogenetic problem of this magnitude requires numerous steps to solve, including increasing the sample of known taxa. Searching for more fossil turtles such as *Microbaena* in middle Cretaceous deposits of North America is a likely step to return further significant findings that can clarify not only the faunal assemblages of the middle Cretaceous of Laramidia, but also the origin and evolution of the enigmatic turtles near the origin of some if not, all modern Testudines.

References

Avrahami, H. M. (2018). *Paleobiodiversity of a New Microvertebrate Locality from the Upper Cretaceous Mussentuchit Member, Cedar Mountain Formation, Utah: Testing Morphometric Multivariate Approaches for Quantifying Shape Variation in Microvertebrate Specimens*.

Bhat, M. S., & Cullen, T. M. (2025). Growth and life history of freshwater chelydrid turtles (Testudines: Cryptodira): A bone histological approach. *Journal of Anatomy*, *247*(3–4), 518–541.

Bonde, J. W. (2008). *Paleoecology and taphonomy of the willow tank formation (albian), southern Nevada*.

Botha, A. E. (2017). Comparative bone histology of Stigmochelys pardalis (leopard tortoise), with specific reference to ontogeny and biomechanics.

Cifelli, R. L., Nydam, R. L., & Eaton, J. G. (1999). MOUNTAIN FORMATION, EMERY COUNTY, UTAH: THE MUSSENTUCHIT LOCAL FAUNA. *Vertebrate Paleontology in Utah*, *99*(1), 219.

Clark, B., Prall, J., Hannebaum, Z. J., Orme, D. A., Panascí, G., & Varricchio, D. J. (2025). The earliest dated Basilemys (Testudines, Nanhsiungchelyidae) in North America informs polar dispersal during middle Cretaceous Hothouse conditions. *Historical Biology*, 1–8.

Danilov, I. G., & Parham, J. F. (2008). A reassessment of some poorly known turtles from the Middle Jurassic of China, with comments on the antiquity of extant turtles. *Journal of Vertebrate Paleontology*, *28*(2), 306–318.

Dyman, T. S., & Nichols, D. J. (1988). *Stratigraphy of mid-Cretaceous Blackleaf and lower part of the Frontier Formations in parts of Beaverhead and Madison Counties, Montana* (Issue 1773). US Government Printing Office.

Ehret, D. J. (2007). *Skeletochronology: A method for determing the individual age and growth of modern and fossil tortoises (Reptilia: Testudines)*. Florida Museum of Natural History.

Evers, S. W., & Benson, R. B. (2019). A new phylogenetic hypothesis of turtles with implications for the timing and number of evolutionary transitions to marine lifestyles in the group. *Palaeontology*, *62*(1), 93–134.

Evers, S. W., Ponstein, J., Jansen, M. A., Gray, J. A., & Froebisch, J. (2023). A systematic compendium of turtle mandibular anatomy using digital dissections of soft tissue and osteology. *The Anatomical Record*, *306*(6), 1228–1303.

Fedorov, A., Beichel, R., Kalpathy-Cramer, J., Finet, J., Fillion-Robin, J.-C., Pujol, S., Bauer, C., Jennings, D., Fennessy, F., & Sonka, M. (2012). 3D Slicer as an image computing platform for the Quantitative Imaging Network. *Magnetic Resonance Imaging*, *30*(9), 1323–1341.

Gaffney, E. S. (1979). *Comparative cranial morphology of Recent and fossil turtles. Bulletin of the AMNH; v. 164, article 2*.

Gentry, A. D., Kiernan, C. R., & Parham, J. F. (2023). A large non-marine turtle from the Upper Cretaceous of Alabama and a review of North American "Macrobaenids." *The Anatomical Record*, *306*(6), 1411–1430.

Goldberg, P. (2000). *Faunal composition, non-marine vertebrates, of the upper Cedar Mountain Formation (Cretaceous: Albian-Cenomanian), central Utah*. The University of Oklahoma.

Herzog, L. L. (2019). *Morphological characteristics and variability of helochelydrid turtles in North America: Evidence for a new species*.

Hipsley, C. A., Aguilar, R., Black, J. R., & Hocknull, S. A. (2020). High-throughput microCT scanning of small specimens: Preparation, packing, parameters and post-processing. *Scientific Reports*, *10*(1), 13863.

Hoffstetter, R., & Gasc, J. P. (1969). Vertebrae and ribs of modern reptiles. In *Biology of the Reptilia* (Vol. 1, pp. 201–310). Academic Press.

Joyce, W. G. (2007). Phylogenetic relationships of Mesozoic turtles. *Bulletin of the Peabody Museum of Natural History*, *48*(1), 3–102.

Joyce, W. G. (2016). A review of the fossil record of turtles of the clade Pan-Chelydridae. *Bulletin of the Peabody Museum of Natural History*, *57*(1), 21–56.

Joyce, W. G., Parham, J. F., & Gauthier, J. A. (2004). Developing a protocol for the conversion of rank-based taxon names to phylogenetically defined clade names, as exemplified by turtles. *Journal of Paleontology*, *78*(5), 989-1013.

Joyce, W. G., Anquetin, J., Cadena, E.-A., Claude, J., Danilov, I. G., Evers, S. W., Ferreira, G. S., Gentry, A. D., Georgalis, G. L., & Lyson, T. R. (2021). A nomenclature for fossil and living turtles using phylogenetically defined clade names. *Swiss Journal of Palaeontology*, *140*(1), 5.

Joyce, W. G., & Bourque, J. R. (2016). A review of the fossil record of turtles of the clade Pan-Kinosternoidea. *Bulletin of the Peabody Museum of Natural History*, *57*(1), 57–95.

Joyce, W. G., Landréat, J., & Rollot, Y. (2023). A pan-chelydrid, Chelydropsis aubasi sp. Nov., from the middle Eocene (MP 15, early Bartonian) of Chéry-Chartreuve, France. *The Anatomical Record*, *306*(6), 1465–1480.

Joyce, W. G., Lyson, T. R., & Kirkland, J. I. (2016). An early bothremydid (Testudines, Pleurodira) from the Late Cretaceous (Cenomanian) of Utah, North America. *PeerJ*, *4*, e2502.

Joyce, W. G., Parham, J. F., Lyson, T. R., Warnock, R. C., & Donoghue, P. C. (2013). A divergence dating analysis of turtles using fossil calibrations: An example of best practices. *Journal of Paleontology*, *87*(4), 612–634.

Joyce, W. G., Sterli, J., & Chapman, S. D. (2014). The skeletal morphology of the solemydid turtle Naomichelys speciosa from the Early Cretaceous of Texas. *Journal of Paleontology*, *88*(6), 1257–1287.

Klein, I. T. (1760). Klassification und kurze Geschichte der Vierfüßigen Thiere (translation by FD Behn). *Jonas Schmidt, Lübeck*.

Krumenacker, L. (2020). Paleontological and chronostratigraphic correlations of the mid-Cretaceous Wayan-Vaughn depositional system of southwestern Montana and southeastern Idaho. *Historical Biology*.

Laurenti, J. N., & Marherr, P. A. (1768). *[Specimen Medicum, Exhibens Synopsin Reptilium Emendatam Cum Experimentis Circa Venena Et Antidota Reptilium Austriacorum]; Josephi Nicolai Laurenti Austriaci Viennensis Specimen Medicum, Exhibens Synopsin Reptilium Emendatam Cum Experimentis Circa Venena Et Antidota Reptilium Austriacorum: Quod Authoritate Et Consensu... Universitatis Rectoris;... Universitatis Cancellarii;... Domini Præsidis;... Pro Summa In Medicina Laurea Eique Annexis Juribus Ac Privilegiis Rite Consequendis Publicæ Disquisition*. Joan. Thoma Trattner.

Lawver, D. R., & Jackson, F. D. (2014). A review of the fossil record of turtle reproduction: Eggs, embryos, nests and copulating pairs. *Bulletin of the Peabody Museum of Natural History*, *55*(2), 215–236.

Menon, J. C., Brinkman, D. B., Hermanson, G., Joyce, W. G., & Evers, S. W. (2024). New insights into the early morphological evolution of sea turtles by re-investigation of Nichollsemys baieri, a three-dimensionally preserved fossil stem chelonioid from the Campanian of Alberta, Canada. *Swiss Journal of Palaeontology*, *143*(1), 27.

Menon, J. C., & Joyce, W. G. (2025). A redescription of Glyptochelone suyckerbuykii (Ubaghs, 1879), an enigmatic fossil sea turtle (Chelonioidea) from the Maastrichtian of the Netherlands and Belgium, sheds new light on fossil sea turtle shell variation and neural bone homology: Menon and Joyce. *Swiss Journal of Palaeontology*, *144*(1), 62.

MEYLAN, P. A., & STERRER, W. (2000). Hesperotestudo (Testudines: Testudinidae) from the Pleistocene of Bermuda, with comments on the phylogenetic position of the genus. *Zoological Journal of the Linnean Society*, *128*(1), 51–76.

Miller, E., Lee, H. W., Abzhanov, A., & Evers, S. W. (2024). The topological organization of the turtle cranium is constrained and conserved over long evolutionary timescales. *The Anatomical Record*, *307*(8), 2713–2748.

Mlynarski, M. (1976). *Testudines*.

Object Research Systems. (2024). *Dragonfly* (Version 2024.1) [Computer software]. https://dragonfly.comet.tech/

Parham, J. F., & Hutchison, J. H. (2003). A new eucryptodiran turtle from the late cretaceous of North America (Dinosaur Provincial Park, Alberta, Canada). *Journal of Vertebrate Paleontology*, *23*(4), 783–798.

Paulina-Carabajal, A., Sterli, J., & Werneburg, I. (2019). The endocranial anatomy of the stem turtle Naomichelys speciosa from the Early Cretaceous of North America. *Acta Palaeontologica Polonica*, *64*(4).

Pereira, A. G., Sterli, J., Moreira, F. R., & Schrago, C. G. (2017). Multilocus phylogeny and statistical biogeography clarify the evolutionary history of major lineages of turtles. *Molecular Phylogenetics and Evolution*, *113*, 59–66.

Pérez-García, A. (2012). The European Early Cretaceous cryptodiran turtle Chitracephalus dumonii and the diversity of a poorly known lineage of turtles. *Acta Palaeontologica Polonica*, *57*(3), 575–588.

PÉREZ-GARCÍA, A., DE LA FUENTE, M. S., & ORTEGA, F. (2012). Hoyasemys jimenezi gen. Et sp. Nov., a freshwater basal eucryptodiran turtle from the Lower Cretaceous of Spain. *Acta Palaeontologica Polonica*.

Peters, S. E., & McClennen, M. (2016). The Paleobiology Database application programming interface. *Paleobiology*, *42*(1), 1–7.

Rabi, M. (2014). *New Insights into the Origin and Phylogeny of Cryptodiran Turtles Based on Key Fossil Taxa from the Mesozoic of Asia*.

Rabi, M., Sukhanov, V. B., Egorova, V. N., Danilov, I., & Joyce, W. G. (2014). Osteology, relationships, and ecology of Annemys (Testudines, Eucryptodira) from the Late Jurassic of Shar Teg, Mongolia, and phylogenetic definitions for Xinjiangchelyidae, Sinemydidae, and Macrobaenidae. *Journal of Vertebrate Paleontology*, *34*(2), 327–352.

Raselli, I. (2018). Comparative cranial morphology of the Late Cretaceous protostegid sea turtle Desmatochelys lowii. *PeerJ*, *6*, e5964.

Rollot, Y., Evers, S. W., Pierce, S. E., & Joyce, W. G. (2022). Cranial osteology, taxonomic reassessment, and phylogenetic relationships of the Early Cretaceous (Aptian-Albian) turtle Trinitichelys hiatti (Paracryptodira). *PeerJ*, *10*, e14138.

Ronquist, F., Huelsenbeck, J., & Teslenko, M. (2019). Draft MrBayes version 3.2 manual: Tutorials and model summaries. *Distributed with the Software from Http://Brahms. Biology. Rochester. Edu/Software. Html*, 1–105.

Ronquist, F., Teslenko, M., Van Der Mark, P., Ayres, D. L., Darling, A., Höhna, S., Larget, B., Liu, L., Suchard, M. A., & Huelsenbeck, J. P. (2012). MrBayes 3.2: Efficient Bayesian phylogenetic inference and model choice across a large model space. *Systematic Biology*, *61*(3), 539–542.

Scheyer, T. M., & Cerda, I. A. (2021). Testudines. In *Vertebrate skeletal histology and paleohistology* (pp. 385–398). CRC Press.

Soltis, P. S., & Soltis, D. E. (2003). Applying the bootstrap in phylogeny reconstruction. *Statistical Science*, 256–267.

Sterli, J. (2015). A review of the fossil record of Gondwanan turtles of the clade Meiolaniformes. *Bulletin of the Peabody Museum of Natural History*, *56*(1), 21-45.

Suarez, C. A., González, L. A., Ludvigson, G. A., Cifelli, R. L., & Tremain, E. (2012). Water utilization of the Cretaceous Mussentuchit Member local vertebrate fauna, Cedar Mountain Formation, Utah, USA: using oxygen isotopic composition of phosphate. *Palaeogeography, Palaeoclimatology, Palaeoecology*, *313*, 78–92.

Sukhanov, V. B. (1964). Subclass Testudinata, Testudinates. In J. A. Orlov (Ed.), *Fundamentals of Palaeontology. Amphibians, reptiles and birds* (pp. 354–438).

Tatarinov, L. (1959). A new turtle of the family Baenidae from the lower Eocene of Mongolia. *Paleontologicheskii Zhurnal*, *1*, 100–113.

Tong, H., & Brinkman, D. (2013). A new species of Sinemys (Testudines: Cryptodira: Sinemydidae) from the Early Cretaceous of Inner Mongolia, China. *Palaeobiodiversity and Palaeoenvironments*, *93*(3), 355–366.

TTWG (Rhodin, A. G. K., J. B. Iverson, R. Bour, U. Fritz, A. Georges, and H. B. Shaffer). 2021. Turtles of the World Annotated Checklist and Atlas of Taxonomy, Synonymy, Distribution, and Conservation Status (9th Ed.). Chelonian Research Monographs 8: 1–472. DOI:10.3854/crm.8.checklist.atlas. v9.2021.

Ullmann, P. V., Varricchio, D., & Knell, M. J. (2012). Taphonomy and taxonomy of a vertebrate microsite in the mid-Cretaceous (Albian–Cenomanian) Blackleaf Formation, southwest Montana. *Historical Biology*, *24*(3), 311–328.

Vandermark, D., Tarduno, J. A., Brinkman, D. B., Cottrell, R. D., & Mason, S. (2009). New Late Cretaceous macrobaenid turtle with Asian affinities from the High Canadian Arctic: Dispersal via ice-free polar routes. *Geology*, *37*(2), 183–186.

Varricchio, D. J., Martin, A. J., & Katsura, Y. (2007). First trace and body fossil evidence of a burrowing, denning dinosaur. *Proceedings of the Royal Society B: biological sciences*, *274*(1616), 1361-1368.

Wyneken, J., Godfrey, M. H., & Bels, V. (Eds.). (2007). *Biology of turtles: from structures to strategies of life*. CRC press.

Zhou, C.-F., & Rabi, M. (2015). A sinemydid turtle from the Jehol Biota provides insights into the basal divergence of crown turtles. *Scientific Reports*, *5*(1), 16299.

CHAPTER THREE

CONCLUSION

The discovery of *Microbaena* from the Ullmann microsite (BL-1) of the Cenomanian Albian Blackleaf Formation in Montana has provided a more thorough reconstruction of the morphology, interrelationships, and ecology of Mesozoic turtles. Morphological features related to the internal carotid artery canals and parabasisphenoid suggest this specimen represents a new member of "Macrobaenidae." The skull shares carotid fenestrae and paired pits on the parabasisphenoid with "Macrobaenidae/Sinemydidae," and uniquely these paired pits are highly reduced. Additionally, this turtle has an apomorphic, squared anterior plastron, formed by large, elongate epiplastra. North American "macrobaenids" are otherwise only known from after the Cenomanian, making *Microbaena* the oldest of these currently known. *Microbaena* not only supplements the known faunal assemblage of the Blackleaf Formation but also has unique phylogenetic and biogeographic significance. This specimen likely represents one of the smallest and most complete mid-Cretaceous North American turtle fossils found, representing an individual with a carapace length of about 15 cm. This study's Bayesian phylogenetic analysis places MOR 14891 within a clade of "macrobaenids/sinemydids" branching just stemward of Testudines. MOR 14891 falls in a polytomy with other "macrobaenids"/sinemydids", with moderate node support. More specifically, MOR 14891 plots as a sister taxon to the "macrobaenid" *Ordosemys* with similarly moderate node support. Like *Microbaena*, *Ordosemys* has a convex ventral margin of the jugal, and a processus trochlearis oticum primarily formed by the prootic.

Microbaena acts as yet another sample of the enigmatic "Macrobaenidae," providing phylogenetic significance and insight into the suite of characters expressed in this group. The fenestra caroticus is a ubiquitous structure in these early turtles (Macrobaenidae, XInjiangchelyidae, Sinemydidae), and has seldom been reported with close-up, high resolution images or scans. Further research exploring this structure could focus on the topology of the fenestrae caroticus relative to other elements in the basicranium, comparative anatomy of the pathways formed by the internal carotid arteries in fossil turtles, and how the thickness of the basicranium correlates to expression of the fenestrae caroticus (W.G.J., pers. comm). Additionally, the braincase of MOR 14891 offers a rich source of characters that can inform further phylogenetic analyses of these turtles. Additional, more detailed segmentation of this region is an ideal next step in revealing the full suite of anatomical features found in this unique turtle.

To supplement these findings, redescriptions of "macrobaenids," "sinemydids," and xinjiangchelyids via CT scanning would prove invaluable in providing context for the importance of these characters at a pivotal point in the evolution of modern turtles, along with their relevance to those found in *Microbaena*. Promising candidates for redescription include *Judithemys* and *Ordosemys*. Eventually, redescribing *Macrobaena* would be a lofty, but ideal next step in resolving the enigmatic origins and phylogeny of "Macrobaenidae." The taxonomic history of this genus renders *Macrobaena* as the internal specifier for the family, making future phylogenetic analyses including this taxon highly valuable in deciphering the interrelationships of these unusual turtles. Overall, redescription of these taxa are of significantly higher value compared to other turtles because of their lack of phylogenetic resolution. For example, the

placement of “macrobaenids” in phylogenetic trees is far more sensitive to changes in character coding brought by redescription. This can prove especially valuable in future studies, considering that “macrobaenids” have been hypothesized to be basal to either chelydrids (snapping turtles) or chelonioids (sea turtles). Overall, further exploration of “macrobaenids” in the field (additional discoveries of middle Cretaceous fossils) or via redescriptions of well-preserved specimens (emphasizing cranial vasculature and internal cranial anatomy) is needed to resolve the origins, proliferation, and evolutionary fate of this enigmatic group of turtles.

Hopefully, a large sample size of more complete and articulated specimens can provide more refined insight into the anatomy and biology of this taxon and in turn, the mysterious “macrobaenids”/”sinemydids.” Combining these conclusions with a more comprehensive approach and sample size in future studies can yield further invaluable data on the development of middle Cretaceous vertebrate clades and ecosystems. Despite its size, this specimen is one of the most complete North American turtle fossils of its time, which suggests a greater possibility of discovering similar specimens than previously thought. In turn, the nature of middle Cretaceous formations of North America can further uncover the evolution of life in this pivotal time and region than previously thought.

Unlike many common Mesozoic turtle fossils, *Microbaena* offers insight into the evolution of turtles in North America in a manner far more expansive than initially expected. “Macrobaenids”/”sinemydids” have escaped phylogenetic resolution for six decades, with taxa spanning across an entire hemisphere for most of the Mesozoic and part of the Cenozoic for “macrobaenids.” A phylogenetic problem of this magnitude requires numerous steps to solve, including increasing the sample of known taxa. Searching for more fossil turtles such as

Microbaena in middle Cretaceous deposits of North America is a likely step towards further significant findings that can clarify not only the faunal assemblages of the middle Cretaceous of Laramidia, but also the origin and evolution of the enigmatic turtles diverging just earlier than some if not, all modern Testudines.

REFERENCES CITED

Allen, H. J., Wilberg, E. W., Turner, A. H., & Varricchio, D. J. (2025). A new, diminutive, heterodont neosuchian from the Vaughn Member of the Blackleaf Formation (Cenomanian), southwest Montana, and implications for the paleoecology of heterodont neosuchians. Journal of Vertebrate Paleontology, 45(2), e2542185.

Avrahami, H. M. (2018). *Paleobiodiversity of a New Microvertebrate Locality from the Upper Cretaceous Mussentuchit Member, Cedar Mountain Formation, Utah: Testing Morphometric Multivariate Approaches for Quantifying Shape Variation in Microvertebrate Specimens*.

Bhat, M. S., & Cullen, T. M. (2025). Growth and life history of freshwater chelydrid turtles (Testudines: Cryptodira): A bone histological approach. *Journal of Anatomy*, *247*(3–4), 518–541.

Bonde, J. W. (2008). *Paleoecology and taphonomy of the willow tank formation (albian), southern Nevada*.

Botha, A. E. (2017). Comparative bone histology of Stigmochelys pardalis (leopard tortoise), with specific reference to ontogeny and biomechanics.

Brinkman, D. B., Densmore, M. J., & Joyce, W. G. (2010). “Macrobaenidae”(Testudines: Eucryptodira) from the late Paleocene (Clarkforkian) of Montana and the taxonomic treatment of “Clemmys” backmani. Bulletin of the Peabody Museum of Natural History, 51(2), 147–155.

Cifelli, R. L., Nydam, R. L., & Eaton, J. G. (1999). MOUNTAIN FORMATION, EMERY COUNTY, UTAH: THE MUSSENTUCHIT LOCAL FAUNA. *Vertebrate Paleontology in Utah*, *99*(1), 219.

Clark, B., Prall, J., Hannebaum, Z. J., Orme, D. A., Panascí, G., & Varricchio, D. J. (2025). The earliest dated Basilemys (Testudines, Nanhsiungchelyidae) in North America informs polar dispersal during middle Cretaceous Hothouse conditions. *Historical Biology*, 1–8.

Danilov, I. G., & Parham, J. F. (2008). A reassessment of some poorly known turtles from the Middle Jurassic of China, with comments on the antiquity of extant turtles. *Journal of Vertebrate Paleontology*, *28*(2), 306–318.

Dyman, T. S., & Nichols, D. J. (1988). *Stratigraphy of mid-Cretaceous Blackleaf and lower part of the Frontier Formations in parts of Beaverhead and Madison Counties, Montana* (Issue 1773). US Government Printing Office.

Ehret, D. J. (2007). *Skeletochronology: A method for determing the individual age and growth of modern and fossil tortoises (Reptilia: Testudines)*. Florida Museum of Natural History.

Evers, S. W., & Benson, R. B. (2019). A new phylogenetic hypothesis of turtles with implications for the timing and number of evolutionary transitions to marine lifestyles in the group. *Palaeontology*, *62*(1), 93–134.

Evers, S. W., Ponstein, J., Jansen, M. A., Gray, J. A., & Froebisch, J. (2023). A systematic compendium of turtle mandibular anatomy using digital dissections of soft tissue and osteology. *The Anatomical Record*, *306*(6), 1228–1303.

Fedorov, A., Beichel, R., Kalpathy-Cramer, J., Finet, J., Fillion-Robin, J.-C., Pujol, S., Bauer, C., Jennings, D., Fennessy, F., & Sonka, M. (2012). 3D Slicer as an image computing platform for the Quantitative Imaging Network. *Magnetic Resonance Imaging*, *30*(9), 1323–1341.

Gaffney, E. S. (1979). *Comparative cranial morphology of Recent and fossil turtles. Bulletin of the AMNH; v. 164, article 2*.

Gentry, A. D., Kiernan, C. R., & Parham, J. F. (2023). A large non-marine turtle from the Upper Cretaceous of Alabama and a review of North American "Macrobaenids." *The Anatomical Record*, *306*(6), 1411–1430.

Goldberg, P. (2000). *Faunal composition, non-marine vertebrates, of the upper Cedar Mountain Formation (Cretaceous: Albian-Cenomanian), central Utah*. The University of Oklahoma.

Herzog, L. L. (2019). *Morphological characteristics and variability of helochelydrid turtles in North America: Evidence for a new species*.

Hipsley, C. A., Aguilar, R., Black, J. R., & Hocknull, S. A. (2020). High-throughput microCT scanning of small specimens: Preparation, packing, parameters and post-processing. *Scientific Reports*, *10*(1), 13863.

Hoffstetter, R., & Gasc, J. P. (1969). Vertebrae and ribs of modern reptiles. In *Biology of the Reptilia* (Vol. 1, pp. 201–310). Academic Press.

Joyce, W. G. (2007). Phylogenetic relationships of Mesozoic turtles. *Bulletin of the Peabody Museum of Natural History*, *48*(1), 3–102.

Joyce, W. G. (2016). A review of the fossil record of turtles of the clade Pan-Chelydridae. *Bulletin of the Peabody Museum of Natural History*, *57*(1), 21–56.

Joyce, W. G. (2017). A review of the fossil record of basal Mesozoic turtles. Bulletin of the Peabody Museum of Natural History, 58(1), 65–113.

Joyce, W. G., Parham, J. F., & Gauthier, J. A. (2004). Developing a protocol for the conversion of rank-based taxon names to phylogenetically defined clade names, as exemplified by turtles. *Journal of Paleontology*, *78*(5), 989-1013.

Joyce, W. G., & Anquetin, J. (2019). A review of the fossil record of nonbaenid turtles of the clade Paracryptodira. Bulletin of the Peabody Museum of Natural History, 60(2), 129–155.

Joyce, W. G., Anquetin, J., Cadena, E.-A., Claude, J., Danilov, I. G., Evers, S. W., Ferreira, G. S., Gentry, A. D., Georgalis, G. L., & Lyson, T. R. (2021). A nomenclature for fossil and living turtles using phylogenetically defined clade names. *Swiss Journal of Palaeontology*, *140*(1), 5.

Joyce, W. G., & Bourque, J. R. (2016). A review of the fossil record of turtles of the clade Pan-Kinosternoidea. *Bulletin of the Peabody Museum of Natural History*, *57*(1), 57–95.

Joyce, W. G., Landréat, J., & Rollot, Y. (2023). A pan-chelydrid, Chelydropsis aubasi sp. Nov., from the middle Eocene (MP 15, early Bartonian) of Chéry-Chartreuve, France. *The Anatomical Record*, *306*(6), 1465–1480.

Joyce, W. G., & Lyson, T. R. (2015). A review of the fossil record of turtles of the clade Baenidae. Bulletin of the Peabody Museum of Natural History, 56(2), 147–183.

Joyce, W. G., Lyson, T. R., & Kirkland, J. I. (2016). An early bothremydid (Testudines, Pleurodira) from the Late Cretaceous (Cenomanian) of Utah, North America. *PeerJ*, *4*, e2502.

Joyce, W. G., Parham, J. F., Lyson, T. R., Warnock, R. C., & Donoghue, P. C. (2013). A divergence dating analysis of turtles using fossil calibrations: An example of best practices. *Journal of Paleontology*, *87*(4), 612–634.

Joyce, W. G., Sterli, J., & Chapman, S. D. (2014). The skeletal morphology of the solemydid turtle Naomichelys speciosa from the Early Cretaceous of Texas. *Journal of Paleontology*, *88*(6), 1257–1287.

Klein, I. T. (1760). Klassification und kurze Geschichte der Vierfüßigen Thiere (translation by FD Behn). *Jonas Schmidt, Lübeck*.

Knell, M. J. (2012). Taphonomic and biostratigraphic analysis of fossil freshwater turtles in the Upper Cretaceous (Campanian) Kaiparowits Formation of southern Utah, USA. Montana State University.

Krumenacker, L. (2020). Paleontological and chronostratigraphic correlations of the mid-Cretaceous Wayan-Vaughn depositional system of southwestern Montana and southeastern Idaho. *Historical Biology*.

Laurenti, J. N., & Marherr, P. A. (1768). *[Specimen Medicum, Exhibens Synopsin Reptilium Emendatam Cum Experimentis Circa Venena Et Antidota Reptilium Austriacorum]; Josephi Nicolai Laurenti Austriaci Viennensis Specimen Medicum, Exhibens Synopsin Reptilium Emendatam Cum Experimentis Circa Venena Et Antidota Reptilium*

Austriacorum: Quod Authoritate Et Consensu... Universitatis Rectoris;... Universitatis Cancellarii;... Domini Præsidis;... Pro Summa In Medicina Laurea Eique Annexis Juribus Ac Privilegiis Rite Consequendis Publicæ Disquisition. Joan. Thoma Trattner.

Lawver, D. R., & Jackson, F. D. (2014). A review of the fossil record of turtle reproduction: Eggs, embryos, nests and copulating pairs. *Bulletin of the Peabody Museum of Natural History*, *55*(2), 215–236.

Menon, J. C., Brinkman, D. B., Hermanson, G., Joyce, W. G., & Evers, S. W. (2024). New insights into the early morphological evolution of sea turtles by re-investigation of Nichollsemys baieri, a three-dimensionally preserved fossil stem chelonioid from the Campanian of Alberta, Canada. *Swiss Journal of Palaeontology*, *143*(1), 27.

Menon, J. C., & Joyce, W. G. (2025). A redescription of Glyptochelone suyckerbuykii (Ubaghs, 1879), an enigmatic fossil sea turtle (Chelonioidea) from the Maastrichtian of the Netherlands and Belgium, sheds new light on fossil sea turtle shell variation and neural bone homology: Menon and Joyce. *Swiss Journal of Palaeontology*, *144*(1), 62.

MEYLAN, P. A., & STERRER, W. (2000). Hesperotestudo (Testudines: Testudinidae) from the Pleistocene of Bermuda, with comments on the phylogenetic position of the genus. *Zoological Journal of the Linnean Society*, *128*(1), 51–76.

Miller, E., Lee, H. W., Abzhanov, A., & Evers, S. W. (2024). The topological organization of the turtle cranium is constrained and conserved over long evolutionary timescales. *The Anatomical Record*, *307*(8), 2713–2748.

Mlynarski, M. (1976). *Testudines*.

Object Research Systems. (2024). *Dragonfly* (Version 2024.1) [Computer software]. https://dragonfly.comet.tech/

Parham, J. F., & Hutchison, J. H. (2003). A new eucryptodiran turtle from the late cretaceous of North America (Dinosaur Provincial Park, Alberta, Canada). *Journal of Vertebrate Paleontology*, *23*(4), 783–798.

Paulina-Carabajal, A., Sterli, J., & Werneburg, I. (2019). The endocranial anatomy of the stem turtle Naomichelys speciosa from the Early Cretaceous of North America. *Acta Palaeontologica Polonica*, *64*(4).

Pereira, A. G., Sterli, J., Moreira, F. R., & Schrago, C. G. (2017). Multilocus phylogeny and statistical biogeography clarify the evolutionary history of major lineages of turtles. *Molecular Phylogenetics and Evolution*, *113*, 59–66.

Pérez-García, A. (2012). The European Early Cretaceous cryptodiran turtle Chitracephalus dumonii and the diversity of a poorly known lineage of turtles. *Acta Palaeontologica Polonica*, *57*(3), 575–588.

Pérez-GarcÍa, A. (2020). A European Cenozoic ‘macrobaenid:’new data about the Paleocene arrival of several turtle lineages to Europe. Journal of Vertebrate Paleontology, 40(4), e1795874.

PÉREZ-GARCÍA, A., DE LA FUENTE, M. S., & ORTEGA, F. (2012). Hoyasemys jimenezi gen. Et sp. Nov., a freshwater basal eucryptodiran turtle from the Lower Cretaceous of Spain. *Acta Palaeontologica Polonica*.

Peters, S. E., & McClennen, M. (2016). The Paleobiology Database application programming interface. *Paleobiology*, *42*(1), 1–7.

Rabi, M. (2014). *New Insights into the Origin and Phylogeny of Cryptodiran Turtles Based on Key Fossil Taxa from the Mesozoic of Asia*.

Rabi, M., Sukhanov, V. B., Egorova, V. N., Danilov, I., & Joyce, W. G. (2014). Osteology, relationships, and ecology of Annemys (Testudines, Eucryptodira) from the Late Jurassic of Shar Teg, Mongolia, and phylogenetic definitions for Xinjiangchelyidae, Sinemydidae, and Macrobaenidae. *Journal of Vertebrate Paleontology*, *34*(2), 327–352.

Raselli, I. (2018). Comparative cranial morphology of the Late Cretaceous protostegid sea turtle Desmatochelys lowii. *PeerJ*, *6*, e5964.

Rollot, Y., Evers, S. W., Pierce, S. E., & Joyce, W. G. (2022). Cranial osteology, taxonomic reassessment, and phylogenetic relationships of the Early Cretaceous (Aptian-Albian) turtle Trinitichelys hiatti (Paracryptodira). *PeerJ*, *10*, e14138.

Ronquist, F., Huelsenbeck, J., & Teslenko, M. (2019). Draft MrBayes version 3.2 manual: Tutorials and model summaries. *Distributed with the Software from Http://Brahms. Biology. Rochester. Edu/Software. Html*, 1–105.

Ronquist, F., Teslenko, M., Van Der Mark, P., Ayres, D. L., Darling, A., Höhna, S., Larget, B., Liu, L., Suchard, M. A., & Huelsenbeck, J. P. (2012). MrBayes 3.2: Efficient Bayesian phylogenetic inference and model choice across a large model space. *Systematic Biology*, *61*(3), 539–542.

Scheyer, T. M., & Cerda, I. A. (2021). Testudines. In *Vertebrate skeletal histology and paleohistology* (pp. 385–398). CRC Press.

Soltis, P. S., & Soltis, D. E. (2003). Applying the bootstrap in phylogeny reconstruction. *Statistical Science*, 256–267.

Sterli, J. (2015). A review of the fossil record of Gondwanan turtles of the clade Meiolaniformes. *Bulletin of the Peabody Museum of Natural History*, *56*(1), 21-45.

Suarez, C. A., González, L. A., Ludvigson, G. A., Cifelli, R. L., & Tremain, E. (2012). Water utilization of the Cretaceous Mussentuchit Member local vertebrate fauna, Cedar

Mountain Formation, Utah, USA: using oxygen isotopic composition of phosphate. *Palaeogeography, Palaeoclimatology, Palaeoecology*, *313*, 78–92.

Sukhanov, V. B. (1964). Subclass Testudinata, Testudinates. In J. A. Orlov (Ed.), *Fundamentals of Palaeontology. Amphibians, reptiles and birds* (pp. 354–438).

Tatarinov, L. (1959). A new turtle of the family Baenidae from the lower Eocene of Mongolia. *Paleontologicheskii Zhurnal*, *1*, 100–113.

Tong, H., & Brinkman, D. (2013). A new species of Sinemys (Testudines: Cryptodira: Sinemydidae) from the Early Cretaceous of Inner Mongolia, China. *Palaeobiodiversity and Palaeoenvironments*, *93*(3), 355–366.

Tong, H., Chanthasit, P., Naksri, W., Ditbanjong, P., Suteethorn, S., Buffetaut, E., Suteethorn, V., Wongko, K., Deesri, U., & Claude, J. (2021). Yakemys multiporcata ngn sp., a large macrobaenid turtle from the basal Cretaceous of Thailand, with a review of the turtle fauna from the Phu Kradung Formation and its stratigraphical implications. Diversity, 13(12), 630.

TTWG (Rhodin, A. G. K., J. B. Iverson, R. Bour, U. Fritz, A. Georges, and H. B. Shaffer). 2021. Turtles of the World Annotated Checklist and Atlas of Taxonomy, Synonymy, Distribution, and Conservation Status (9th Ed.). Chelonian Research Monographs 8: 1–472. DOI:10.3854/crm.8.checklist.atlas. v9.2021.

Ullmann, P. V., Varricchio, D., & Knell, M. J. (2012). Taphonomy and taxonomy of a vertebrate microsite in the mid-Cretaceous (Albian–Cenomanian) Blackleaf Formation, southwest Montana. *Historical Biology*, *24*(3), 311–328.

Vandermark, D., Tarduno, J. A., Brinkman, D. B., Cottrell, R. D., & Mason, S. (2009). New Late Cretaceous macrobaenid turtle with Asian affinities from the High Canadian Arctic: Dispersal via ice-free polar routes. *Geology*, *37*(2), 183–186.

Varricchio, D. J., Martin, A. J., & Katsura, Y. (2007). First trace and body fossil evidence of a burrowing, denning dinosaur. *Proceedings of the Royal Society B: biological sciences*, *274*(1616), 1361-1368.

Wyneken, J., Godfrey, M. H., & Bels, V. (Eds.). (2007). *Biology of turtles: from structures to strategies of life*. CRC press.

Zhou, C.-F., & Rabi, M. (2015). A sinemydid turtle from the Jehol Biota provides insights into the basal divergence of crown turtles. *Scientific Reports*, *5*(1), 16299.

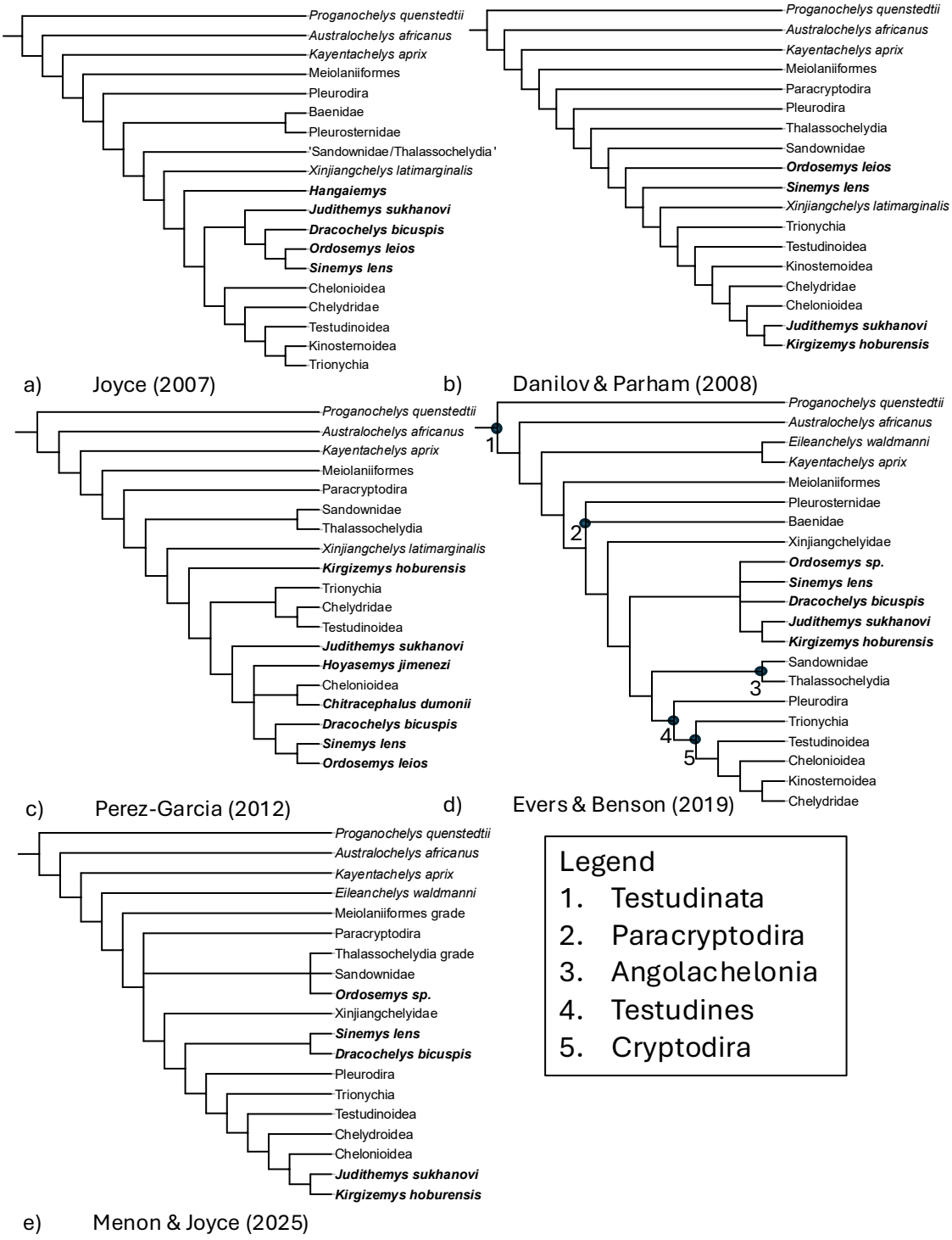

Figure 1: Hypotheses of turtle phylogeny proposed by a) Joyce (2007), b) Danilov & Parham (2008), c) Perez-Garcia (2012), d) Evers & Benson (2019) with labels of higher taxa, and e) Menon & Joyce (2025). “Macrobaenids/sinemydids” bolded.

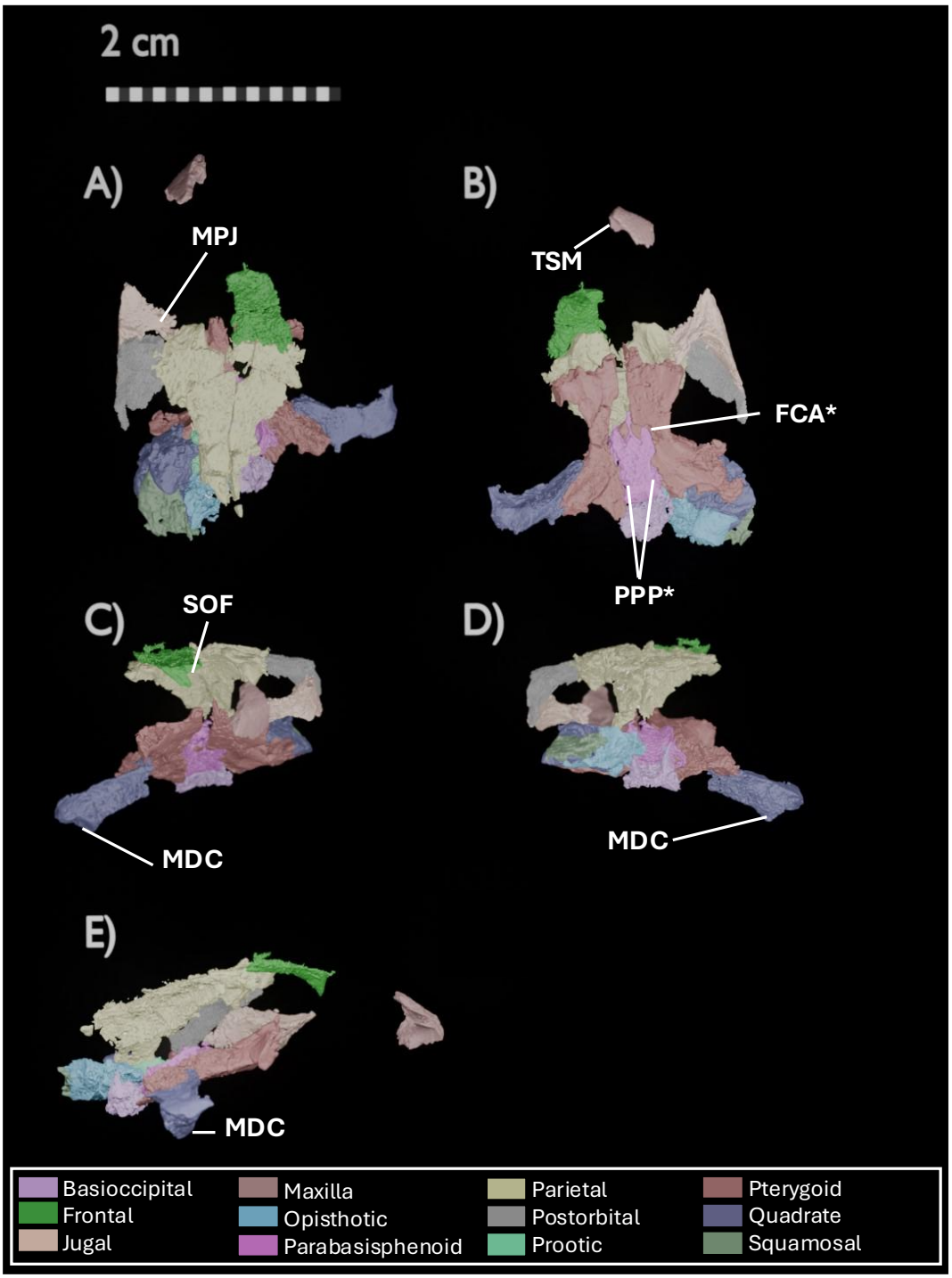

Figure 2: Reconstructed skull of *Microbaena quadratosternon* (MOR 14891) in A) dorsal view, B) ventral view, C) anterior view, D) posterior view, E) right lateral view. Abbreviations: FCA*, fenestra caroticus; MDC, mandibular condyle of quadrate; MPJ, medial process of jugal; PPP*, paired pits of parabasisphenoid; SOF, sulcus olfactorius of frontal; TSM, triturating surface of maxilla.

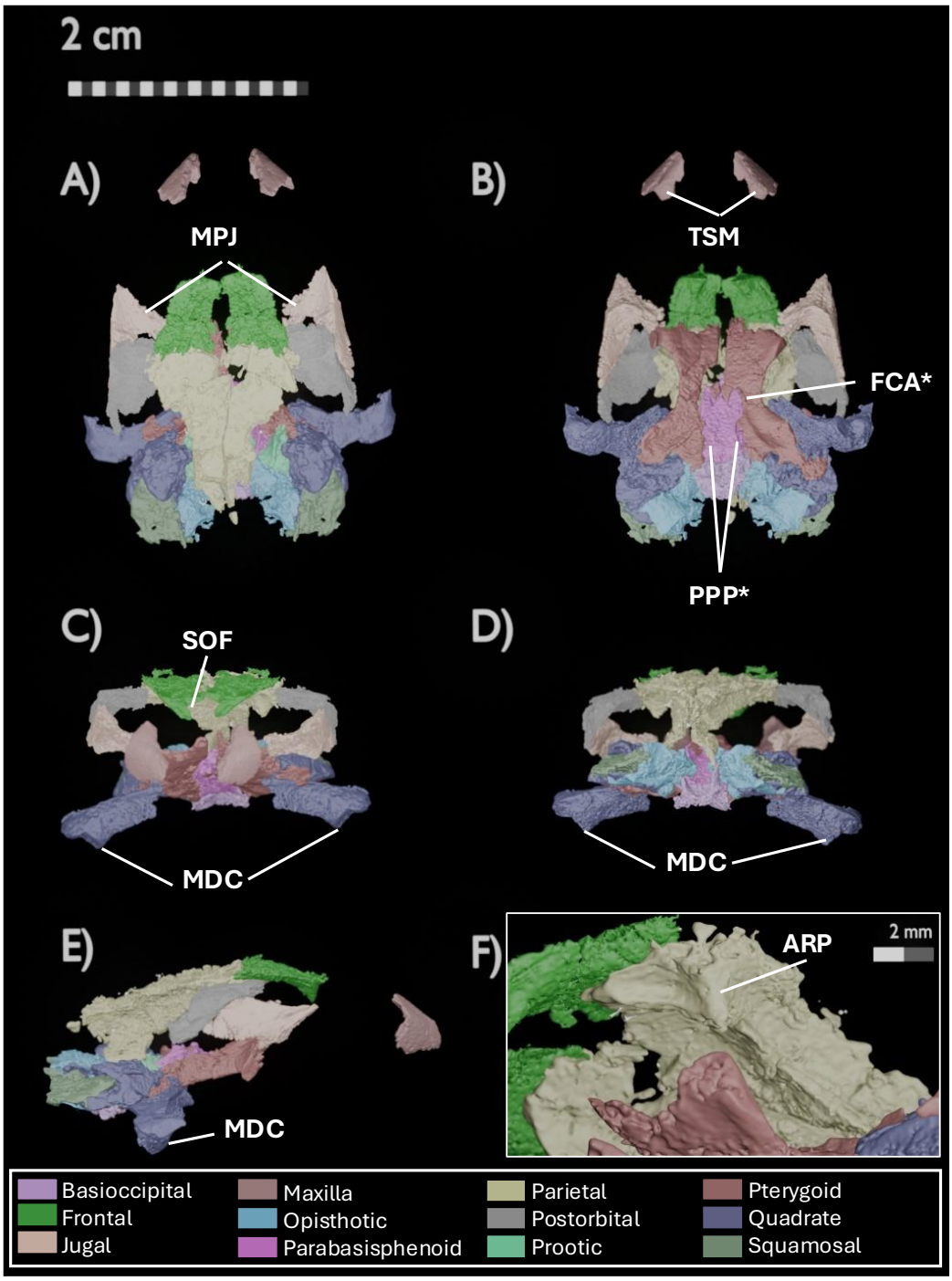

Figure 3: Reconstructed skull of *Microbaena quadratosternon* (MOR 14891) using mirrored elements in A) dorsal view, B) ventral view, C) anterior view, D) posterior view, E) right lateral view, and F) inset in left ventrolateral view exposing the ventral aspect of the parietal. Abbreviations: ARP, anterior ridge of parietal; FCA*, fenestra caroticus; MDC, mandibular condyle of quadrate; MPJ, medial process of jugal; PPP*, paired pits of parabasisphenoid; SOF, sulcus olfactorius of frontal; TSM, triturating surface of maxilla.

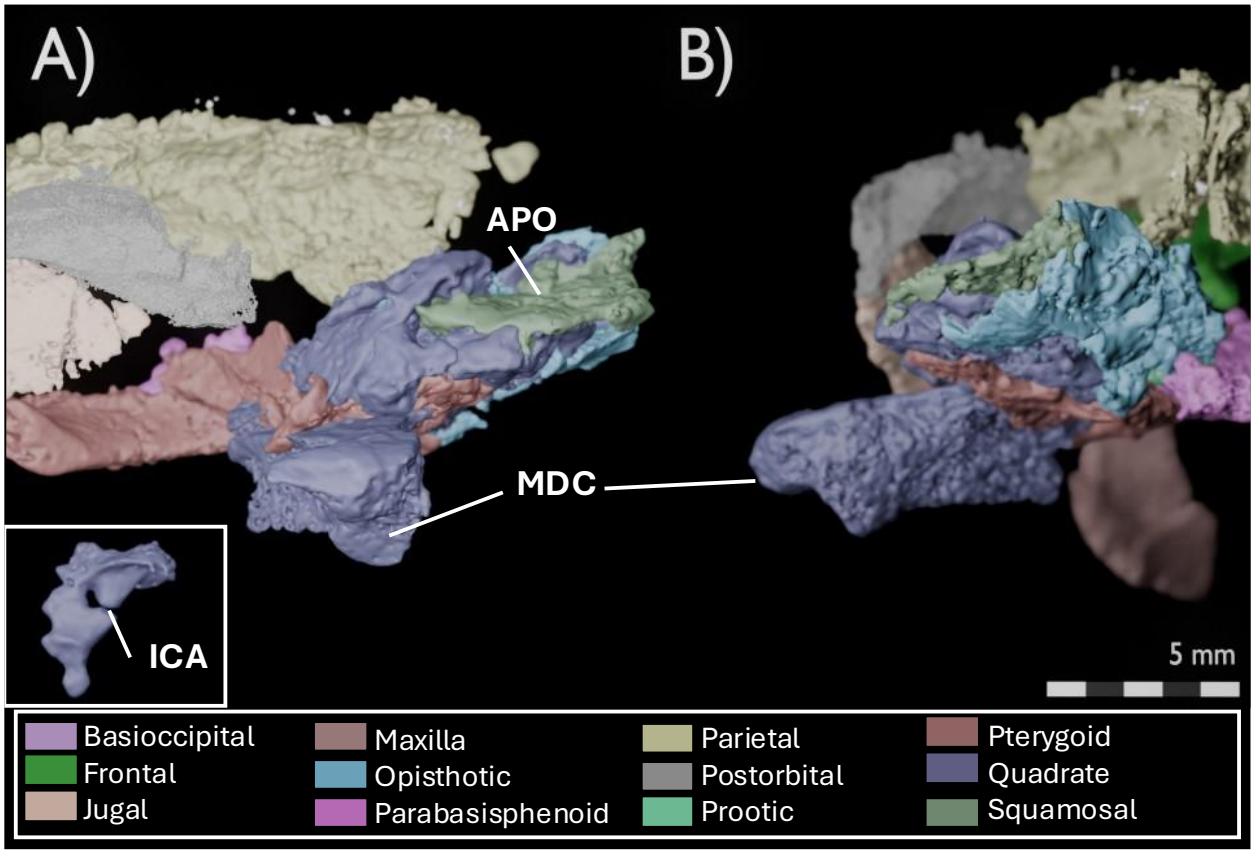

Figure 4: Quadrate and surrounding elements of *Microbaena quadratosternon* (MOR 14891) in A) left lateral view, and B) posterior view. Abbreviations: APO, antrum postoticum; MDC, mandibular condyle of quadrate.

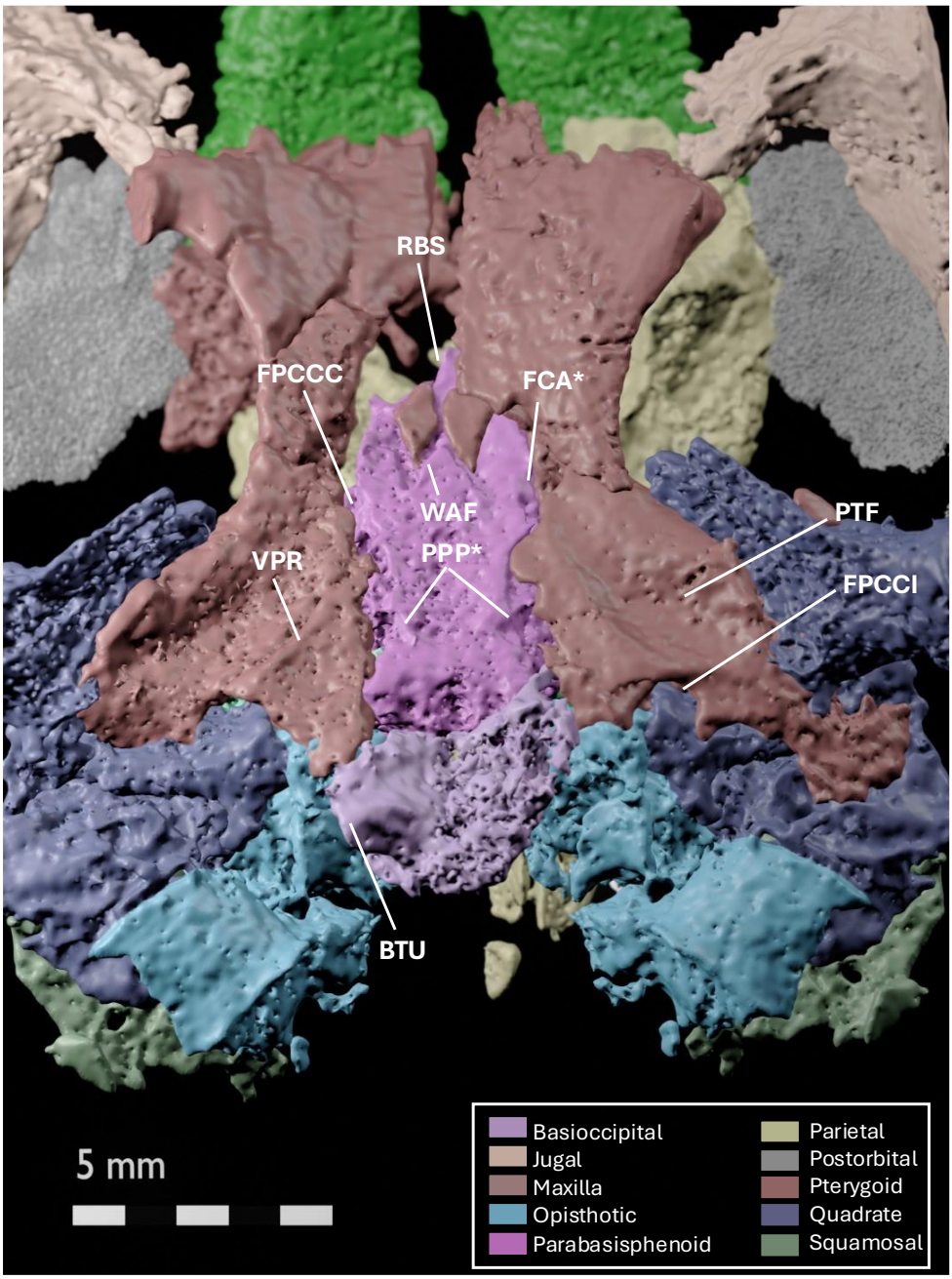

Figure 5: Reconstructed basicranium and fenestrae carotici of *Microbaena quadratosternon* (MOR 14891) in ventral view. Abbreviations: BTU, basal tubera of basioccipital; FCA*, fenestra caroticus; FPCCC, foramen posterius canalis caroticus cerebralis; FPCCI, foramen posterius canalis caroticus interni; PPP*, paired pits of parabasisphenoid; PTF, pterygoid fossa; RBS, rostrum basisphenoidale of parabasisphenoid; VPR, ventral pterygoid ridge; WAF, W-shaped articular facet of parabasisphenoid.

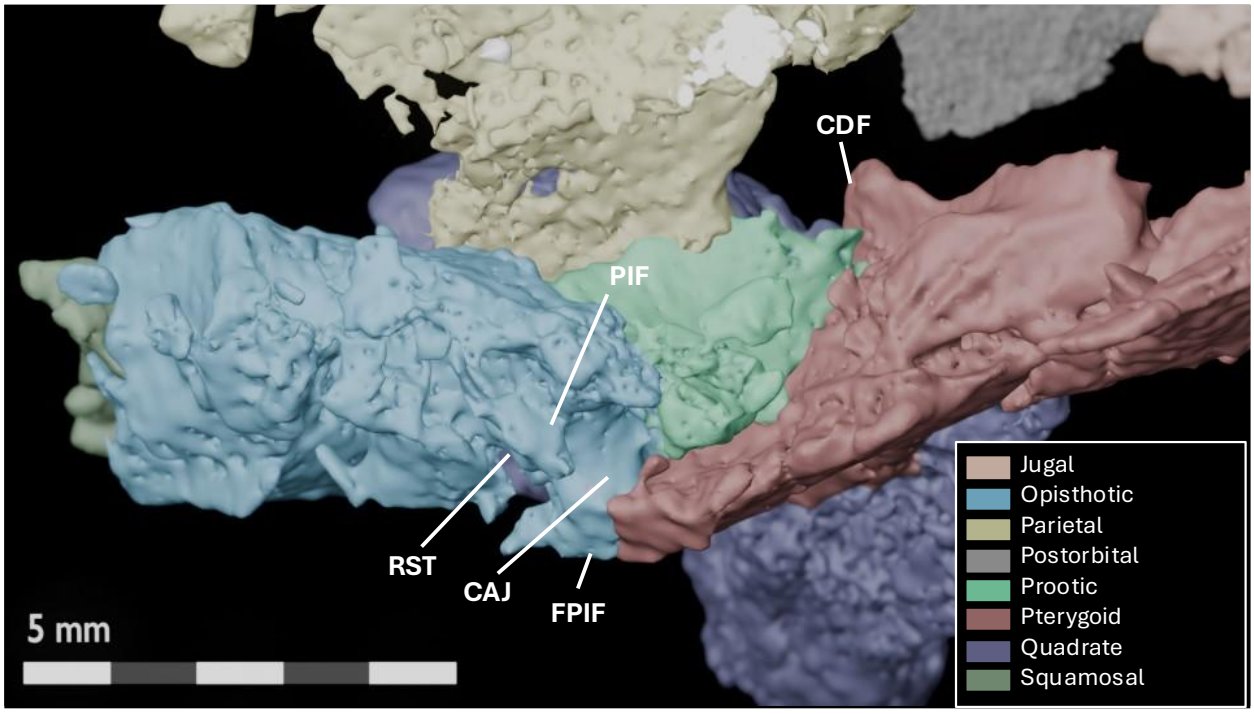

Figure 6: Medial view of the cranium of *Microbaena quadratosternon* (MOR 14891) with the basioccipital and parabasisphenoid removed. Abbreviations: CAJ, cavum acustico-jugulare; CDF, "cryptodire flange" of pterygoid; FPIF, footplate of processus interfenestralis; PIF, processus interfenestralis of opisthotic; RST, recessus scalae tympani.

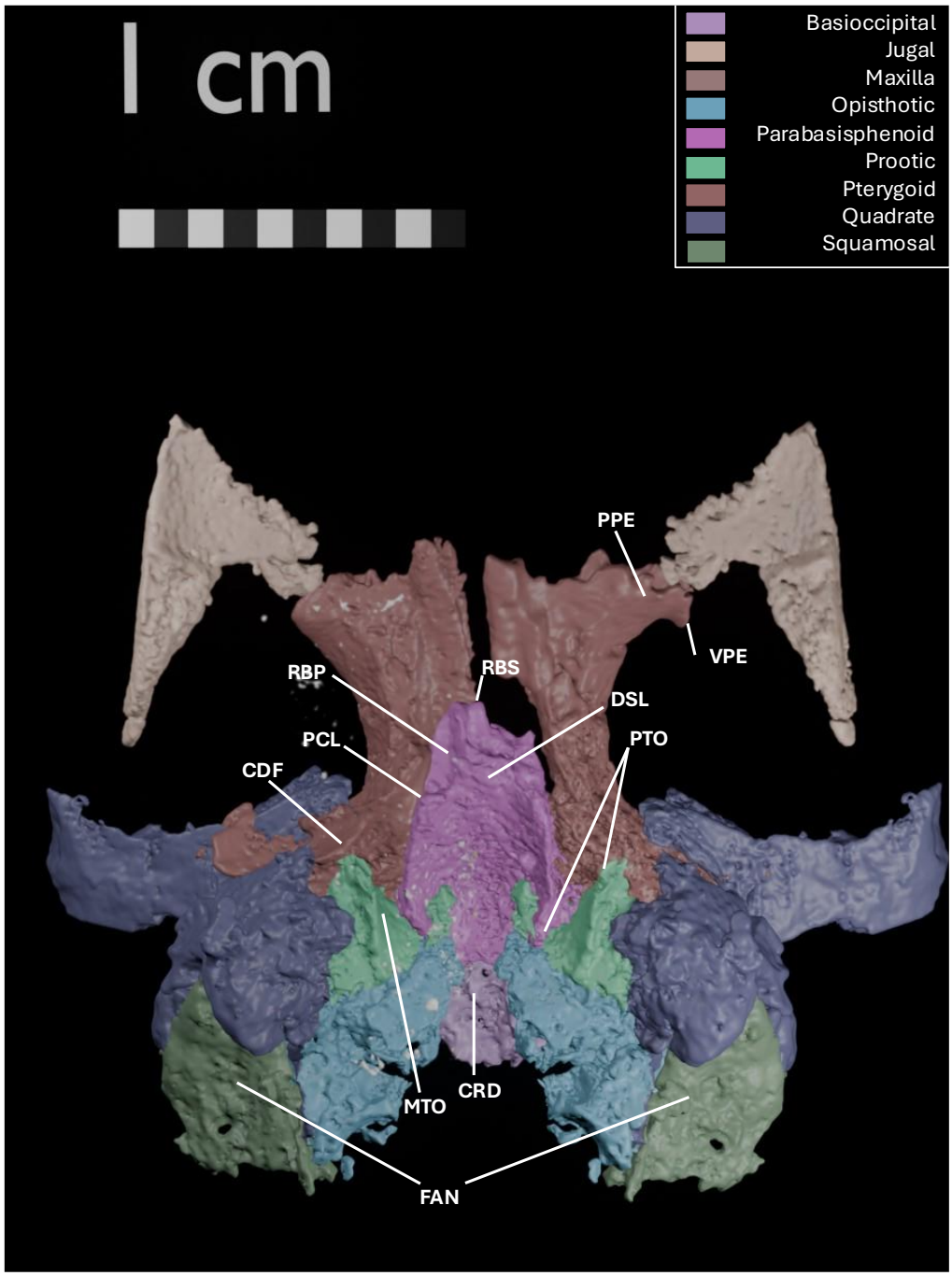

Figure 7: Cranium of *Microbaena quadratosternon* (MOR 14891) in dorsal view with the skull roof removed. Abbreviations: CDF, "cryptodire flange" of pterygoid; CRD, crista dorsalis of basioccipital; DSL, dorsum sellae of parabasisphenoid; FAN, quadrate fenestra leading into antrum postoticum; MTO, musculatory facet of processus trochlearis oticum; PCL, processus clinoidei of parabasisphenoid; PPE, processus pterygoideus externis; PTO, processus trochlearis oticum; RBS, rostrum basisphenoidale (broken); RBP, retractor bulbi pits of parabasisphenoid; VPE, "vertical flange" of pterygoid.

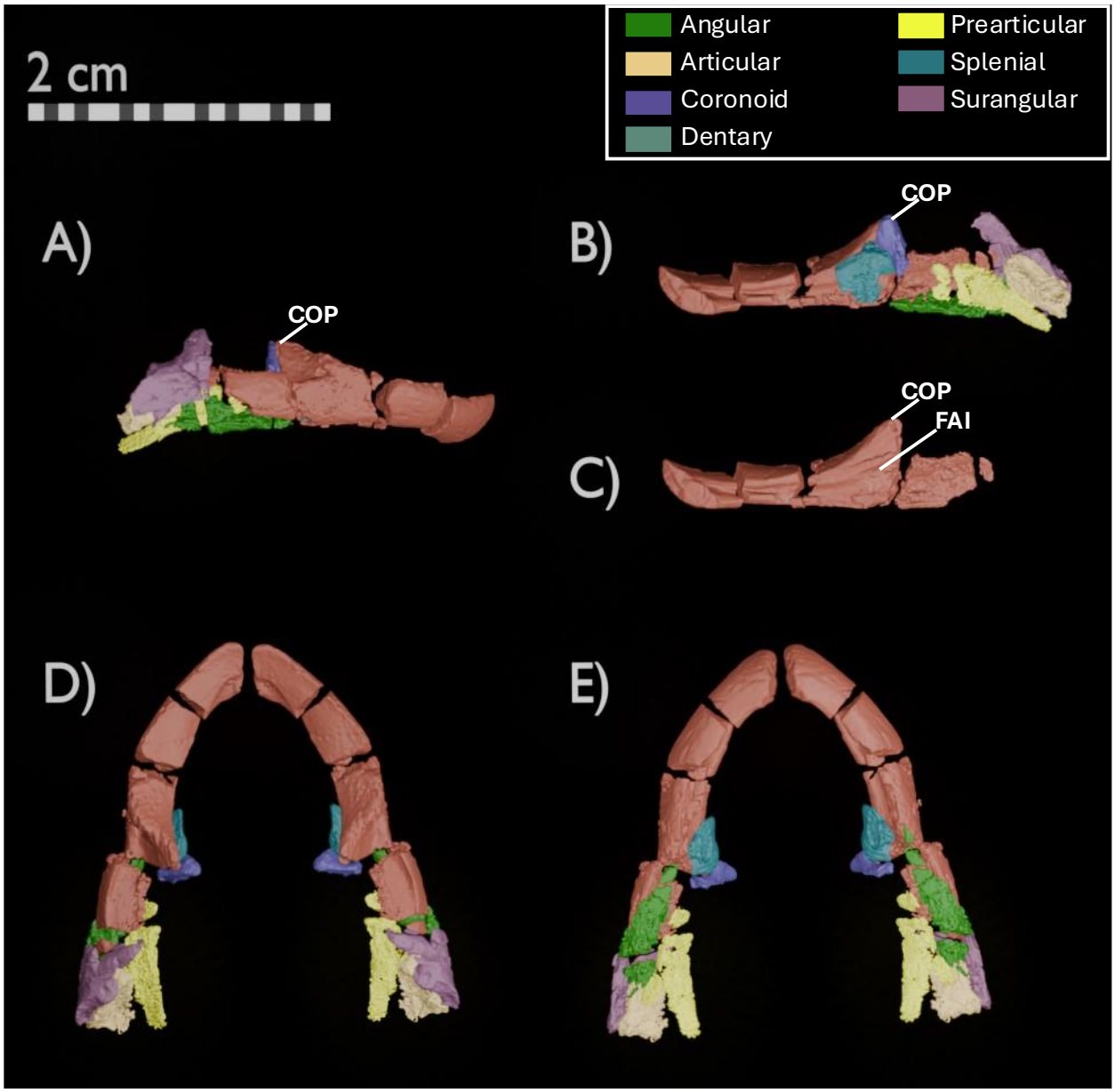

Figure 8: Right hemimandible of *Microbaena quadratosternon* (MOR 14891) in A) right lateral view, B) medial view, and C) medial view with the post-dentary elements removed. Mirrored mandibular elements in D) dorsal view, and E) ventral view. Abbreviations: COP, coronoid process; FAI, foramen alveolare inferius.

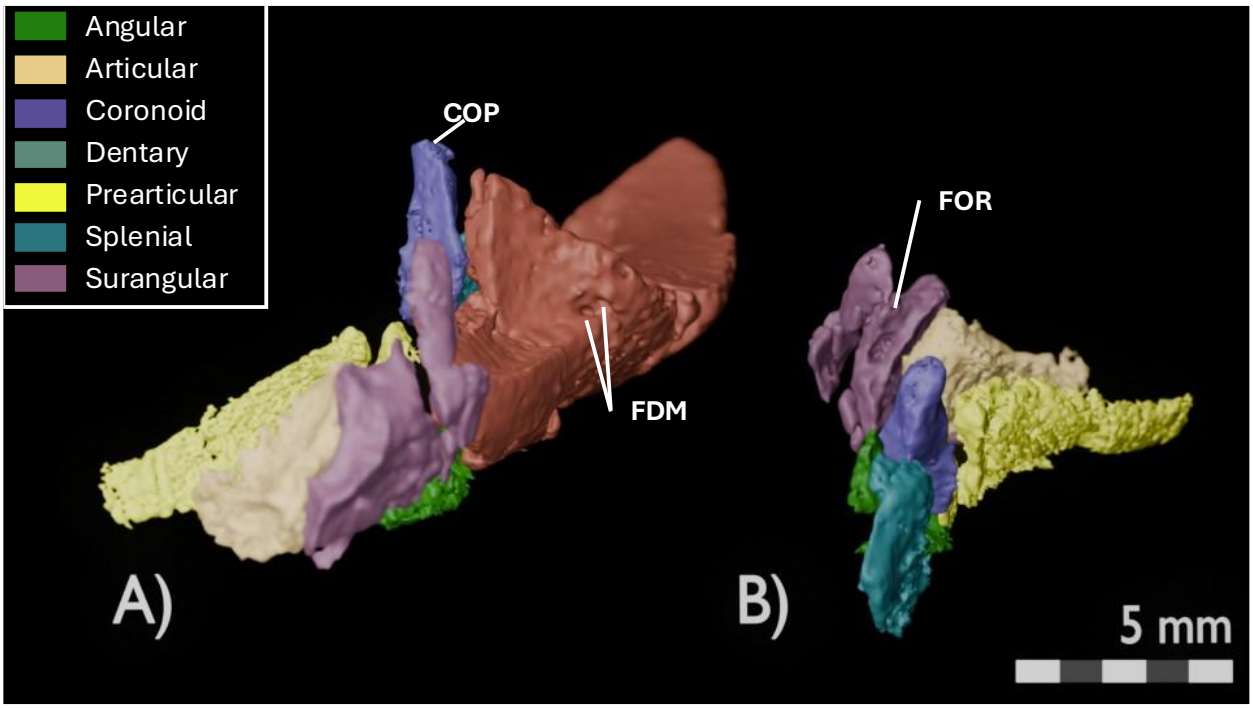

Figure 9: Right hemimandible of *Microbaena quadratosternon* (MOR 14891) in A) posterolateral view, and B) anterior view with the dentary removed. Abbreviations: COP, coronoid process; FDM, foramen dentofaciale majus; FOR, unnamed foramen of the surangular.

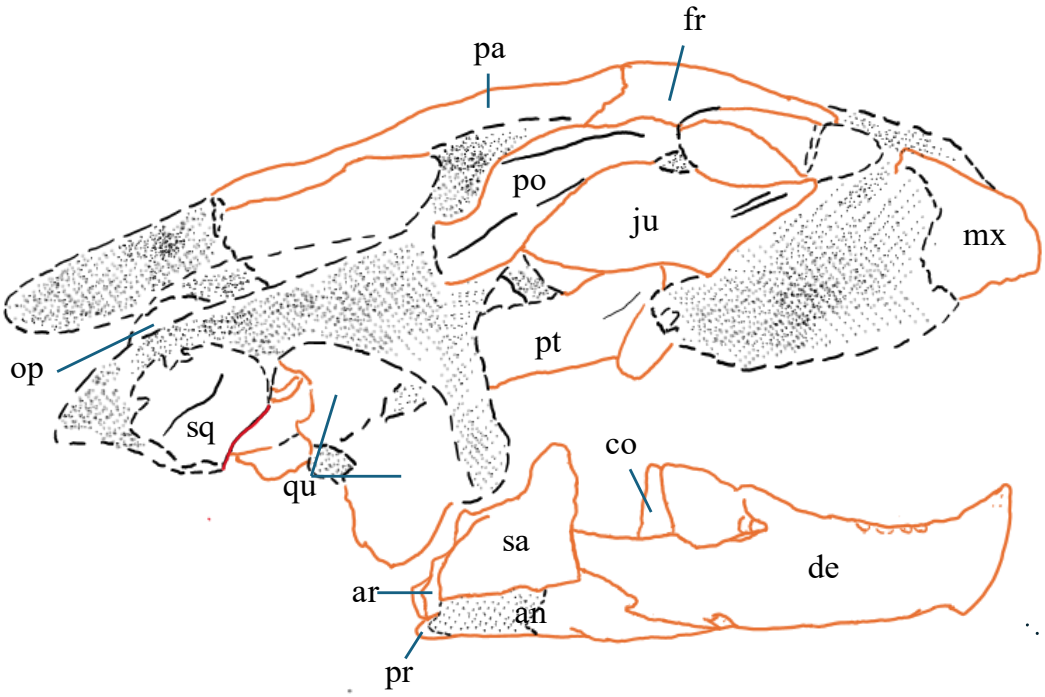

Figure 10: Line drawing of the reconstructed cranium and mandible of *Microbaena quadratosternon* (MOR 14891) in right lateral view. Red denotes complete edges on elements, black dashed lines delimit regions with missing material, and stippling indicates reconstructed missing areas of the skull. Abbreviations: an, angular; ar, articular; co, coronoid; de, dentary; fr, frontal; ju, jugal; mx, maxilla; op, opisthotic; pa, parietal; po, postorbital; pr, prearticular; pt, pterygoid; qu, quadrate; sa, surangular; sq, squamosal.

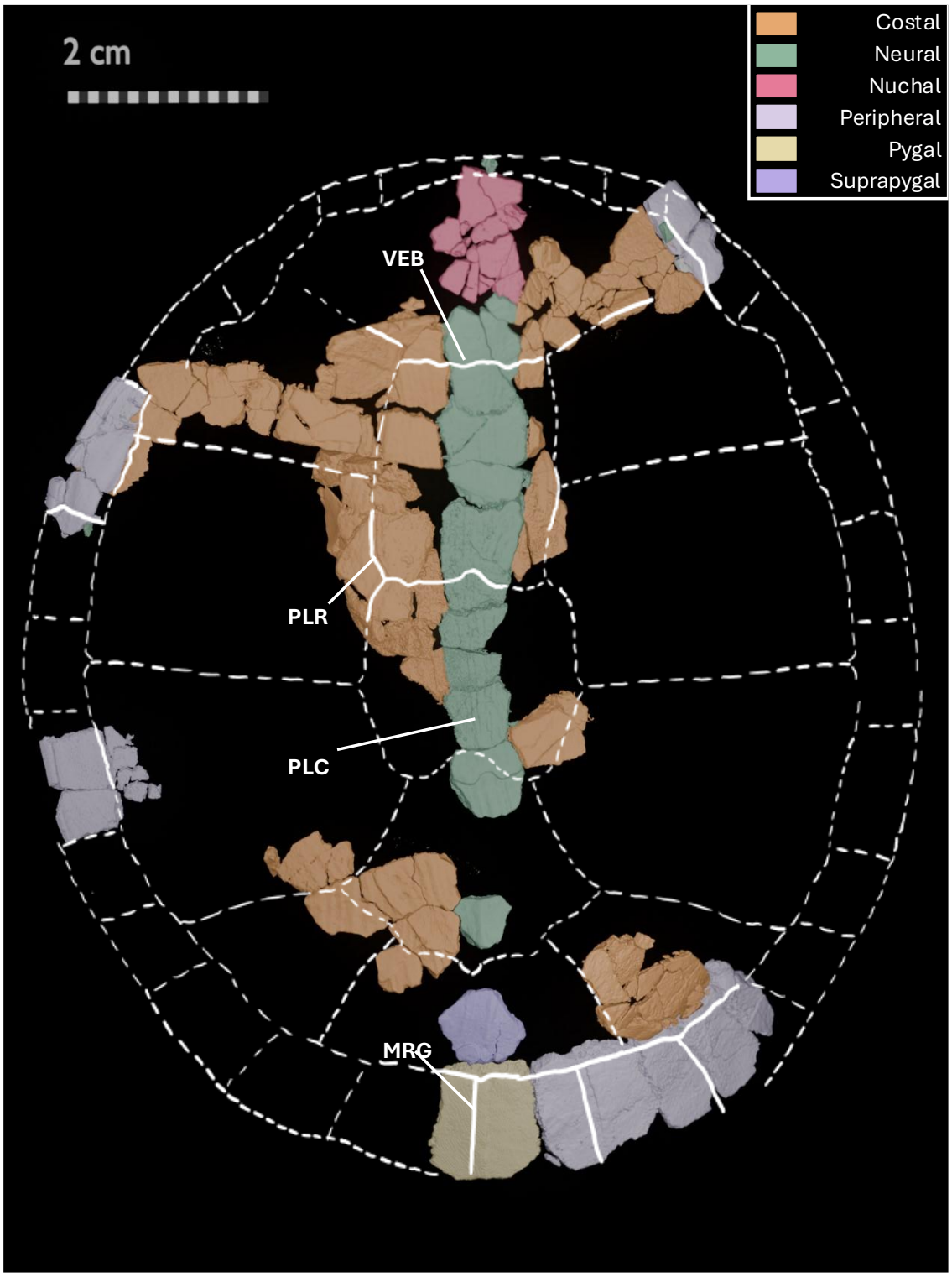

Figure 11: Reconstructed carapace fragments of *Microbaena quadratosternon* (MOR 14891) in dorsal view. Abbreviations: MRG, marginal scutes; PLC, plications; PLR, pleural scutes; VEB, vertebral scutes.

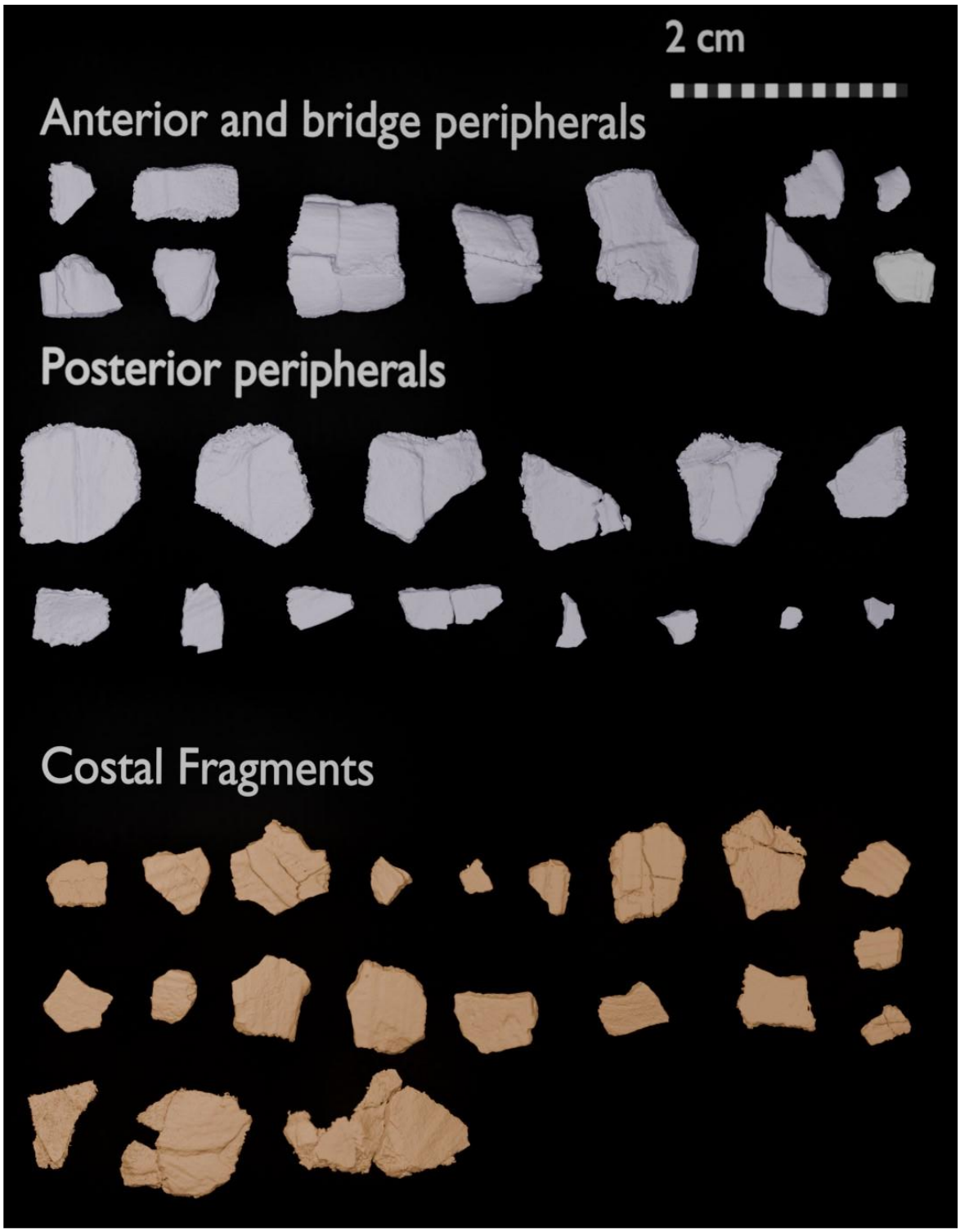

Figure 12: Unfitted carapace fragments of *Microbaena quadratosternon* (MOR 14891) in dorsal view.

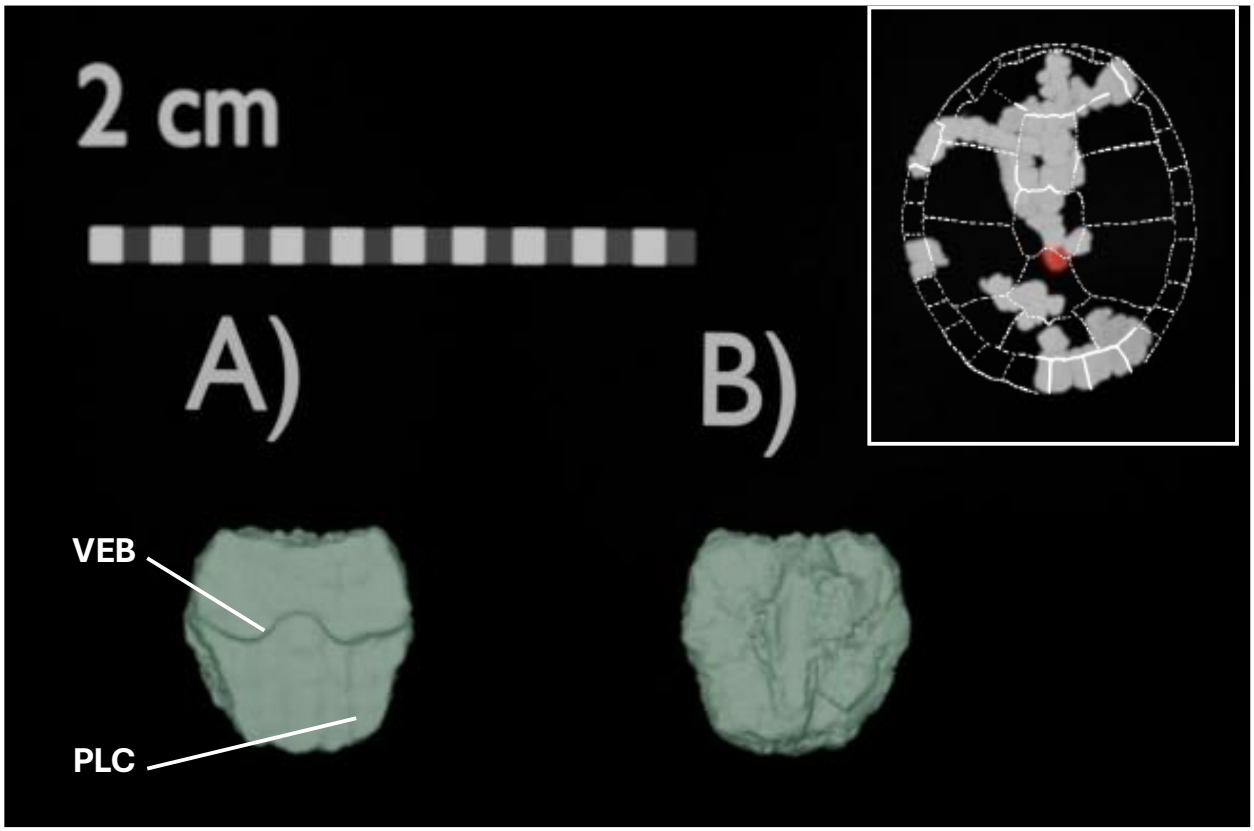

Figure 13: Sixth neural of *Microbaena quadratosternon* (MOR 14891) in A) dorsal view, and B) ventral view, displaying the anteriorly embayed sulcus separating the third and fourth vertebral scutes. Abbreviations: PLC, plications; VEB, vertebral scutes.

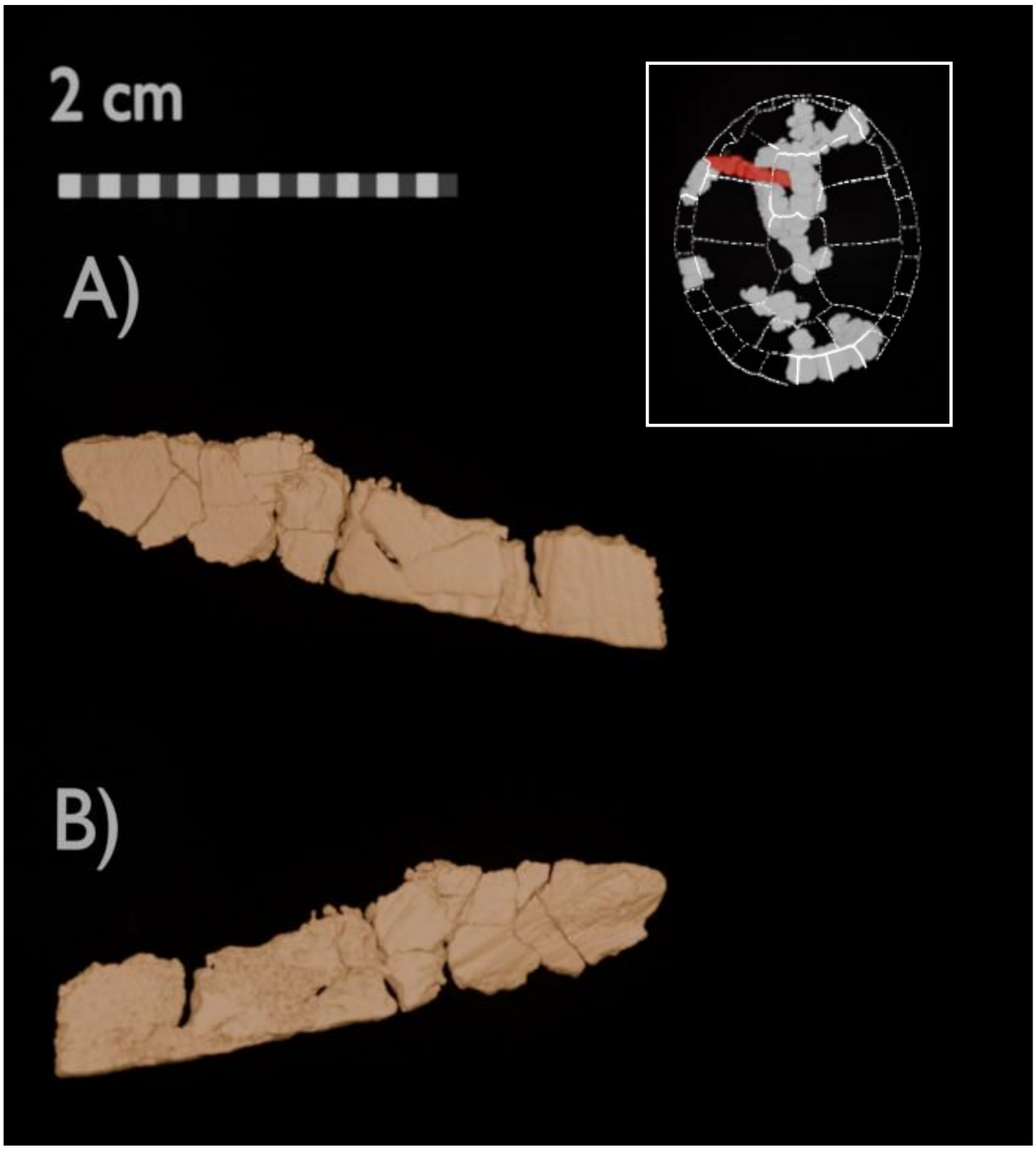

Figure 14: Second costal of *Microbaena quadratosternon* (MOR 14891) in A) dorsal view, and B) ventral view.

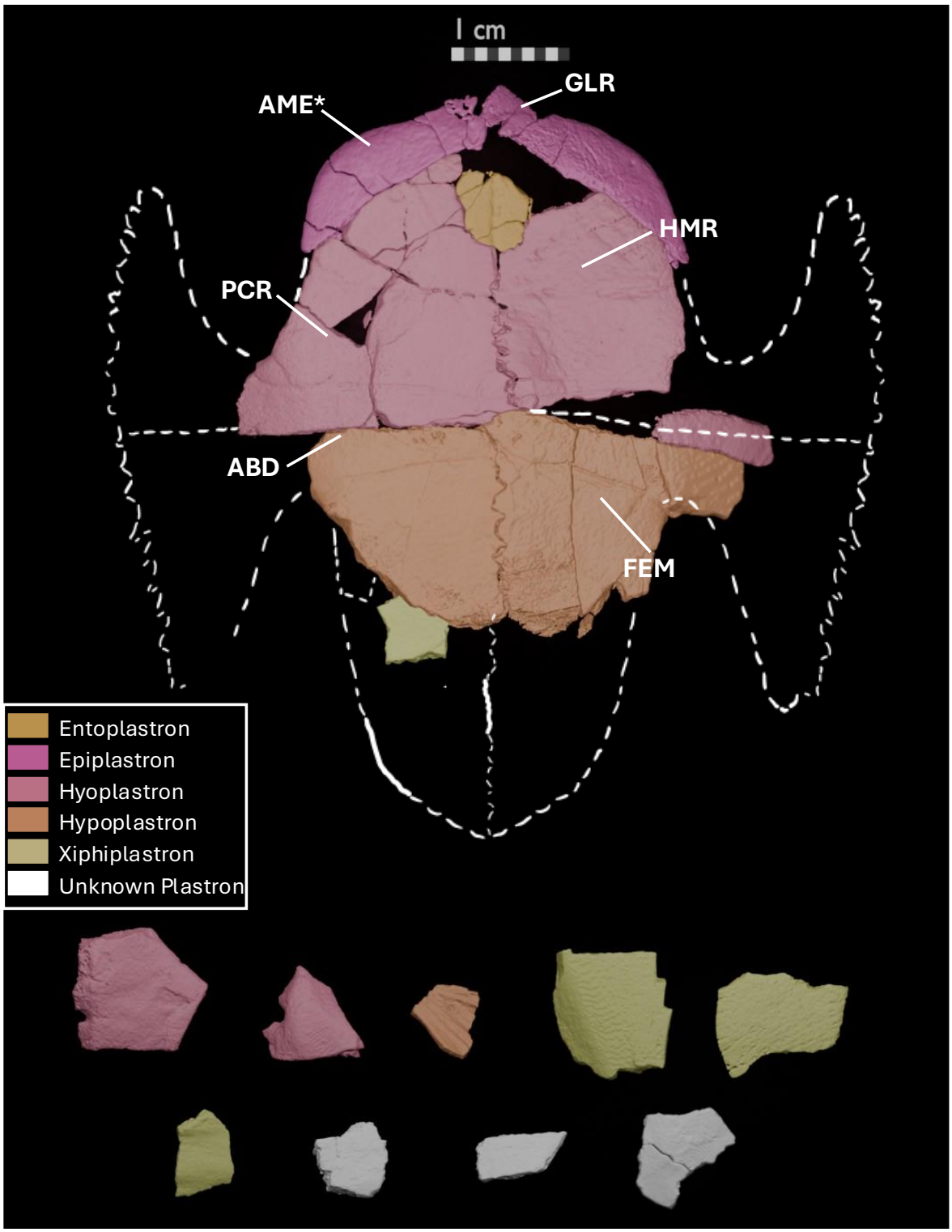

Figure 15: Reconstructed plastron of *Microbaena quadratosternon* (MOR 14891) in ventral view. Abbreviations: ABD, abdominal scute; AME*, anterior marginal of epiplastra; FEM, femoral scute; GLR, gular scute; HMR, humeral scute; PCR, pectoral scute.

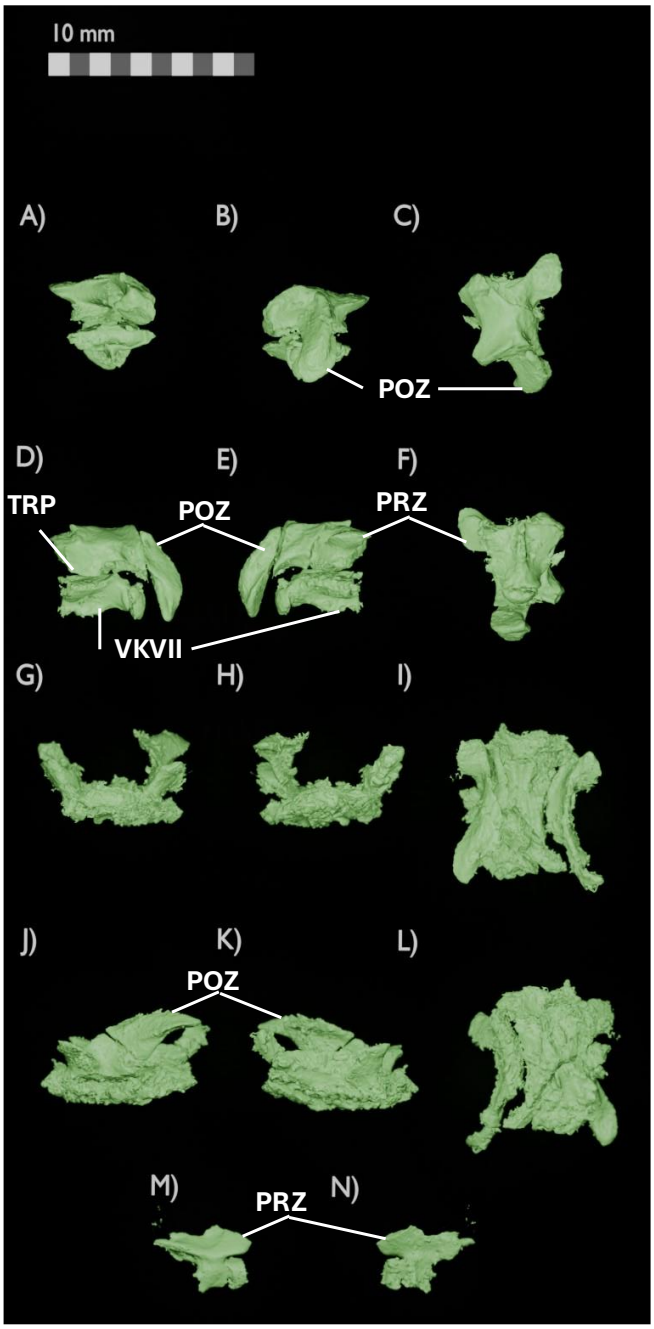

Figure 16: Eighth cervical vertebra of *Microbaena quadratosternon* (MOR 14891) in A) anterior, B) posterior, C) dorsal, D) left lateral, E) right lateral, and F) ventral views. Unidentified cervical vertebra in G) anterior, H) posterior, I) dorsal, J) left lateral, K) right lateral, and L) ventral views. Unidentified right half of a neural arch in M) right lateral, and N) medial views. Abbreviations: POZ, postzygapophysis; PRZ, prezygapophysis; TRP, transverse process; VKVII, ventral keel of CV VIII.

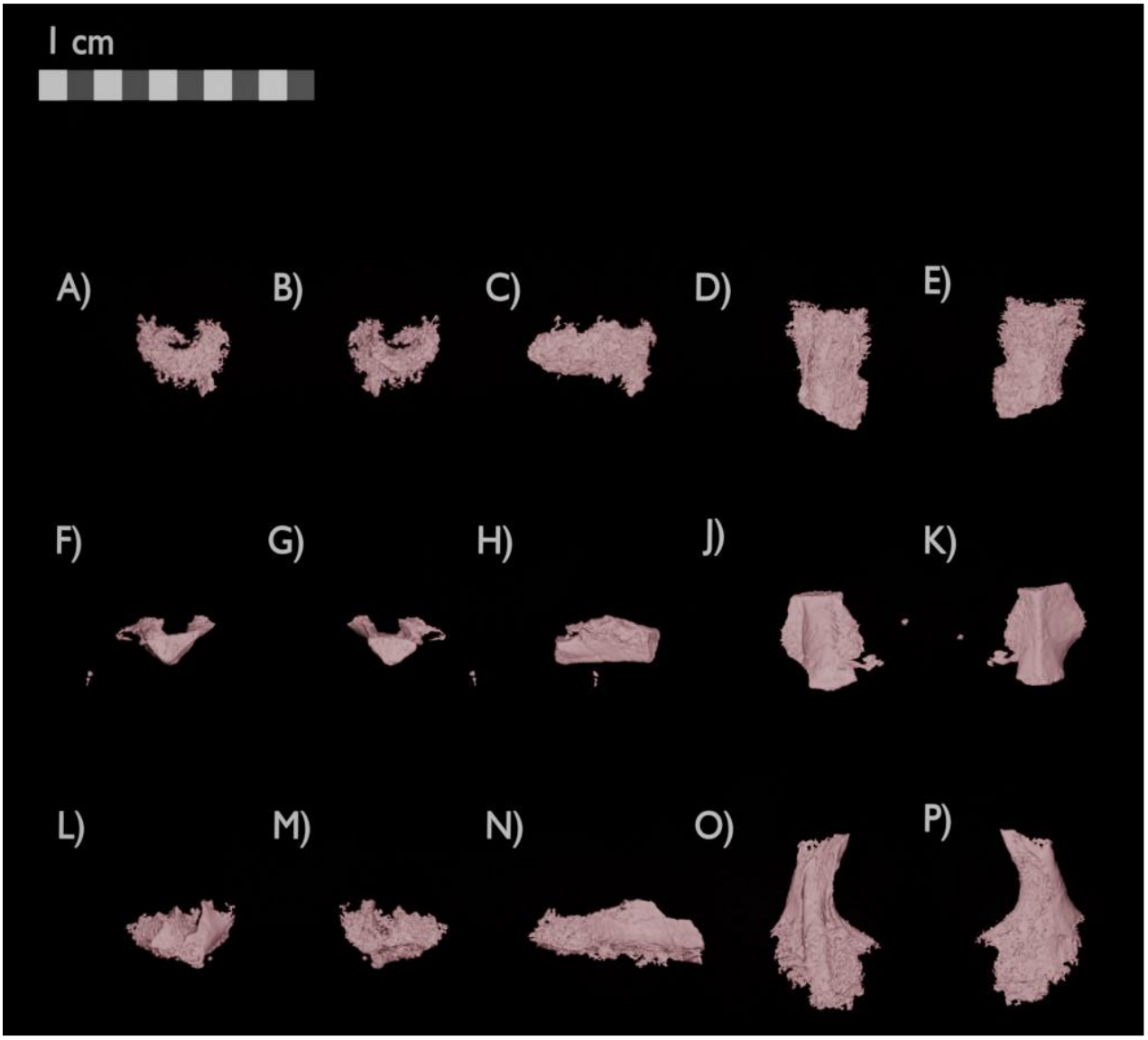

Figure 17: Three unidentified dorsal centra of *Microbaena quadratosternon* (MOR 14891) in A, F, & L) anterior view, B, G, & M) posterior view, C, H, & N) right lateral view, D, J, & O) dorsal view, and E, K, & P) ventral views.

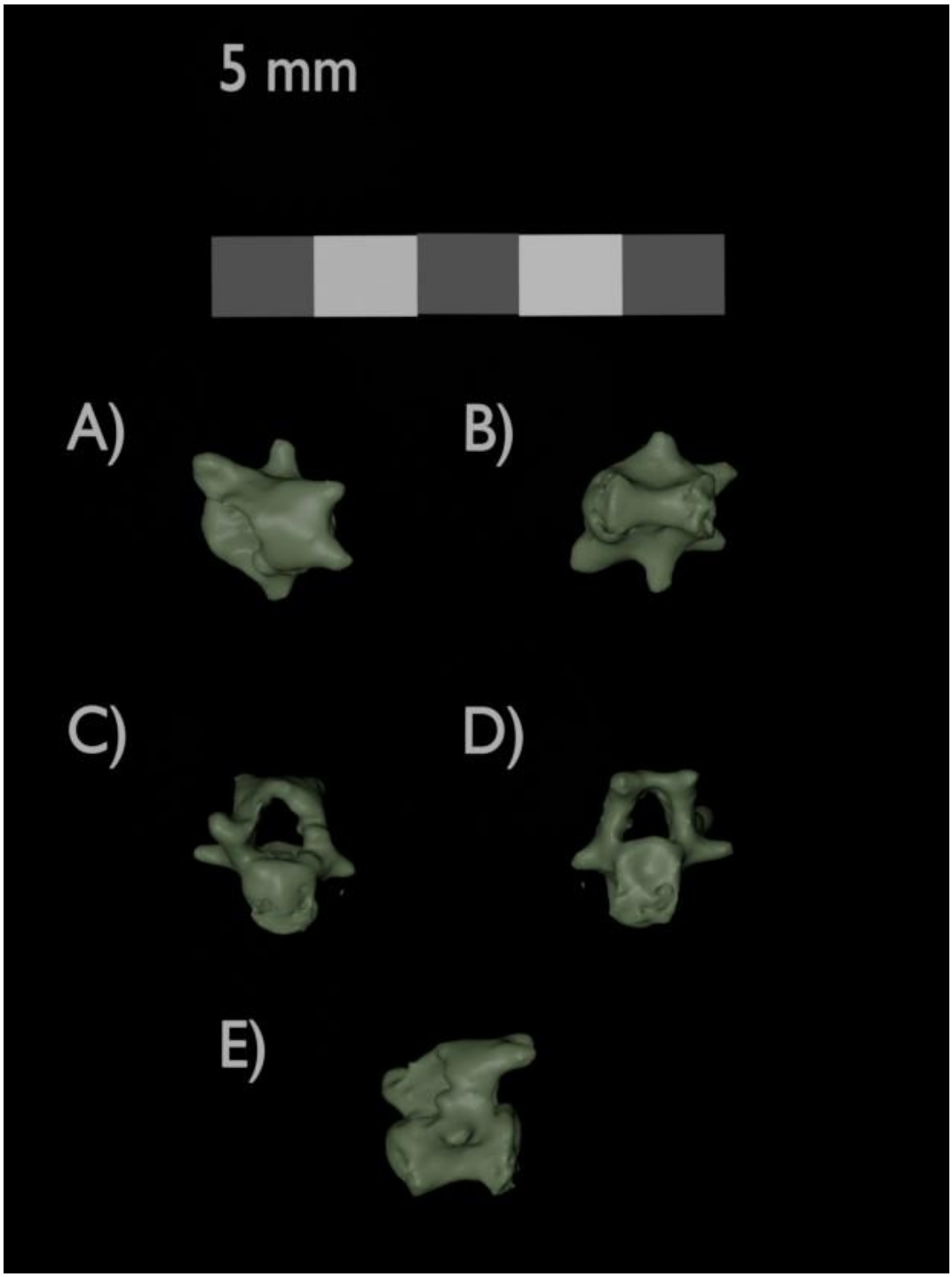

Figure 18: Unidentified caudal vertebra of *Microbaena quadratosternon* (MOR 14891) in A) dorsal, B) ventral, C) anteriot, D) posterior, and E) left lateral views.

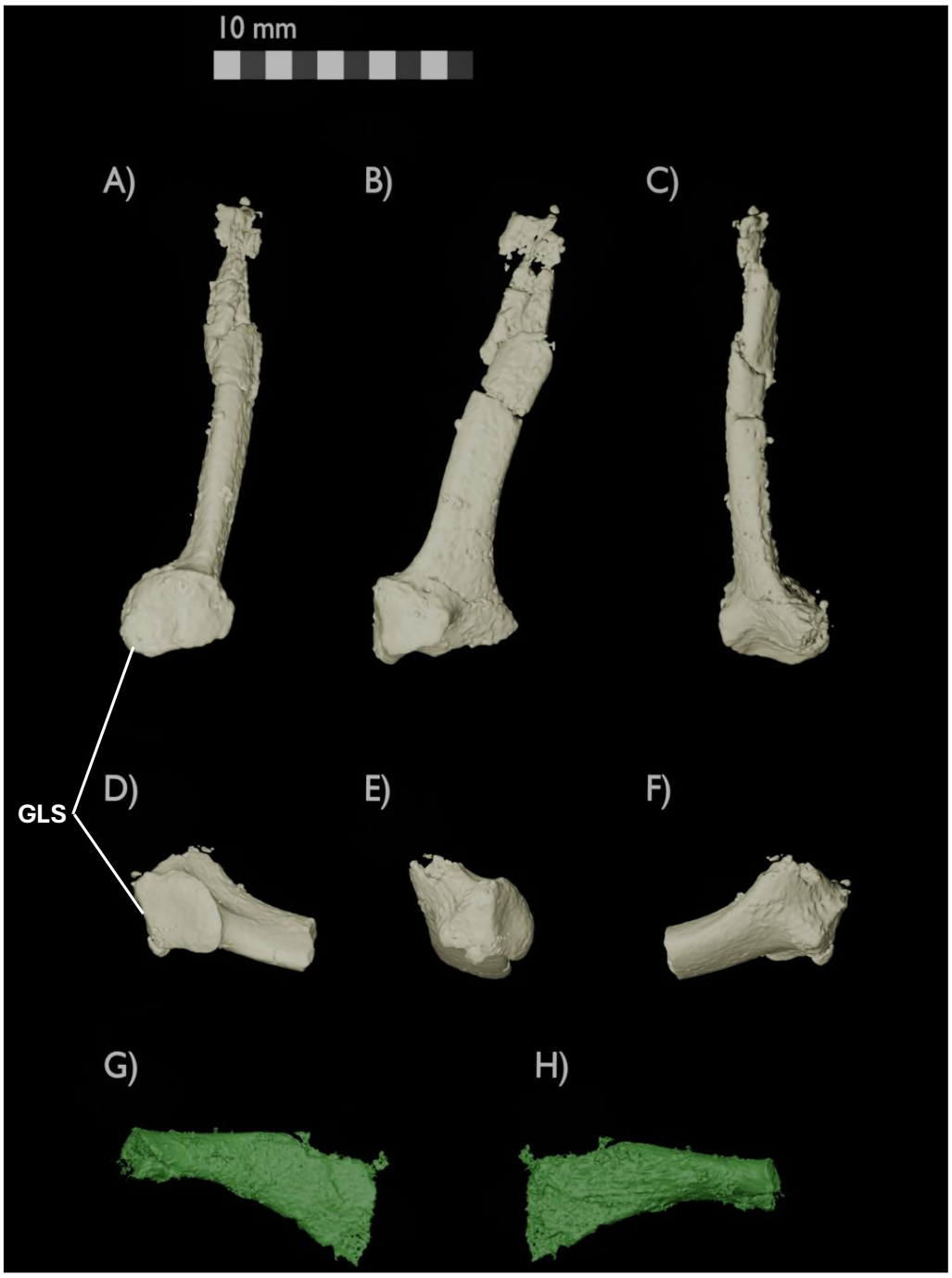

Figure 19: Left scapula of *Microbaena quadratosternon* (MOR 14891) in A) anterior, B) lateral, and C) posterior views. Right scapula of *Microbaena quadratosternon* (MOR 14891) in D) anterior, E) lateral, and F) posterior views. Right coracoid of *Microbaena quadratosternon* (MOR 14891) in G) dorsal, and H) ventral views. Abbreviations: GLS, glenoid of scapula.

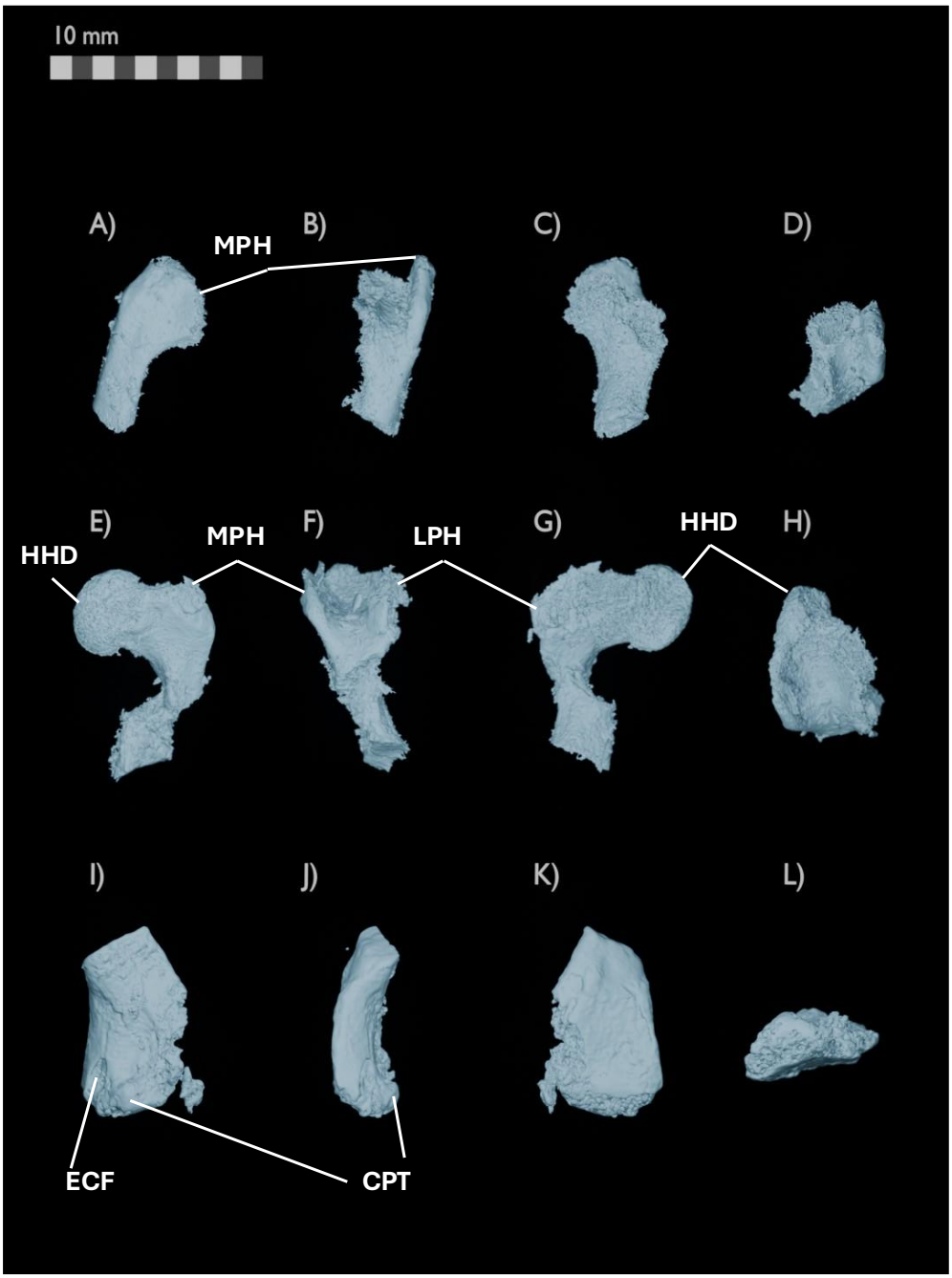

Figure 20: Left proximal humerus of *Microbaena quadratosternon* (MOR 14891) in A) anterior, B) ventral, C) posterior and D) proximal views. Right proximal humerus of *Microbaena quadratosternon* (MOR 14891) in E) anterior, F) ventral, G) posterior and H) proximal views. Left distal humerus of *Microbaena quadratosternon* (MOR 14891) in I) dorsal, J) posterior, K) ventral and L) distal views. Abbreviations: CPT, capitulum of humerus; ECF, ectepicondylar foramen; HHD, humeral head; LPH, lateral process of humerus; MPH, medial process of humerus.

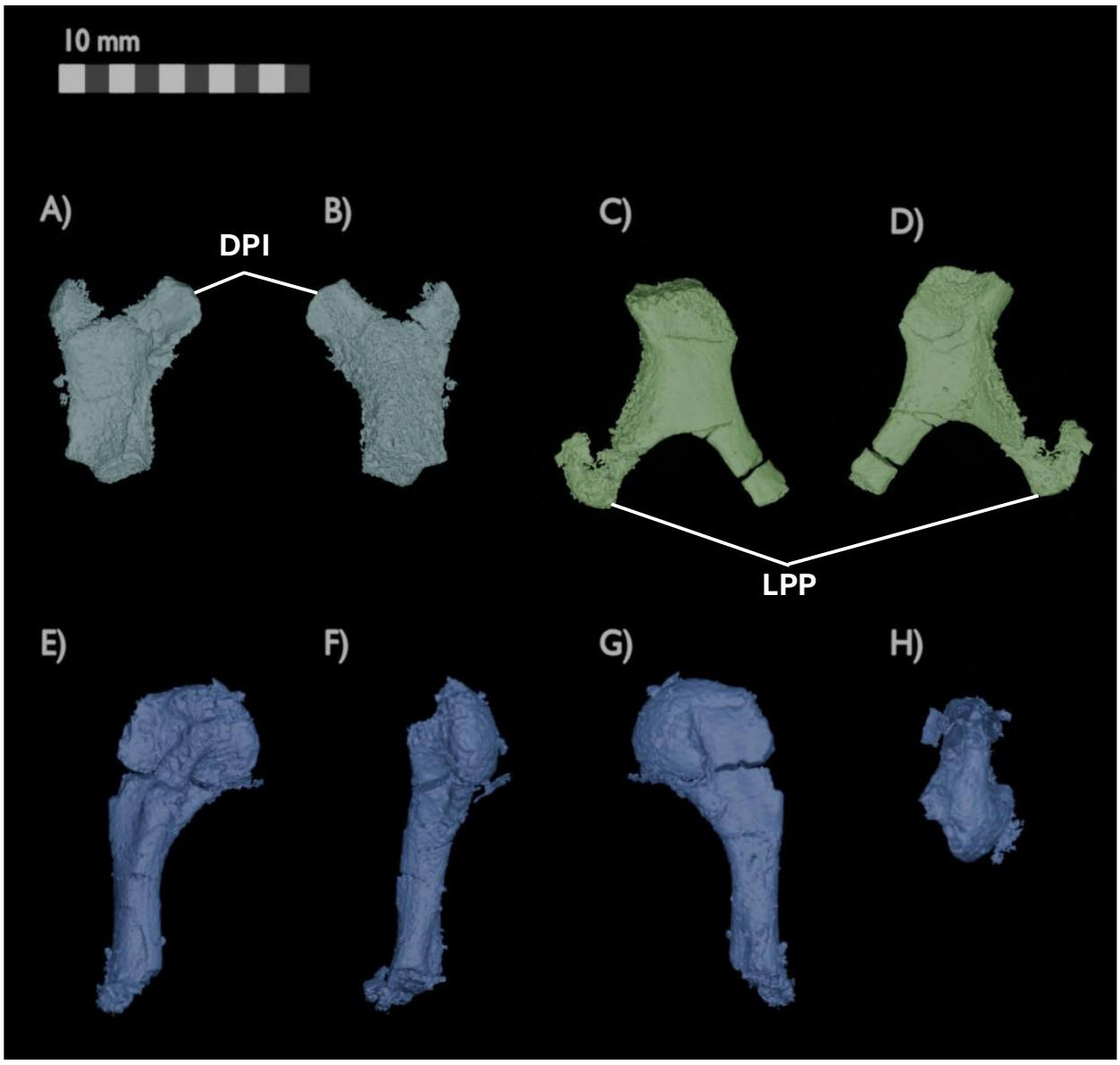

Figure 21: Illium of *Microbaena quadratosternon* (MOR 14891) in A) lateral, and B) medial views. Pubis of *Microbaena quadratosternon* (MOR 14891) in C) ventral, and D) dorsal views. Right femur of *Microbaena quadratosternon* (MOR 14891) in E) posterior, F) dorsal, G) anterior, and H) proximal views. Abbreviations: DPI; dorsal process of illium, LPP; lateral process of pubis.

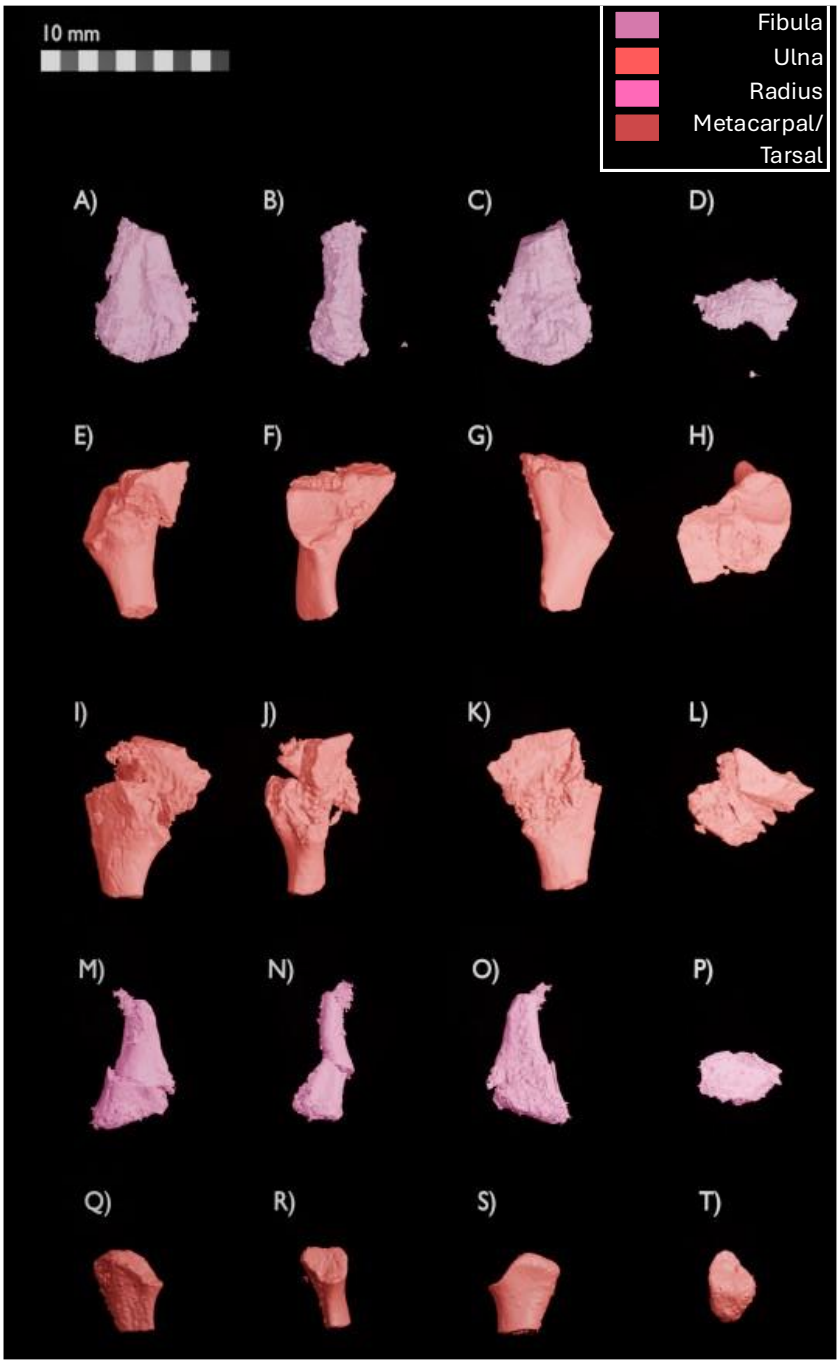

Figure 22: Left distal fibula of *Microbaena quadratosternon* (MOR 14891) in A) ventral?, B) medial?, C) dorsal?, and D) distal views. Left ulna of *Microbaena quadratosternon* (MOR 14891) in E) dorsal, F) medial, G) ventral, and H) proximal views. Right ulna of *Microbaena quadratosternon* (MOR 14891) in in I) dorsal, J) medial, K) ventral, and L) proximal views. Radius of *Microbaena quadratosternon* (MOR 14891) in Q) dorsal?, R) posterior?, S) ventral?, and T) distal views. First metacarpal of *Microbaena quadratosternon* (MOR 14891) in Q) dorsal?, R) posterior?, S) anterior?, and T) proximal views.

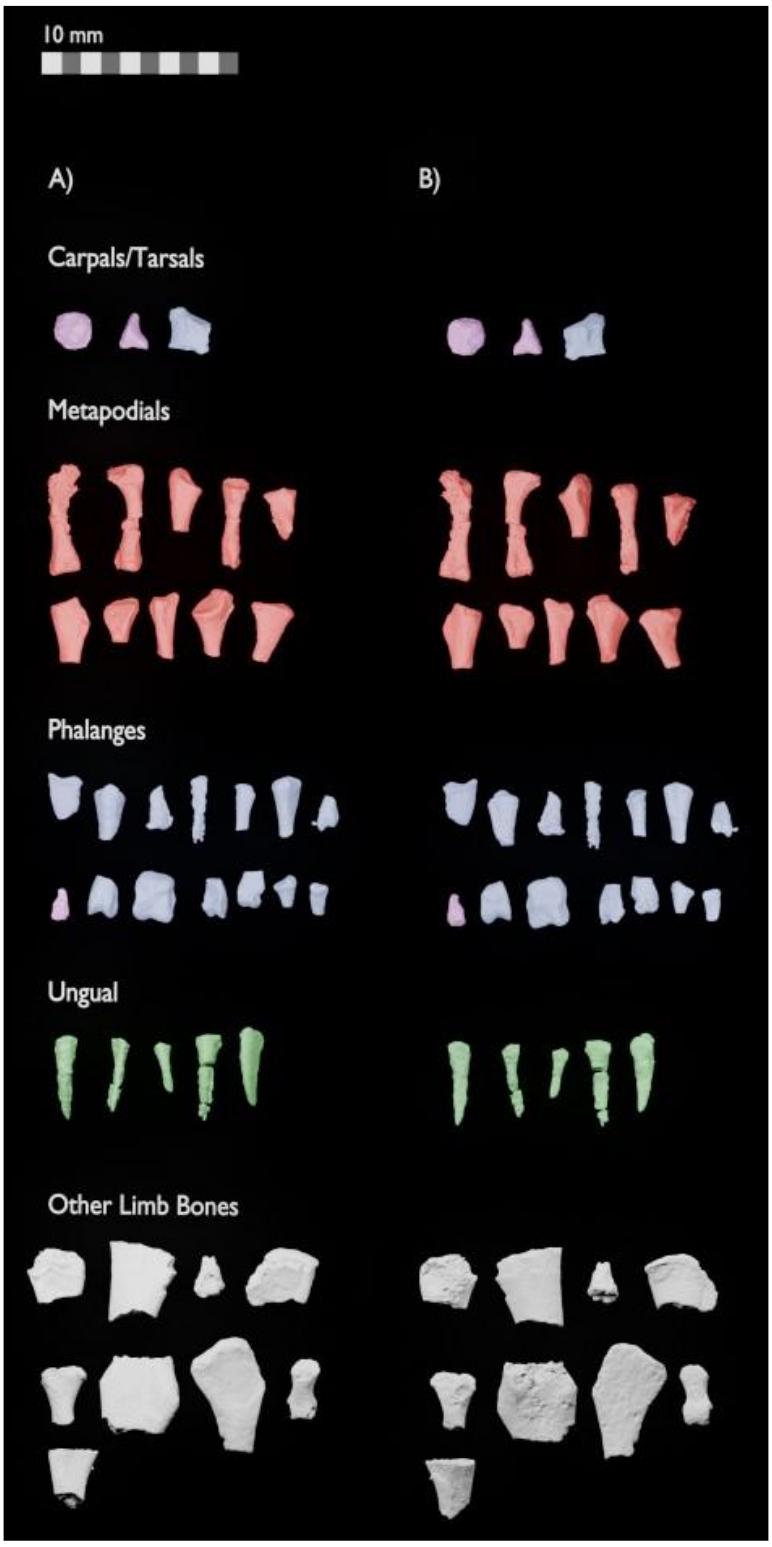

Figure 23: Carpals/tarsals, metapodials, phalanges, and other unidentified limb bones of *Microbaena quadratosternon* (MOR 14891) in A) dorsal?, and B) ventral? views.

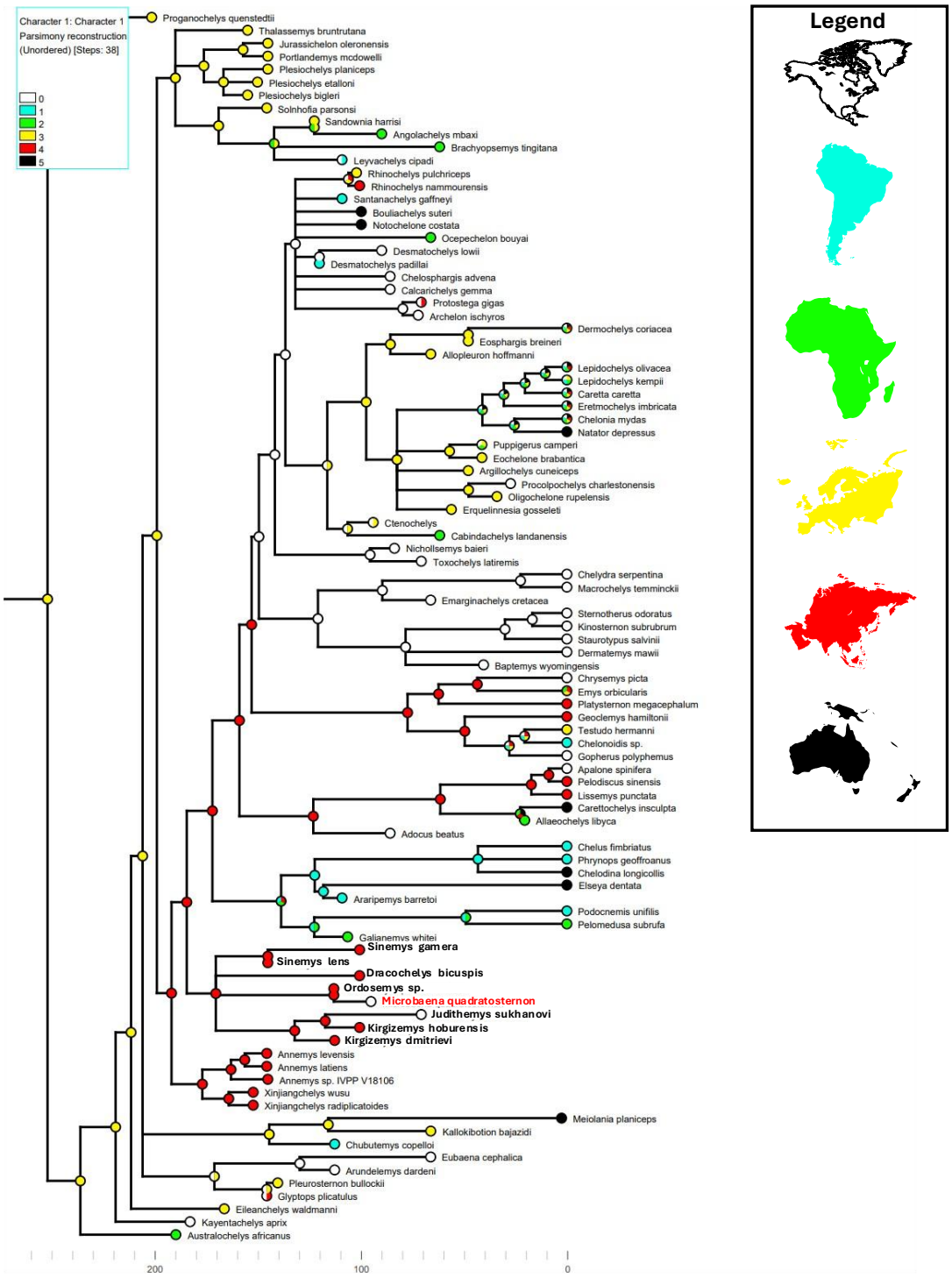

Figure 24: Bayesian consensus timetree (from the latest Triassic through the Cretaceous) with estimated geographic origins for nodes using parsimony ancestral state reconstruction. Taxa with over 75% missing data removed. *Microbaena quadratosternon* in red. Members of "Macrobaenidae/Sinemydidae" bolded.

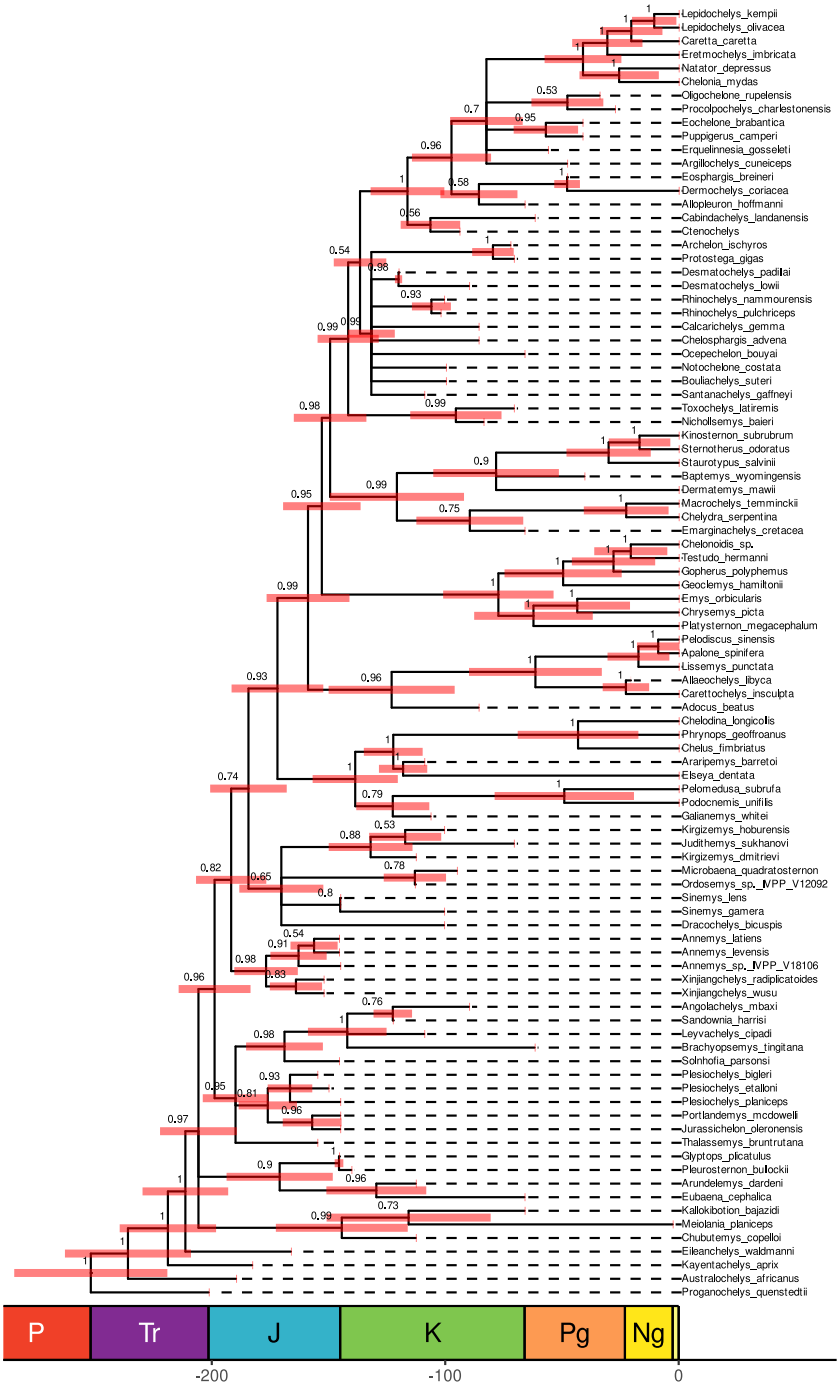

Figure 25: Bayesian consensus timetree displaying all taxa included in matrix. Taxa with over 75% missing data removed. Node support displayed as posterior probability in decimal format. Bars represent 95% highest posterior density (HPD) intervals for node ages. *Microbaena quadratosternon* in red. Members of "Macrobaenidae/Sinemydidae" bolded.

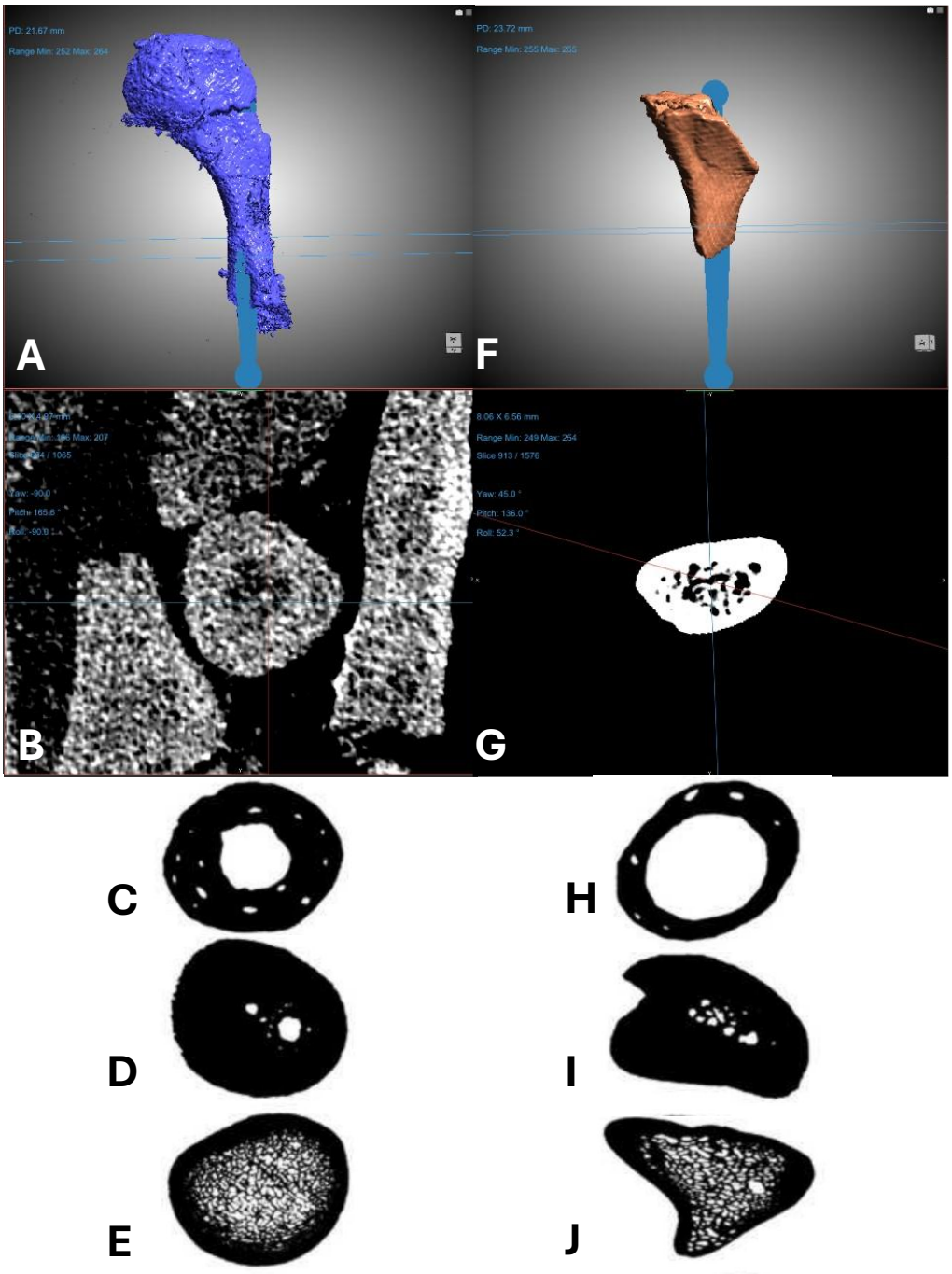

Figure 26: Plane of cross section in A) femur of MOR 14891 and B) corresponding cross section in CT data. Comparative cross sections modified from Botha (2023) of *Stigmochelys pardalis* representing the femur of a C) juvenile, D) young sub adult, and E) old subadult. Plane of cross section in F) ulna of MOR 14891 and G) corresponding cross section in CT data. Comparative cross sections of ulnae from a H) juvenile, I) young sub adult, and J) old subadult of *Stigmochelys pardalis* modified from Botha (2023).